Università degli Studi di Cagliari

PhD DEGREE

Molecular and translational medicine

Cycle XXXII

Radiogenomic features of CNS tumors and MiRNAs correlation phenotypes analysis

Scientific Disciplinary Sectors

MED/27-MED/36-MED/04

PhD Student: ***Federico Loi***

Coordinator of the PhD Programme ***Prof. Sebastiano Banni***

Supervisor ***Prof. Luca Saba***

Final exam. Academic Year 2018 – 2019

Thesis defence: January-February 2020 Session

Acknowledgements

Un sentito ringraziamento al Prof. Amedeo Columbano, che già dal Corso di Medicina e Chirurgia ha iniziato a darmi le migliori basi per affrontare al meglio tre distinti percorsi universitari, per i suoi insegnamenti che sono andati oltre l'ambito accademico, e soprattutto per la Sua filosofia di crescita personale, culturale e civile al fine di contrastare l'anonima mediocrità, che penso sia il più grande degli insegnamenti.

Il grande ringraziamento è destinato al Prof. Luca Saba, che con il suo lavoro, i suoi successi è la rappresentazione viva di "chi non si accontenta mai" rappresentando per me un grande esempio da seguire. Il ringraziamento inoltre per avermi supportato e spronato nel miglior modo possibile, senza mai farmi perdere di vista ciò che più è importante.

Un ringraziamento molto importante lo dedico al Dott. Carlo Conti, direttore della S.C. di Neurochirurgia dell'Ospedale Brotzu, che mi ha sempre incentivato a portare avanti questo progetto di ricerca, e che senza il suo importante contributo non si sarebbe potuto portare avanti.

Un ringraziamento va inoltre a tutti i Colleghi e tutto il Personale delle Sale Operatorie della S.C. di Neurochirurgia dell'Ospedale Brotzu che hanno collaborato al progetto.

Un enorme ringraziamento al collega e soprattutto amico Michele Porcu, che con il suo aiuto ha reso divertenti anche le parti più difficili di questo lavoro.

Un ringraziamento a tutti coloro che hanno collaborato al progetto, chi mi fatto vedere come si fanno le cose per bene e a chi con mi ha fatto capire come non vanno fatte.

Un ringraziamento particolare ai Miei Genitori, Daniela, Giammichele, Annina e Daniele.

Grazie a Chiara per tutto.

Radiogenomic features of CNS tumours and MiRNAs correlation phenotypes analysis

1 Introduction

1.1 Gliomas - General overview

Gliomas are the most common tumors of the central nervous system, representing 81% of primitive malignant brain tumors (Ostrom QT 2014). These neoplasms have highly invasive and aggressive behavior and represent a very broad diagnostic category. The most malignant and common form is the glioblastoma (Louis et al., 2007). Gliomas are named after their morphological similarity to glial cells, in fact they derive from astrocytic cells, ependymal cells, oligodendrocytic cells or from a mixture of all cell types and may develop from all central nervous system districts. Such common cellular origin determines that gliomas share similar features, including indistinct margins and malignant progression, and they may only be distinguished by genetic alterations or gene expression profiles (Walker C 2011)

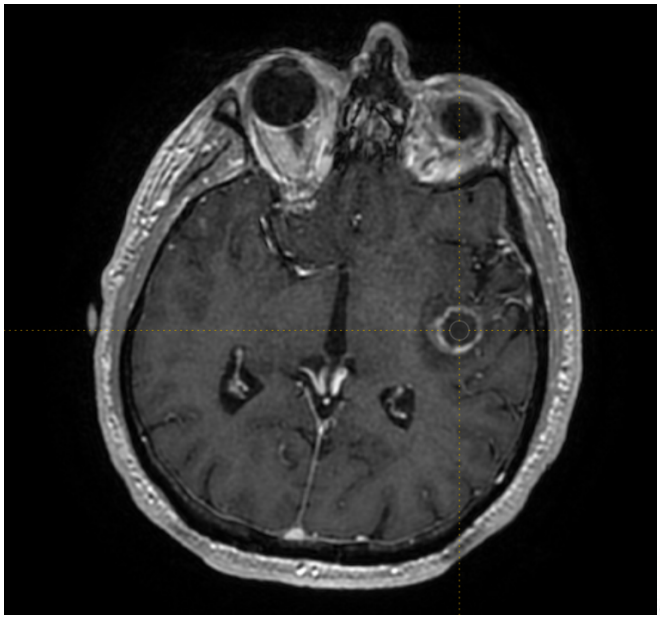

C.E. T1 –insular left glioma (A.O. Brotzu)

Graphic representation of left insular glioma (Mayo Foundation)

Glial cells were thought to have only supporting functions for neurons, but research studies showed that they also play a role in the homeostasis of the microenvironment and of the development of the nervous system (Dimou and Götz, 2014).

It has been shown that glial cells, through the constitution of a network of cells interconnected with each other and connected to neurons, form a structural scaffold with supporting roles (Giaume et al., 2010). participate in the regulation of synapses and in the formation of new synapses (Gundersen et al., 2015).

In recent years the identification of molecular markers gave a major contribution to better classifying, understanding and treating gliomas; in clinical use it enables to stratify patients more accurately, especially in clinical research to assess the efficacy of new pharmacological protocols or new drugs. (Riemenschneider et al., 2010). The rapid expansion of imaging techniques determined the ability to acquire ever better images, with increasingly higher resolution and a greater ability to identify smaller lesions (Shijun Wang et al., 2012). Clinical treatment also presented adjuncts. surgery is now supported by neuronavigation systems, intraoperative tumor tracers, which improved surgical performance, chemotherapy and new radiotherapy techniques.

Despite the progress made in research, only 5% of patients survived after 5 years (Ostrom QT et al., 2014), the results of the other patients with gliomas remain scarce and patients will eventually die from complications of this devastating disease.

Only early diagnosis of gliomas, early surgery and further treatment improvements will be the most effective method to deliver better results to patients (Pellerino et al., 2018).

1.2 Classification of WHO gliomas

Until a few years ago the classification principle for gliomas was based on their morphological characteristics, cytoarchitecture and immunohistological heritage, high cellularity and mitotic index, proliferation of endothelial cells and necrosis (Louis DN et al., 2007).

The international classification based on classical histology, has been recently revised and presents important modifications for the incorporation of different molecular biomarkers such as the IDH1 / 2 status, the 1p / 19q co-deletion and the methylation of the MGMT promoter (Reifenberger G et al., 2017) , mutation of H3 K27M; WNT and SHH activation; thus defining new groupings of

diagnosis and the need for standardization of the nomenclature including genetic and molecular characteristics (Louis DN et al., 2017)

For tumor types without molecular diagnostic tests, a diagnostic designation of the NOS is allowed (ie not otherwise specified). A NOS designation implies that there is no molecular information characterizing the lesion. In this context, the NOS in most cases, include tumors that do not show diagnostic genetic alterations. The NOS defines a group of lesions that cannot be classified, but can be the subject of future studies that could classify them. (Louis et al., 2017)

In text format, italics are used for symbols of specific genes. Linear hyphens are used in some designations. The WHO degrees are written with Roman numerals (I, II, III, IV). (Louis et al., 2017)

By simplifying we can distinguish diffuse or circumscribed gliomas, with a special mention for embryonic tumors.

All diffusely infiltrating gliomas (whether astrocytic or oligodendroglial) are grouped together, they include:

Diffuse Gliomas		Other astrocytomas	
Diffuse astrocytoma, IDH-mutant	Grade sec WHO II	Pilocytic Astocytoma	Grade sec WHO I
Anaplastic astrocytoma, IDH-mutant	Grade sec WHO III	Subependyma giant cell astrocytoma	Grade sec WHO I
Glioblastoma, IDH-wildtype	Grade sec WHO IV	Pleomorphic astrocytoma	Grade sec WHO II
Glioblastoma, IDH-mutant	Grade sec WHO IV	Anaplastic pleomorphic astrocytoma	Grade sec WHO III
Diffuse midline glioma, H3 K27M-mutant	Grade sec WHO IV		
Oligodendroglioma, IDH-mutant and 1p / 19q-codelected	Grade sec WHO II	Embryonal tumors	
Anaplastic oligodendroglioma, IDH-mutant and 1p / 19q codelected	Grade sec WHO III	Medulloblastoma (all subtypes)	Grade sec WHO IV

In patients diagnosed with glioblastoma without clinical or histological evidence of a less malignant precursor lesion, primary glioblastoma is defined. Glioblastomas diagnosed in a patient

with a previous diagnosis of low-grade diffuse astrocytoma or anaplastic astrocytoma are called secondary glioblastomas. (Ohgaki et al., 2013)

1.3 Incidence and survival of glioma.

There are many articles in the literature describing the incidence of gliomas.

The incidence rate of gliomas was 7.7 / 100,000 in the decade 1990-2006 and 7.3 in 2007-2016 in Finland (Natukka et al.,2019).

In the United Kingdom, the incidence rate of 7.1 / 100,000 in 2014 (Sehmer et al., 2014).

The incidence of malignant brain tumors in the US brain (CBTRUS) in the United States was 5.74 / 100000 (95% confidence interval = 5.77-5.78). The highest incidence in Northern Europe (AAIR = 6.59, 95% CI = 6.52-6.66) and Canada (AAIR = 6.53, 95% CI = 6.41-6.66). Incidence was instead found to be lower in Southeast Asia (AAIR = 2.55, 95% CI = 2.44-2.66), India (AAIR = 2.85, 95% CI = 2.78-2, 93) and East Asia (AAIR = 3.07, 95% CI = 3.02-3.12) (Leece R et al 2017)

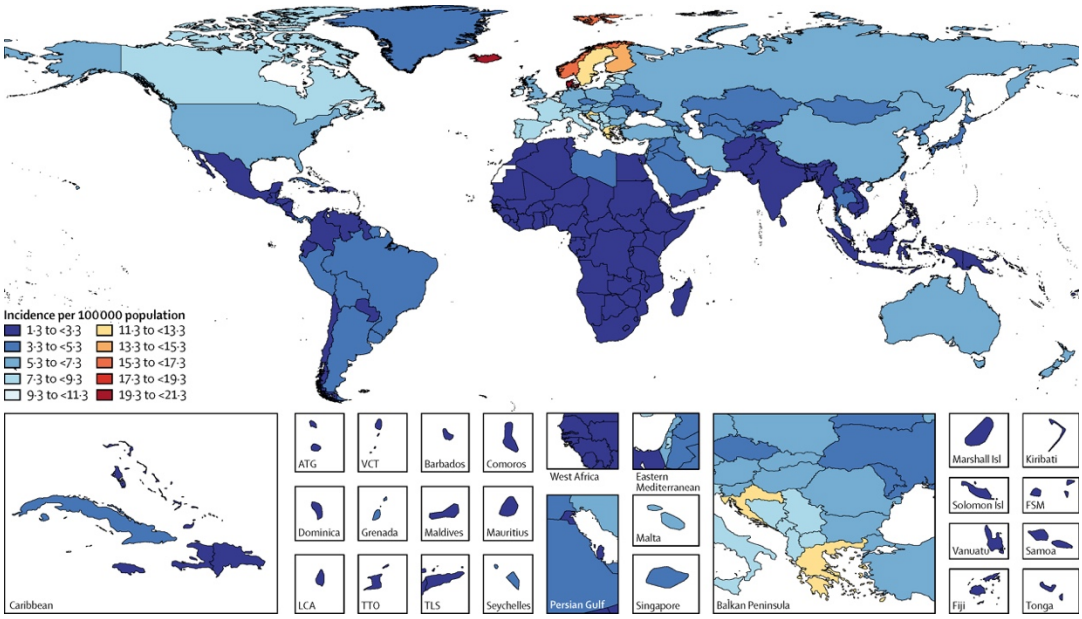

Age-standardised incidence of CNS cancer per 100 000 population for both sexes, 2016
The Lancet Neurology 2019 18, 376-393DOI: (10.1016/S1474-4422(18)30468-X)

Median survival time is 14.6 months after surgery and subsequent chemotherapy and radiotherapy. The five-year survival rate is 0.05% -4.7%, representing GBM as the most lethal primary brain tumor (Huang SW 2018), five-year survival rates show a women / men ratio = 20 , 7% / 18.7% (Crocetti et al., 2012).

Survival was consistently longer among females than males. The female gender can be considered as a prognostic factor (Franceschi et al., 2018)

The prevalence of glioblastomas is 86% (Sehmer et al., 2014). The age-related incidence is different between the different subtypes of glioma. The astrocytic type is typical of childhood with a peak in the first decade, the lowest incidence in the second decade and then reappears at 50-60 years (Feltbower RG et al., 2004). Glioblastomas occur in adults between 45 and 75 years of age, with a low increase starting at age 30 (Louis et al., 2007b) with an incidence of 3.32 cases per 100,000 person-years in males and 2, 24 in females (Ohgaki et al., 2004).

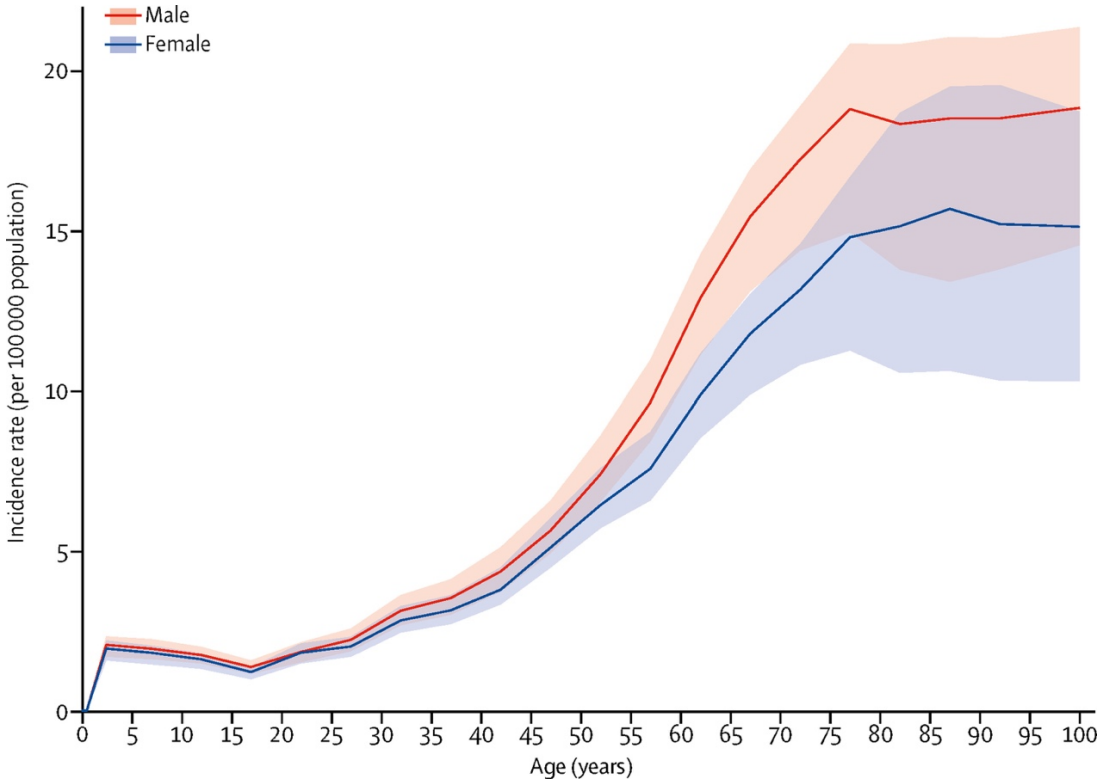

Global age-standardised incidence rate per 100 000 population of CNS cancer by age and sex, 2016
The Lancet Neurology 2019 18, 376-393DOI: (10.1016/S1474-4422(18)30468-X)

Overall survival at 1 year and 2 years for glioblastoma are 19.15% and 3.27% (Ghosh M et al., 2017). In patients under the age of 50, the median survival is 8.8 months compared to patients aged 50 to 59 years who have a median survival of 7.3 months (Ohgaki et al., 2004). Patients with anaplastic grade III astrocytoma have a 2-year survival rate of 58% (Laws et al., 2003).

1.4 Biomarkers for Glioma

The biomarkers currently used for glioma include hypermethylation of the O6 methylguanine-DNA-methyltransferase (MGMT) promoter, combined hetrozygosity (LOH) loss of the 1p and 19q chromosomes, chromosome 10q LOH, isocitrate dehydrogenase (IDH) mutations and epidermal growth mutations factor receptor (EGFR) BRAF duplication / fusion.

1.4.1 MGMT

MGMT, a protein with enzymatic function of DNA repair that catalyzes the removal of methyl groups from the O6 position of guanine to cysteine (Von Deimling et al., 2011) reversing the cytotoxic effect of alkylating agents. The methylation of the MGMT promoter determines the absence of one of the main DNA repair systems thus making the tumor cells more susceptible to the arrest of the replicative cycle. The MGMT status is an important predictive factor in the success of chemotherapy treatment with alkylating agents such as Temolozomide (Hegi et al., 2005). It is known that the gliomas with promoter methylation and the MGMT gene silencing will respond better to TMZ, resulting in higher survival rates.

1.4.2 IDH

The IDH (isocitrate dehydrogenase) family of enzymes catalyze the transformation of the isocitrate by oxidative carboxylation into α-ketoglutarate, NADP + -dependent (IDH1 and IDH2) and independent NAD + -ID3). There are different forms of IDH; IDH1 is found in cytosol and peroxisomes and IDH2 and 3 are confined within the mitochondria and collaborate in the citric acid cycle for energy production (Zhang, C. et al., 2013).

In astrocytomas, oligodendrogliomas and oligoastrocytomas and in secondary glioblastomas, mutations in the IDH1 and IDH2 genes (Von Deimling et al., 2011) are present in precisely 86% of grade II astrocytomas and oligodendroglioma and in 82% of III grade disease (Yan et al., 2009).

Mutations in IDH1 and IDH2 are rare in primary glioblastomas de novo and in ependymal tumors and are a well-established method of differential diagnosis (Von Deimling et al., 2011). IDH mutations determine the accumulation of 2-HG, this may have a toxic effect on mutated cells for IDH1 / 2, on the other hand, it would seem to promote angiogenesis in the tumor by protein stabilization (HIF1). IDH mutations generally increase sensitivity to chemotherapy and are generally associated with a disease-free survival (Houillier et al., 2010)

1.4.3 EGFR

The over-expression and frequent mutations of epidermal growth factor (EGFR) receptor had been found in 30% of gliomas in and 60% of glioblastomas (Jansen et al., 2010). The most common EGFR mutation is the EGFR III variant (EGFRvIII). the mutation determines the absence of a ligand-binding domain and as a consequence EGFRvIII is constitutively activated causing the uninterrupted activation of the EGFR-phospho-inositide 3-kinase pathway increasing cell proliferation (Stommel et al., 2007).

Glioblastomas with the EGFRvIII mutation are more aggressive and with a more rapid proliferation, patients with mutated EGFR can benefit from targeted treatments (Jeuken et al., 2009).

1.4.4 Duplication / fusion of BRAF in pilocytic astrocytoma.

Pilocytic astrocytoma classified as grade I glioma according to WHO and is a non-infiltrating brain lesion (Louis et al, 2007; Louis et al, 2017).

About 50-70% of pilocytic astrocytomas have fusions of the B1 gene (BRAF) of the murine oncogene v-RAF murine with the KIAA1549 gene which causes the loss of the N-terminal inhibitory domain of BRAF and simultaneous doubling of the resulting activation domain in the expression of the BRAF mutant protein (Siegal et al., 2015). The expression of the BRAF: KIAA1549 fusion gene allows the differential diagnosis between glioblastoma and pilocytic astrocytoma, which despite the different biological behavior histologically share the proliferative microvascular plot (Siegal et al., 2015).

1.4.5 Co-deletion of chromosomal arms 1p and 19q

The oligodendroglioma is classified among the diffused gliomas (Louis et al.,2017), it derives from the oligodendrocytes, glial cells that in the healthy tissue exhibit a branched morphology and are involved in the myelin production (Louis et al., 2007a).

1p19q aberration is characterized by an unbalanced translocation, with loss of the short arm of chromosome 1 along with the long arm of chromosome 19 in tumor cells or loss of heterozygosity in these chromosomal regions (Ręcławowicz et al., 2013)

The combination of the deletion of 1p and 19q chromosomes in patients with anaplastic oligodendroglioma is associated with longer overall survival and better response to therapy (Jenkins et al., 2006) following alterations of the CIC gene on chromosome 19q and the FUBP1 gene on chromosome 1p (Bettegowda et al., 2011)

2.0 MiRNA

2.1 Biological meaning and features of MiRNA

MicroRNAs are small non-codifying RNAs (18-24 azotate bases) that play a fundamental role in eukariots post-transcriptional genome expression (Bartel et al., 2004). They are leading molecules in the RNA silencing process (Ha, Kim, 2014). Nonetheless, up until microRNAs were discovered, RNA was merely considered as a protein carrier molecule. Thanks to multiple scientific papers (Lagos-Quintana, M. 2001 Lee, R. C. 2001), the scientific world now recognizes their physiological role: microRNAs negatively regulate genome expression in the post-transcriptional phase by binding RNA. The MiRNA function is to regulate cellular behavior (Wang et al., 2011) and modulate gene expression at the post-transcriptional level by suppressing translation (Baraniskin et al., 2012).Other scientific studies demonstrated that microRNAs are always involved in development and pathological processes in animals: such as emopoiesis, miogenesis, and brain development; also, they may regulate cellular proliferation, differentiation, apoptosis and carcinogenesis.(Sassen S et al, 2008) interacting with most protein-coded transcripts (Ha and Kim, 2014).

Victor Ambros and colleagues in 1993 discovered miRNA, a small RNA encoded by the lin-4 locus, during the study of developmental progress in Caenorhabditis elegans (Lee et al., 1993 Wightman et al., 1993). It was determined that the lin-4 gene produces RNA of about 22 non-coding nitrogenous bases that binds to sequences in the 3 "untranslated region (3" UTR) of lin-14 mRNA (Lee R et al., 1993). The interaction between lin-4 and lin-14 determines the translational repression of lin-14 mRNA (Lee R et al., 1993). Another small non-coding RNA, let-7, binds to the 3 'URL of lin-41 mRNA and suppressed LIN-41 protein levels (Berezikov et al., 2011). let-7 has been preserved in a wide range of animals, suggesting that in other organisms there may be other regulatory RNAs ~ 22 nt (Pasquinelli, A. E. et al., 2000).

The importance of miRNAs in mammalian development was initially demonstrating that the loss of both phases of miRNA biogenesis driven by Dicer and DGCR8, causes embryonic lethality (Bernstein et al., 2003; Wang et al., 2007)

Today we know that miRNAs control a wide range of biological processes such as embryonic development mechanisms, cell differentiation, apoptosis, control of cell growth and regulation of metabolic processes (He and Hannon, 2004). Given their role in so many physiological process, it does not come as a surprise to see the microRNAs' levels are altered in the course of a pathological

event (carcinogenesis, metastatical progression).(Blenkiron and Miska, 2007; Zhang et al., 2007; Ma and Weinberg, 2008).

Since the discovery of the first miRNA in 1993 (Lee et al., 1993), as of 2012, 2,588 miRNA human genes, biogenesis and miRNA maturation have been well studied (Graves and Zeng, 2012).Their biology has been thoroughly studied and still remains an important subject to develop, infact several of them still appear without an evident function despite potentially regulate nearly all cellular pathways (Chen 2004)

2.2 Biogenesis of microRNA*s*

miRNA genes are found within introns of coding and non-coding transcripts, those found in introns of protein-coding genes share the promoter sequence (Ozsolak et al., 2008).
Mature microRNAs are generated through a two-step nuclear and cytosolic processing pathway to produce about small RNAs of about 22 nucleotides that regulate gene expression at the post-transcriptional level (Denli et al., 2004).
The basic process of miRNA biogenesis starts with the transcription from the RNA polymerase II from the DNA, to produce a primary miRNA (pri-miRNA), the pri-miRNAs are therefore single-stranded RNA molecules that fold in a "hairpin" forming a partial double helix following the pairing of complementary sequences (Lee et al., 2002). MiRNA transcription is regulated by epigenetic mechanisms and transcription factors including histone modification (Scott et al., 2006) and DNA methylation (Saito et al., 2006). The stem of the pri-miRNA is asymmetrically cut out at the level of the base of the "hairpin" by a type III RNA-endonucles, Drosha, an RNase III endonuclease, and DGCR8, (Denli et al., 2004) to create a fork more small with a projection of 3 "becoming precursor miRNA precursor, the pre-miRNAs (Bartel, 2004). In many cases a single pri-miRNA contains a cluster of several microRNAs and will thus be responsible for the origin of multiple miRNAs.
The recognition by Drosha requires the interaction of this enzyme with a second protein, Pasha (Partner of Drosha), which recognizes the secondary structure of the base of the "hairpin" and sequences flanking this region, generally located at no more than 125 nucleotides of distance (Lee et al., 2003; Yeom et al., 2006).
Subsequently the pre-miRNAs are actively translocated to the cytoplasm thanks to the synergistic action of Ran-GTP and Exportin-5 (Bartel, 2004).
Once in the cytoplasm the pre-miRNAs are subjected to the catalytic action of a highly conserved protein: type III RNA-endonuclease: Dicer. (Bernstein, E 2001). With this step the pre-miRNA

filaments are processed in the duplex form of about 23 base pairs These double-helix RNA molecules are referred to as miRNAs: miRNA *, in which miRNA is the strand that will be included in the "RNA- Induced Silencing Complex ”(RISC); the miRNA * strand will instead be degraded (Bartel, 2004). RISC's decision on which wire degrades is based on the stability of the base pair at the 5 'ends of the duplex. RISC is a ribonucleo-protein complex composed of single-stranded miRNA and a variety of proteins, among which the proteins of the Argonaute family are fundamental for the activity of the complex (Bartel, 2004).

The 5 'monophosphate of the guide wire is anchored to a 5' phosphate-binding pocket inside AGO and the 3 'end binds to the PAZ domain of the AGO protein (Schirle and MacRae, 2012). The seed sequence of the guide wire has a helix-shaped conformation in the shape of an A, a short compact helical structure with bases not perpendicular to the helix axis, which allows the target mRNA to be scanned for mRNA complementation and cleavage target from the PIWI domain (Ha and Kim, 2014). Mature miRNAs with 2-8 nucleotides in common are from the same family (Bartel, 2009). Mature miRNAs derived from separate loci are identified with numerical suffixes such as miR-125a-1 and 125a-2.

MiRNAs that differ by one or two nucleotides in the sequence are "miRNA sisters" and usually have the same goals, identified by suffixes with letters such as miR-125a and 125b (Ha and Kim, 2014).

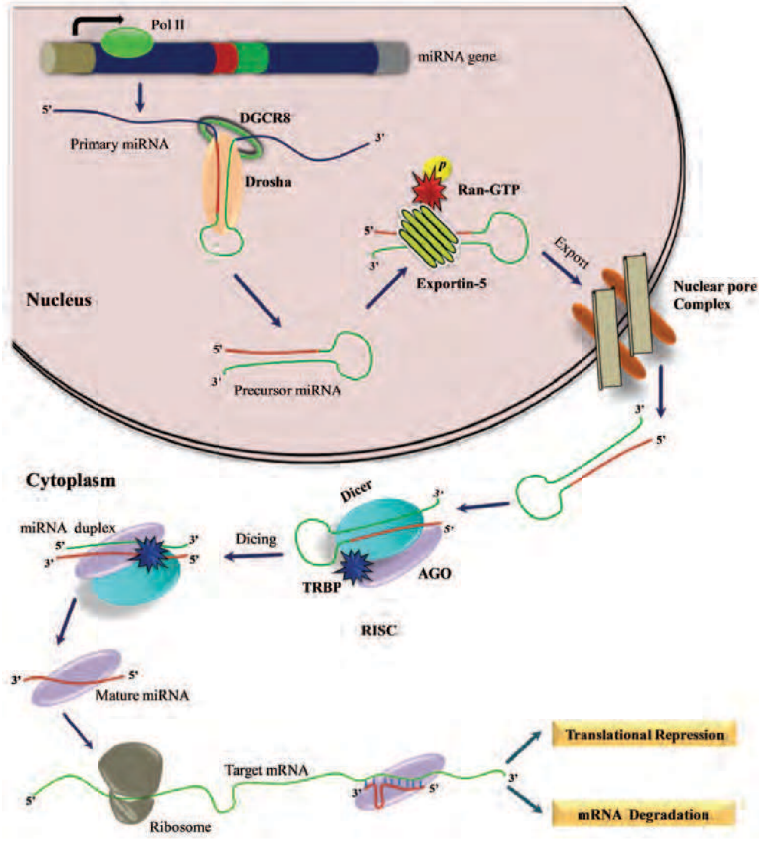

(Kumaravel Somasundaram, Soumya Alige Mahabala Rao, Zahid Nawaz
MicroRNA (miRNA) Regulation in Glioma: Implications in Development, Progression, Grading, Prognosis and Therapy Published in 2011)

2.3 Current MiRNA detection and CNS association

MicroRNAs are deeply involved in molecular biology of gliomas. In 2005 Chan demonstrated that miR-21 is highly overregulated in gliomas cells and this feature induces an increased antiapoptosis activity: we can then presume that miR-21 works an oncogene by silencing antiapoptosis genes(Chan, 2005). Chan's work became a stimolo to analyze and assess microRNAs expression both in gliomas cells and in gliomas bioptical sample (Ciaffré 2005). Subsequently comparative studies were carried out, betweeb pathological and normal tissues samples. These studies allowed the scientific world to learn that not only miR-21 is highly expressed in gliomas but also miR-10b, miR-92b, miR-183, miR-106b, while miR-302c, miR-379, miR-329, miR-134, miR-221 appear to be underexpressed in gliomas compared to normal cerebral tissue (Sasavama 2009). Subsequently many studies have demonstrated the role of miRNAs as regulators of the processes of proliferation, differentiation, apoptosis, migration and invasion (Karsy 2012).

The following table 1 summarizes the most cited and known miRNAs whose role is known in the natural history of gliomas.

miRNA	Targets	Functional Assay	Tumor Grade	Reference
hsa-miR-101	TRIM44	Cell proliferation, Cell migration, Cell viability, Angiogenesis, Cell invasion	Grade IV	(Li et al., 2019)
hsa-miR-10b	BCL2L11, p16/CDKN2A, p21/CDKN1B	Cell proliferation, Cell cycle regulator	Grade III-IV	(Gabriely et al., 2011)
hsa-miR-106	TIMP-2	Cell invasiveness	Grade III-IV	(Wang et al., 2015)
hsa-miR-124	Gli2/miR-124/AURKA	Cell proliferation, Angiogenesis, Cell invasion	Grade-III-IV	(Xu et al., 2017)
hsa-miR-125b	Wnt/β-catenin	Cell cycle regulator, Apoptosis / Stemness	Grade-III-IV	(Yuan et al., 2018, Shi et al., 2015)
hsa-miR-133b	FOXC1	Cell migration and Cell invasion	Grade IV	(Liu et al., 2018)
hsa-miR-134	KRAS	Cell Proliferation, Cell invasive	Grade III-IV	(Wang et al., 2018)
hsa-miR-137	RASGRF1, RTVP1, c-KIT, YBX1, AKT2, CDC42, CDK6, TGFβ2	Cell proliferation, Cell migration, Apoptosis, Stemness	Grade IV and Glioma Stem Cells	(Deng et al., 2016, Bier et al., 2013, Tamim et al., 2014)
hsa-miR-146a	Notch1 / TGFβ, Smad4 / TRAF6, IRAK1, IRAK2	Cell proliferation, Cell viability, Apoptosis and Chemosensitivity / Regulate NF-κB Signaling Pathway	Grade IV	(Mei et al., 2011) (Lv et al., 2015) (Park et al., 2015,)
hsa-miR-148a	BIM (BCL2L11), MIG6	Reduced EGFR trafficking	Grade IV	(Kim et al., 2014)
hsa-miR-154	PIWIL1	Cell proliferation, Cell migration Cell invasion	Grade IV	(Wang et al., 2017)
hsa-miR-155	EAG1, GABRA1, MAPK13, MAPK14, MXl1, FOXO3a	Cell proliferation, Cell invasion, Apoptosis and Chemoresistance	Grade IV	(D'Urso et al., 2012, Liu et al., 2015, Meng et al., 2012, Zhou et al., 2013)
hsa-miR-17-92 cluster	TGFβRII, Smad4, CAMTA1, CTGF, POLD2	Cell viability, Cell proliferation, Apoptosis and Angiogenesis	Grade III-IV	(Dews et al., 2010, Ernst et al., 2010, Miele et al., 2014)
hsa-miR-181a/b/c	BCL2, Cyclin B1	Cell proliferation, Apoptosis, Cell invasion, Angiogenesis, Radiosensitivity, Chemosensitivity	Grade-III-IV	(Zhang et al., 2014 Ciafre et al., 2005, Conti et al., 2009)
hsa-miR-182	HIF2A, BCL2L12, c-MET	Cell proliferation, Cell invasion, Angiogenesis, Apoptosis and Chemoresistance	Grade IV	(Kouri et al., 2015)
hsa-miR-183	NEFL LRIG1	Cell proliferation	Grade IV	(Fan et al., 2018, Wang et al., 2016)
hsa-miR-18a	CTGF Smad3	Cell proliferation, Cell migration, Apoptosis and Cell invasive	Grade III-IV	(Fox et al., 2013)
hsa-miR-19a/b	RUNX3 via β-catenin/Tcf-4 signaling	Cell proliferation, Cell survival and Cell invasion	Grade III-IV	(Sun et al., 2017, Wang et al., 2018)
hsa-miR-200a/b	DNMT1 and EZH2	Cell proliferation, Cell invasion	Grade IV	(Ning et al., 2015)
hsa-miR-203	ATM-dependent interferon PLD2, Robo1, ERK, MMP9	Cell proliferation, Cell migration Cell invasion	Grade IV	(Yang et al. 2017, Dontula et al., 2013)
hsa-miR-20a	TIMP2	Cell invasiveness	Grade III-IV	(Wang et al., 2015)
hsa-miR-21	HNRPK, TAp63, PDCD4	Cell proliferation, Cell Invasive, Apoptosis	Grade III-IV	(Conti et al., 2009, Gaur et al., 2011, Papagiannakopoulos et al., 2008, Quintavalle ey al., 2016)
hsa-miR-210	HIF3A TMZ-resistant	Cell survival and Chemoresistance	Grade IV	(Lee et al., 2015 Agrawal et al., 2014)
hsa-miR-218	Robo1	Cell proliferation, Apoptosis, Cell invasion, Cell survival, Cell migration	Grade IV	(Gu et al., 2016)

hsa-miR-219	CD164	Cell proliferation, Cell migration Cell invasion	Grade IV	(Shi et al., 2014)
hsa-miR-221/222	SUN2,/ TIMP3/p57 PI3-K/Akt signaling	Cell cycle progression and anti-apoptosis	Grade III-IV	(Hsieh et al., 2014, Zhang, 2012, Chen et al., 2012 Xie et al. 2014)
hsa-miR-296-3p	SOCS2, STAT3	Cell invasiveness	Grade IV	(Lee et al., 2016)
hsa-miR-296-5p	CASP8, NGFR	Cell invasiveness	Grade IV	(Lee et al., 2017)
hsa-miR-296-5p	SOX2	Stemness	Glioma Stem Cells	(Lopez-Bertoni et al., 2016)
hsa-miR-302	DOCK4	Cell proliferation and Apoptosis	Grade III-IV	(Debruyne et al. 2018)
hsa-miR-320	Cyclin D1 and CDK6	Cell cycle progression Cell invasivness	Grade III-IV	(Li ey al. 2018)
hsa-miR-329	E2F1	Cell proliferation	Grade III-IV	(Xiao et al., 2013)
hsa-miR-335	cAMP/protein kinase A	Cell survival, Cell proliferation, Cell invasion and Cell stemness	Grade III-IV	(CShu et al., 2012)
hsa-miR-34a	PD-L1 c-Met, NOTCH1, NOTCH2, PDGFRA, CDK6, SMAD4, CCND1, SIRT1	Cell survival, Cell proliferation, Cell migration, Apoptosis, Cell invasion, Stemness	Grade-III-IV	(Wang et al., 2017, Di Bari et al., 2018, Genovese et al., 2012, Silber et al., 2012)
hsa-mIR-372	FER1L4/miR-372/E2F1	Cell proliferation, Cell invasion and Apoptosis	Grade III-IV	(Xia et al., 2019)
hsa-mIR-379	C14MC; MEF2; MEG3	Cell proliferation, Cell invasion and Apoptosis	Grade IIII	(Kumar et al., 2018)
hsa-miR-381	BRD7	Cell proliferation	Grade III-IV	(Tang et al., 2014)
hsa-miR-429	SOX2	Cell proliferation, Cell invasion	Grade IV	(Dong et al., 2017)
hsa-miR-451	mTOR/HIF-1α/VEGF PI3 K, AKT, CAB39	Cell proliferation, Apoptosis, Stemness	Grade IV and Glioma Stem Cells	(Nan et al., 2018, Tian et al., 2012)
hsa-miR-491	TRIM28, IGFBP2, CDK6, BCL2L1, EGFR, MMP9, TRIM28	Cell proliferation, Cell invasion, Stemness	Grade IV	(Qi et al., 2016, Li et al., 2015, Yan et al., 2011,)
hsa-miR-520b	AKT1, PIK3CA and SOS1	Cell proliferation	Grade IV	(Cunha et al., 2017)
hsa-miR-595	SOX7	Cell proliferation	Grade IV	(Hao et al., 2016)
hsa-miR-610	MDM2, CCND2, AKT3	Cell proliferation, Cell migration, Cell viability	Grade IV	(Yan et al., 2016 Mo et al., 2016)
hsa-miR-7	IGF-1R	Cell proliferation, Cell migration,	Grade-III-IV	(Wang et al., 2014)
hsa-miR-9	JAK, STAT3, OL18A1, THBS2, PTCH1 and PHD3	Stemness Cell proliferation, Cell migration,	Glioma Stem Cells	(Kim et al., 2011 Chen et al., 2019)
hsa-miR-92a	BCL2L11 / KLF4	Cell proliferation and Apoptosis	Grade IV	(Niu et al., 2012)
hsa-miR-92b	CHIP/miR-92b/PTEN	Cell Proliferation, Cell invasive	Grade IV	(Xu et al., 2017)
hsa-miR-93	RBL2	Cell proliferation, Cell migration and Angiogenesis	Grade III-IV	(Liu et al., 2018)
hsa-miR-98	IKBKE/NF-κB	Cell apoptosis	Grade III-IV	(Wang et al., 2017)
let-7b	PBX3/MEK/ERK1/2/LIN 28	Cell proliferation, Cell migration, Cell invasion	Grade IV	(Xu et al., 2018)

Table 1

For some miRNAs the true biological meaning has not yet been completely clarified, in fact for some of them the scientific publications do not agree on the univocity of action, sometimes exactly opposite behaviors are described.

3 Radiology and radiogenomics

3.1 Basic principles in instrumental study and brain imaging

When a brain tumor is clinically suspected, radiology imaging is the main and most useful resource in order to obtain diagnostic confirmation and to plan the therapy (both clinical and surgical).

In clinical practice, different imaging modalities are used for the study of the central nervous system. The imaging modalities of the Central Nervous System can provide structural and functional information.

The structural or anatomical modalities allow to highlight the different structures and tissues of the Central Nervous System. Among these, the most used for Neuroimaging are computerized tomography (CT) and magnetic resonance (MR) imaging.

CT imaging uses the differences in X-ray absorption as X-Rays through the different tissues of a patient's body. CT scans are obtained by the emission of X-rays from an X-Rays source that rotates around the patient's head. Each ray produces a 2D image from with a specific angle, the sum of all the 2D images are subsequently used to construct a 3D volume using tomographic reconstruction. CT scans are sharp, high-resolution images that are obtained very quickly. The main disadvantage of TC is the fact that it uses potentially dangerous ionizing radiation.

Magnetic Resonance uses the magnetic properties of hydrogen nuclei present in large quantities in the human body. Today it represents the gold standard for brain studies thanks to the contrasting qualities of tissues and the fact that ionizing radiation is not used. Techniques developed in recent years as Diffusion Tensor Imaging (DTI) which, by measuring the anisotropic diffusion of water within the tissues, allows us to reconstruct the traits of the white substance by connecting the different parts of the neural networks in the brain. The presence of a tumor causing the rupture, displacement or infiltration of fibers has a direct impact on the fiber structures (Wei 2007). Further information for the diagnosis and study of brain tumors from MRI spectroscopy, that is, measurement of metabolites in tumor tissue and measurement of relative cerebral blood volume using a contrast agent (Soffietti 2010).

The use of functional imaging is useful in studying the Central Nervous System in relation to physiological changes caused by brain activity.

Electroencephalography (EEG) and magnetoencephalography (MEG) are techniques that allow us to quantify brain activity. Both of these methods use electrodes positioned on the scalp; EEG detects electrical impulses in the brain due to neuronal activity, while MEG measures flow changes. The methods are commonly used by neurologists due to their simplicity, non-invasiveness and their very high temporal resolution, while they lack spatial signal accuracy.

Position emission tomography (PET) and single photon emission computed tomography (SPECT) measure changes in cerebral blood flow and tissue metabolism and how they are altered by brain disorders using nuclear imaging techniques, marking a biological molecule with a radioactive isotope.

The labeled molecule injected into the bloodstream is accumulated in areas where the molecule has an affinity, for example, the radioactive isotope fluorodeoxyglucose (FDG) behaves like glucose molecules and therefore the ematoencephalic barrier is able to trace the metabolic activity of the brain.

The advantage is that the radioactive tracer specifically designed to target specific organs or processes related to a disease makes it very specific. This technique is invasive and potentially harmful due to the use of radioactive tracers and isotope production is expensive and available in certain centers. The CT and PET technologies combined in a single device, allowing you to sum up the anatomical information from CT scans with the metabolic information provided by PET scans.

Functional magnetic resonance imaging (fMRI) with BOLD (Blood Oxygen Level Dependent) contrast has been used for over 25 years to detect localized neural activity in the cortex and to detect changes in neuronal activity related to functional activity of the brain induced by sensorimotor or cognitive activity (Gore 2019). Neuronal activation causes a selective increase in blood flow in a given brain area to compensate for oxygen consumption and therefore reduces the amount of deoxygenated hemoglobin molecules. Changes in hemoglobin oxygenation are detected by exploiting the paramagnetic properties of deoxygenated hemoglobin that affect the measured NMR signal. fMRI is a tumor surgery planning tool for the purpose of identifying the spatial relationship between the lesion and the functional area. The time spent in signal acquisition means that fMRI images do not have a great structural resolution.

3.2 MR features of CNS tumors

Nuclear magnetic resonance imaging is a non-invasive imaging technique with the ability to study the structure and function of tissues from the cellular level to the whole organ level. The traditional magnetic resonance imaging is based on the properties of protons (present in very high quantities as they are part of the water molecules present in the tissues) subjected to specific magnetic fields, with an intensity between 0.2 T and 3 T for uses clinical (it reaches 7 T for experimental use only).
The potential of magnetic resonance was discovered in 1946 by two groups of scientists: the first directed by Felix Bloch, of the University of Stanford, the second directed by Edward Mills Purcell, at Harvard University.
The differences in the composition of the various tissues give rise to the intrinsic contrast of the specific image for each organ, which, however, can be further optimized through the use of contrast media that allow specific highlighting of organs and tissues.
In clinical routine the great use is due to three factors:

1. sensitivity of the magnetic resonance signal in discriminating characteristics between normal and pathological tissues.
2. possibility of obtaining images with excellent spatial resolution and high discriminating power between the various soft tissues.
3. the development of software and methods for image processing that allow the recognition of alterations at the molecular level beyond the human visual spectrum.

Magnetic resonance imaging is the most complete imaging test for detection of gliomas and the application of different magnetic resonance techniques it allows a first classification of the different types of gliomas (Wang et al., 2019).
Although there is not a specific MR protocol for the study of brain tumors, in 2015 the Society for Neuro-Oncology (SNO), the European Organization for Research and Treatment of Cancer (EORTC) and United States National Brain Tumor Society (NBTS) released a consensus document for a standardized imaging protocol for brain tumor assessment in clinical trials (Ellingson BM 2015). The same recommendations were also confirmed in 2018 by the paper by *Thust SC et al.* (Thust SC 2018) for glioma imaging assessment.
The minimum standard protocol for 1.5 and 3 Tesla MR scanner consists of the following five sequences (Ellingson BM 2015, Thust SC 2018):

1. Pre-contrast and post-contrast isotropic T1-weighted 3D (T1-3D): these sequences are fundamental for evaluation of enhancement of the tumoral lesion, according to the fact that

high-grade gliomas on MR show areas of increased enhancement after gadolinium-based contrast medium infusion. The contrast enhancement is due to the leakage of contrast medium in the interstitial space due to the neoangiogenesis (Wesseling et al., 1998). The isotropic acquisition guarantees a volumetric acquisition in order to reconstruct the images on multi-planar reconstructions and to give better information to the surgeon for biopsy and preoperative planning (Thust et al., 2018). The preferable resolution is 1 x 1 x 1 mm, and the maximum recommended is 1.5 x 1.5 x 1.5 mm (Thust et al., 2018).

2. Axial 2D T2-weighted: this sequence is fundamental for the evaluation of non-enhancing parts of gliomas, especially in low-grade gliomas that do not show typical enhancement on post-contrast T1-3D images. In fact, they appear hyperintense in T2 sequences (Weisman et al., 1972). Slice thickness should be not over 4 mm (with no interslice gap) for 1.5 T scanners, and not over 3 mm (with no interslice gap) for 3 T scanners.
3. Axial 2D Fluid Attenuated Inversion Recovery (FLAIR): FLAIR sequences use a combination of T1- and T2- weighting in order to suppress signal originated form cerebrospinal fluid (CSF) (Ellingson et al., 2015). This sequence offers a better visualization of vasogenic edema, surgery-induced and radiotherapy induced radiation, and tumor infiltration near cortex and in periventricular regions (Ellingson et al., 2015). Slice thickness recommended is the same for axial 2D T2-weighted sequence (Ellingson et al., 2015).
4. Axial 2D Diffusion Weighted Imaging (DWI): this sequence is important for identification of early ischemic injury and infection/abscess (Ellingson et al., 2015). Apparent Diffusion Coefficient (ADC) maps can be generated from DWI sequences, and they reflect the magnitude of water motion inside of the cells (Ellingson et al., 2015). The restriction of diffusion of water molecules can be due by cytotoxic edema (due for example by ischemic injury) or high cellular density, like observed in lymphomas (Ellingson et al., 2015, Guo AC 2002), and it appears as areas of high signal on DWI images, with low values on ADC maps. The scanning protocol recommended suggest the collection of 3 b-values (0, 500 and 1000 mm^2/s) collected in 3 directions (x,y and z), with the slice thickness recommended for axial 2D FLAIR and T2 sequences.

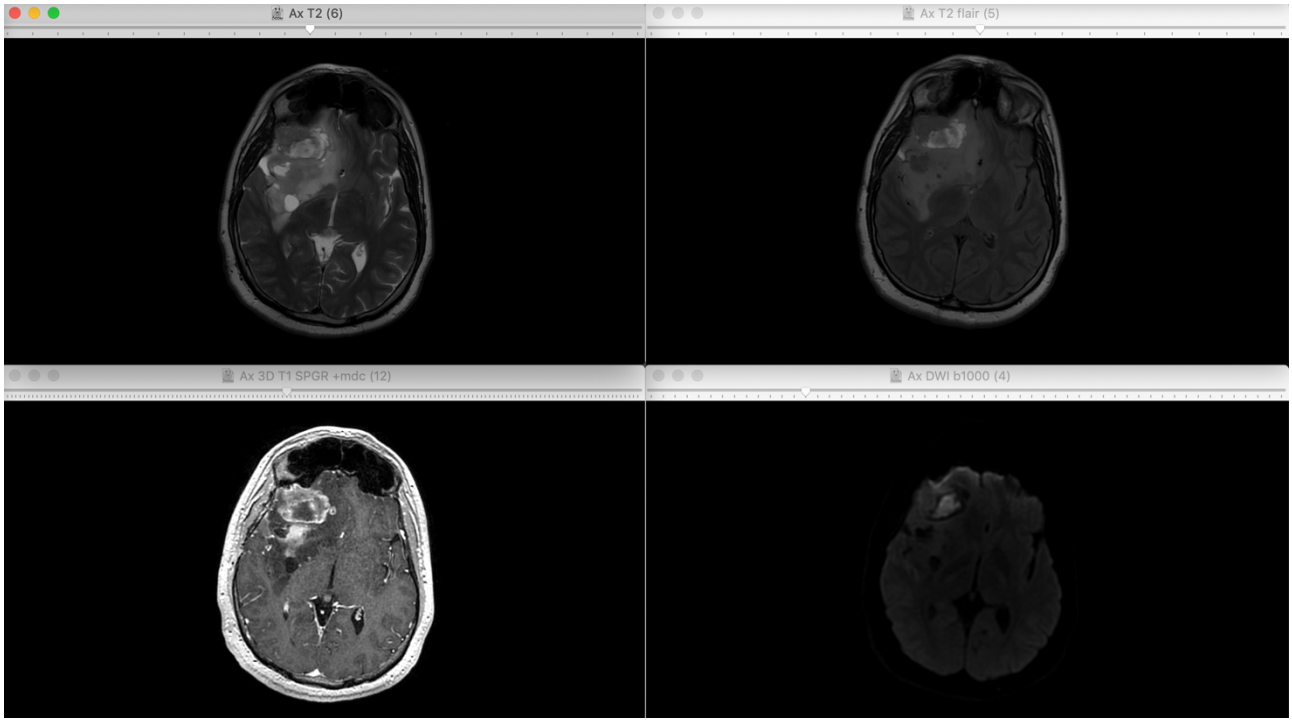

(Representation of MR images of the lesion seen in the different sequences (from left to top T2 and T2 Flair; below C.E. T1 and DWI) (AO-Brotzu)).

Other advanced imaging techniques are not essential, but their use can help characterizing of gliomas even though they are not extensively validated or integrated into clinical practice (Thust SC 2018). In particular:

- Perfusion MRI (pMRI): as reported in the name, this kind of sequences are able to estimate the blood perfusion at the level of capillaries, expressing quantitative data measured in ml/100 gram of tissue (Jahng et al., 2014). High grade gliomas tend to have increased values of perfusion metrics (Essig et al., 2013). This technique can be performed with the use of contrast medium by using dynamic susceptibility contrast (DSC) or dynamic contrast enhanced (DCE) methods, and without contrast medium by usingthe Arterial Spin Labeling (ASL) method (Jahng GH 2014 , Essig M2013).
- MR Spectroscopy (MRS): this technique is able to characterize the chemical composition of a given preselected areas of the tumor (Horská et al., 2010). Data are exposed in terms of spectra, and usually in gliomas there is a direct correlation between Choline (Cho) concentration and grading of the tumor (Horská et al., 2010). This technique can be applied by using the single or the multi-voxel approach (Horská et al., 2010).
- Diffusion Tensor Imaging (DTI): this is a technique able to map and characterize diffusion of water on the three dimensions of space as a function of spatial location, and to identify microstructural changes of white matter (Alexander et al., 2007). This technique can be used

for a better comprehension of the relationships between tumor and white matter, in particular of eloquent areas (Alexander et al., 2007).

- Functional MR (fMR): this technique exploits the Blood Oxygen Level Dependent (BOLD) signal in order to identify cortex activation at rest or during tasks (Weng et al., 2018). Its use can be useful in the preoperative phase to assess the relationship between tumor and eloquent cerebral areas like language area and motor areas (Weng et al., 2018).

3.3 Limitations of Magnetic Resonance in the study of primitive CNS tumors

Physical limitations

Magnetic Resonance (MR) exam is contraindicated for patients who, due to accidents or previous surgeries, have different types of metal devices in their bodies, especially if they are near vital organs; the magnetic field produced by the scanner may induce movements or overheating.

Also, crystalline prostheses used for cataracts before the mid-eighties of the last century and metal heart valves are an absolute contraindication to MR exam.

Cardiac pacemakers and old-type neurostimulators may not be subjected to MR, because magnetic fields alter their functioning; though, in more recent years, radiologists are accustomed to preventing such events by turning off new devices before the exam and turning them on after the exam.

Furthermore, in the past decade new surgical materials were introduced to avoid magnetic fields interference.

All patients who worked as bodybuilders, turners, welders, metal paint workers or have experienced hunting accidents or were the victims of explosions may unconsciously have metal splinters in their bodies.

Pregnancy does not represent a contraindication to MR, although it is advised to avoid such an exam in the first 12 weeks, unless it is utmost and urgent.

Diagnostic limitations

Despite the radiological models of different types of brain tumors and the improvement of imaging techniques, radiological diagnosis is profoundly limited by the similarity of brain tumors imaging features.

Radiological brain tumors may, in fact, present overlapping image profiles with vascular lesions, inflammatory lesions, lymphoproliferative lesions, metastasis and infectious pathologies; thus hindering images reading and demanding biopsy or surgical exeresis of the suspect tissue (Anderson et al., 2014).

In the last 30 years, the progressive improvement of techniques has allowed radiologists to visually highlight edemigenic components, peritumoral gliosis and response to experimental drugs, which has subsequently called for an updated version of the "Macdonald response criteria" (Macdonald et al., 1990) which identified four categories of response: complete response (CR), partial response (PR), stable disease (DS) and progressive disease (PD).

In 2012, the RANO Response Assessment Neuro-Oncology criteria (Gállego et al 2012) were proposed, significantly reforming the "Macdonald response criteria" with the inclusion of the increased evaluation of tumor progression, pseudoprogression (PsP) and pseudoresponse and recommendations for the evaluation of misunderstanding imaging changes.

RANO criteria and subsequent RANO modifications are explained in detail in various review articles (Ellingson et al., 2014).

There are important limits that need to be overcome in the definition of glioma, from the distinction of the tumor mass from the surrounding healthy tissue to the recognition of progression and response to treatment. The complex characteristics of the glioma make these differences difficult to be reliably detected even by an experienced radiologist with only visual evaluation, due to morphology and tissue type, which manifests itself with little differences between the MR exams. Moreover, with the administration of contrast medium, the highlighted components not always indicate true tumor activity; as yet the enhancement changes related to chemotherapy or radiotherapy are not known (Upadhyay et al., 2011).

3.4 Radiogenomic

In the past, the role of medical imaging was limited to diagnosis and staging in the oncology field. In recent years, the progression of hardware and software allowed us to identify imaging markers derived from routine clinical images that are increasingly sought after in order to obtain more information on the tumor in a non-invasive way, thus taking an increasingly important role in the clinical process in oncology.

An expert radiologist diagnoses parameters deriving from the observation of images and applies diagnostic criteria based on his study and experience, with qualitative and quantitative evaluations such as tumor size, signal in the different MR sequences.

In radiomics, information is extracted with the help of specific mathematical algorithms and subsequently reworked by specialized computer software. In this way the radiological features provide a wide range of quantified parameters and have been shown to diversify and stratify precise imaging phenotypes beyond what is visible to the naked eye (Yip et al.,2017)

Radiomics is the rapidly growing field of radiological research in which routine patient images are converted into quantitative data (Aerts et al., 2014) that can decode the tumor phenotype by improving the diagnosis and also providing indications on prognosis and response therapeutic (Tang 2018). Radiomics refers to the study in which MR scans are converted into quantitative data whereas radiogenomics is a specific application in which imaging, radiomic features are linked to genomic profiles (Rutman et al., 2009). In recent years, radiogenomics has become the link between biological parameters such as genomics, proteomics and metabolomics (Peeken et al., 2018) although this method still needs to be standardized to enter everyday use.

The quantitative characteristics extracted from radiological images and linked to specific results generate a workflow defined in the literature as a "radiomic pipeline" where imaging functions are extracted, processed and analyzed (Park at al., 2018) This workflow is structured in a precise sequence of general steps: acquisition of the image followed by reconstruction of the images to be analyzed and then the data is extracted.

After the image acquisition phase, two general approaches emerge, depending on how the radiomic features derive and in which phase artificial intelligence is applied, if at all: classical radiomics (Paul et al., 2018), with or without machine learning (Parmar et al., 2015) and the radiomics of deep learning that have already been used to predict mutation status of isocitrate dehydrogenase 1 in low-grade gliomas (Li et al., 2017).

In classical radiomics, selected hand-made imaging attempts to describe lesions through intuitive shape parameters through visible plot differences (Wang et al., 2014) is characteristic of conventional radiomics. The data selected in the image are then processed with statistical models or automatic learning, to compare them to specific results.

Radiomics based on deep learning (DLR) has been developed to obtain a considerable amount of information from radiological images, excluding manual selection providing a staging or

classification without the need for detailed delineation (Aerts 2016). The functions of radiomics based on deep learning are best exalted in the extraction from multiple modes of magnetic resonance images.
The performance of radiomics based on deep learning was tested in the study of tumors of the central nervous system with the aim of predicting the mutation status of isocitrate dehydrogenase 1 (IDH1) were validated in a data set of 151 glioma patients of low grade (Li et al. 2017).

3.5 Texture analysis

Texture analysis is a non-invasive radiomic technique, which determines the heterogeneity of macroscopic tissue comparing it to the heterogeneity of microscopic tissue, overcoming the limits of human visual perception (Soni et al., 2019).
The texture analysis is a relatively recent method of investigation, can be defined as the analysis of the texture parameters of digital images in order to extract features and properties of its texture, with the aim of increasing the information obtainable from medical images (Castellano et al., 2004),

The analysis can be conducted by using some dedicated software able to evaluate several quantitative parameters of an image, for example the skewness, the mean value of intensity of pixels and the kurtosis (Miles et al., 2013). In medical research, these parameters can be combined and analyzed in group in order to find correlation with determined variables, such as for example the type of tumor analyzed, the pattern of response to a therapy, or the molecular profile of the tumor (Miles et al., 2013).
There are three possible approaches:

• Statistical: the texture is characterized by describing the level of regularity, smoothness, or coarseness of a digital image; this is obtained by quantifying the displacement of the pixel intensity of the image by calculating statistical parameters. It is the most used method for the generalization of its results and the simplicity of the calculation.

• Structural: it is the recognition of patterns within the texture of the image, identified, for example, by the recurrence of repeated geometric structures that is repeated primitive textures (texels), which, combined give rise to the complex pattern that constitutes the image sample .

• Spectral: describe the directionality or periodicity of particular image patterns, which manifest with brighter points on the sample's Fourier spectrum.

Below is a brief description of the main parameters used in the texture analysis of Magnetic Resonance: Media, variance, skewness and kurtosis are the first four moments of a distribution and fall under the "descriptive statistics";

- Mean

Mean is the sum of the sampled values divided by the number of items in the sample

$$\bar{x} = \frac{1}{N}\sum_{i=1}^{N} x_i$$

- Variance

Variance

$$\sigma^2 = \frac{1}{N-1}\sum_{i=1}^{N}(x_i - \bar{x})^2$$

x_i represents the value of each pixel of the image (N - 1 in the denominator, since the value of $\bar{x}$ is not known, but it is estimated by the data; on the contrary we should replace N - 1 with N).

- Skewness

In theory and probability statistics, Skewness is a measure of the asymmetry of the probability distribution of a real value random variable on its average. The value of Skewness can be positive or negative or undefined. The skewness is positive when the distribution has a tail that extends towards the positive values of x, vice versa it will be negative; `is equal to zero for symmetric distributions, like the Gaussian.

$$Skw = \frac{1}{N}\sum_{i=1}^{N}\left[\frac{x_i - \bar{x}}{\sigma}\right]^3$$

Standard error Skewness $\sqrt{\frac{6}{N}}$

- Kurtosis

Kurtosis (from the Greek: κυρτός, kyrtos or kurtos, which means "curved, arched") is a measure of the "tail" of the probabilistic distribution of a random variable of real value. Similarly, to the concept of asymmetry, kurtosis describes the form of a probability distribution. Kurtosis also varies between

positive and negative values, approaching zero for normal distributions; it assumes values all the more positive the more the distribution presents a peak (leptokurtica), vice versa, if the distribution is flat (platikurtica) of a Gaussian, the kurtosis will be negative.

$$Krt = \left\{ \frac{1}{N} \sum_{i=1}^{N} \left[\frac{x_i - \bar{x}}{\sigma} \right]^4 \right\} - 3$$

Standard error Kurtosis $\sqrt{\frac{24}{N}}$

- Mode

The mode of a sample is the element that occurs most often in the collection.

- Uniformity

$$U(x) = \sum_{i=1}^{N} p^2(x_i)$$

- Entropy

$$S(x) = -\sum_{i=1}^{N} p(x_i) log_2(p(x_i))$$

These two measures represent the frequency $p(x_i)$ with which a certain value xi occurs within the histogram. The uniformity will assume a maximum value of 1 if the gray levels of the image are all the same; on the contrary, since entropy measures variability, for images with gray levels it will be equal to 0.

4 Aim of the study

The primary tumors of the central nervous system, in fact, although they are relatively rare tumors, always have a higher frequency, due to the increase in the average age of the population and a considerable improvement in the diagnosis thanks to advances in imaging. It should be remembered that the therapies found so far do not overcome the negative aspects of surgery (often very aggressive) and of chemotherapy.

The work here presented is divided into three main sections:

Our main purpose is to correlate microRNAs (extracted from gliomas samples) and the extracted MRI plot analysis features.

Secondly, in order to overcome the current diagnostic model, we aim to identify and create a radiological protocol, applicable in clinical practice, to increase prognostic and predictive information: providing information on the evolution times of the disease and on the therapeutic response of a particular tumor.

Lastly, my intention is to create a multidisciplinary circuit between neurosurgery, biology and radiology to connect scientific research from the laboratory to the clinical practice. This purpose is well represented by the sentence “from bench to bedside”, thus creating a protocol for the early diagnosis of tumor phenotypes and subsequent clinical management.

5.0 Material and Methods

According to the recent guidelines, all patients with clinical and radiological suspicion of a primary brain tumor undergo magnetic resonance imaging with and without contrast material injection for assessment of the lesion and planning of the surgical intervention.

In September 2017 we sent our project to UR&S of A.O. Brotzu to ensure the feasibility.

In October 2017, UR&S asked the Independent Ethics Committee of the A.O.U. Cagliari to assess the compliance with the Italian and European legislation. We received approval on May 30th, 2018.

The project was approved by the General Management of the A.O. Brotzu on June 26th, 2018.

5.1 Collection of samples

This research project has the purpose to include patients undergoing neurosurgical intervention of glioma's exeresis in the Neurosurgery Department of the A.O. Brotzu directed by Dr. Carlo Conti and, after a valid informed consent from the patient, samples of tumor tissue and (when possible) sample of surrounding tissue were collected.

The surgical operation was performed with the Zeiss OPMI Pentero intraoperative microscope and with the support of the Medtronic S7 Surgical Navigation System.

Once the glioma is excised, part of it is stored in a formaldehyde solution, which will be analyzed by the Pathology department of A.O. Brotzu to obtain a definite diagnosis and to set up a treatment accordingly; whereas a tumor sample and a surrounding tissue sample are extracted and immediately soak in RNAlater.™ ThermoFisher (Suhovskih et al.,2019) stored for 24 hours at + 4 ° and subsequently stored at -20 °.

All samples are made anonymous and only have one alpha numeric code.

5.2 RNA Extraction

In the Unit of Oncology and Molecular Pathology directed by Prof. Amedeo Columbano, Total RNA from surrounding and tumor samples 48 hours later were subjected to the procedure of RNA extraction by using the miRNeasy mini Kit from Qiagen according to manufacturers instructions, at the end, the RNA was eluted with RNAse-free distilled water and stored at -80°C. This procedure appears to be more advantageous than others, such as extraction with Trizol, for both the tumoral and, especially for the surrounding tissue samples, because it allows the recovery of

suitable amounts of nucleic acids, despite the small size samples (tissue volume less than 0,5 mm^3) (Trakunram et al., 2019).

5.3 Determination of the quantity of RNA

In the same Unit, RNA samples were vortexed, centrifuged and placed on ice. Using as a tool the NanoDrop 1000 spectrophotometer (Thermo Scientific) for the measurement of total RNA concentrations and purity ratios (260/280 and 260/230) was performed.

5.4 Determination of RNA Integrity

RNA integrity was assessed by RNA Integrity Number (RIN) from Agilent Bioanalyzer 2100 instrument (Agilent Technologies) in the Unit of Oncology and Molecular Pathology .

The procedures were performed according to the manufacturer's standard protocol. For the extracted samples the majority had a RIN of 3.52. Only RNA samples with a RIN equal to or greater than 2 were considered in the study. In order to evaluate whether very low RIN RNA samples could provide good indications on the expression of microRNA, we analyzed the expression of two microRNAs: miR21 and miR125b from RNA samples extracted from healthy and tumor tissues of 10 glioma patients.

In accordance with scientific data, we chose miR21 and 125b because they are the most up-regulated and down-regulated in gliomas.

The analysis was performed in Real-time PCR using specific probes and primers for each microRNA (Taq Man microRNA assay).

5.5 RNA Sequencing

Sanger sequencing was the first method to obtain an almost complete sequence of the human genome (sanger et al. 1977 and *[1]*) Sanger's sequencing is a "first generation" technology, which requires a lot of manpower and resources.

In the last decade, Sanger sequencing has been supplanted by "new generation" sequencing (NGS), which allows sequencing millions of parallel DNA fragments. NGS applications allow genome and variant sequencing, RNA sequencing, study of DNA methylation, mapping of structural rearrangements and CHiP-seq (Shendure et al., 2008) The preparation of libraries is carried out in vitro with sequences fragmented DNA adapters, these are immobilized on a surface and subsequently amplified clonally (Metzker 2010).

Illumina HiSeq3000 System up the CRS4 – Pula

5.5 Medical Image acquisition and selection of ROIs

Diagnostic images have been acquired in the Radiology department of the Brotzu Hospital in Cagliari directed by Dr. Paolo Siotto.

Every patient performed a MR scan using a 1.5 GE Signal Excite HD scanner (General Electric, Boston, USA), with a 32 channels head coil, and the following dedicated protocol that included the following sequences: a) 3D isotropic Fluid Attenuated Inversion Recovery (FLAIR) sequence (TE = 85.596 ms, TR = 8902 ms, Inversion Time = 2225 ms, flip angle 90°, slice thickness = 5 mm); b) structural pre-contrast T1-weighted (T1) sequence (TE = 10.088 ms, TR= 400 ms, flip angle = 90°, slice thickness = 5 mm); c) a post-contrast isotropic 3D T1-weighted (CE T1) sequence (TE = 5.02 ms, TR= 11.112 ms, flip angle = 20°, slice thickness = 1 mm); d) a Diffusion-Weighted Imaging (DWI) sequence (TE = 81.8 ms; TR = 6000 ms; B-values: 0 and 1000 s/mm2; acquisition matrix = 128 x 128; slice thickness = 5 mm); e) a T2-weighted (T2) sequence (TE = 98.736 ms, TR= 4860 ms, flip angle = 90°, slice thickness = 5 mm).

Horos version 3.3.5 software was used to view MR images and 3D reconstructions (https://horosproject.org). Texture analysis have been studied in the Radiology Department A.O.U Cagliari directed by Prof. Luca Saba.

The texture analysis is performed on data taken from specific regions of interest (ROI): one ROI in the tumor tissue and another one, similar in size, in a healthy tissue area.

ROI tracking is performed manually on the T1-weighted 3D isotropic post-contrast images (C.E. T1) through the LifeX 4.70 software (https://www.lifexsoft.org). Subsequently on the ROI track on the EC T1, the tracks on the T1, T2, T2 Flair and DWI sequences were selected to be analyzed with the LifeX 4.70 software. For the extraction of data from the different resonance sequences it was decided to set the software for the analysis of a reduced gray scale (256).

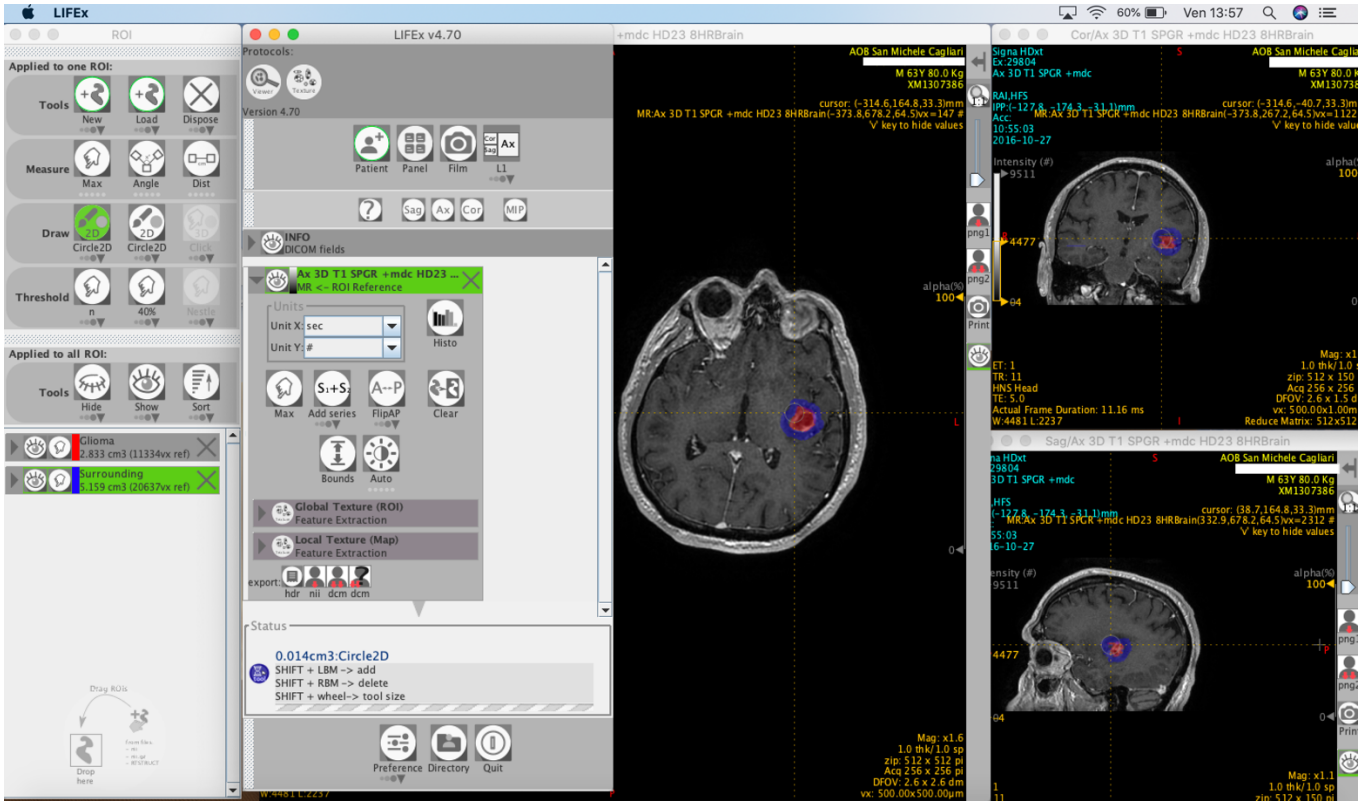

(an example of manual tracking of a ROI on C.E. T1 MR image – red= glioma, blue surrounding tissue)

6 Results

6.1 Pathological diagnosis

From July to December 2018, 13 patients were selected, including 6 females and 7 males, aged between 43 and 75, who underwent surgery due to suspicion of a primary tumor of the central nervous system.

The pathological analysis performed by Dr Cristina Manieli confirmed the diagnosis of glioma; shown below in table 2.

GENDER	AGE	DIAGNOSIS	GRADING ACCORDING TO WHO
M	69	GLIOBLASTOMA	IV
M	64	OLIGODENDROGLIOMAS	III
F	73	GLIOBLASTOMA	IV
F	49	GLIOBLASTOMA	IV
M	30	OLIGODENDROGLIOMAS	III
M	51	GLIOBLASTOMA	IV
F	58	GLIOBLASTOMA	IV
M	75	GLIOBLASTOMA	IV
M	66	GLIOBLASTOMA POST-IRRADIATION	IV
F	55	GLIOBLASTOMA	IV
F	62	GLIOBLASTOMA	IV
M	43	GLIOBLASTOMA	IV
F	67	GLIOBLASTOMA	IV

Table 2

6.2 miRNAs

Following the extraction of the miRNAs, the determination of their quantity and integrity through R.I.N., the samples were sent for deep sequencing through Illumina HiSeq3000.

The analysis led to a large number of data, table 3 shows the differentially expressed miRNAs between the glioma sample and the surrounding tissue sample; for each of them an accurate bibliographic research was made to identify their biological function; for some of them there is no description in the literature of a known biological function. The samples whose target is 0, means that they have never been described in the primitive tumor processes of the Central Nervous System.

miRNA	Targets	Status	Functional Assay	Tumor Grade	Reference	Total number miRNA surrounding sample	Total number miRNA glioma sample	mean difference
miR-122-5p_mature	SATB1	Upregulation	promotes cell proliferation, Cell cycle regulator	grade III-IV	Liu et al., 2019	2108,846154	1545,923077	562,9230769
miR-122b-5p_mature	SATB1	Upregulation	promotes cell proliferation, Cell cycle regulator	grade III-IV	Liu et al., 2019	20,61538462	24,23076923	-3,615384615

miRNA	Targets	Status	Functional Assay	Tumor Grade	Reference	Total number miRNA surrounding sample	Total number miRNA glioma sample	mean difference
miR-124-5p_mature	LAMB1	Upregulation	inhibits the growth	grade III-IV	Chen et al., 2014	22293,82051	6541,769231	15752,05128
miR-1260b_mature	GATA4	Upregulation	inhibits the migration and invasion	Grade I-II	Xu et al., 2017	106,1538462	224,3846154	-118,2307692
miR-128-1-5p_mature	mimics into LN229 and U251	Upregulation	inhibit proliferation and invasion	Grade III-IV	Lin et al., 2018	157734,2308	61122,46154	96611,76923
miR-128-2-5p_mature	mimics into LN229 and U251	Upregulation	inhibit proliferation and invasion	Grade III-IV	Lin et al., 2018	125236,6923	47826,30769	77410,38462
miR-129-5p_mature	DNMT3A	Upregulation	inhibits cell proliferation and induces cell cycle arrest	Grade III-IV	Gu et al., 2018	6710,307692	2601,153846	4109,153846
miR-1307-5p_mature	0		0	0	0	3173,461538	2019	1154,461538
miR-136-5p_mature	E2F1	Downregulation	development of chemoresistance	Grade III-IV	Chen et al., 2014	10257,30769	3992	6265,307692
miR-137-5p_mature	RASGRF1	Upregulation	inhibit proliferation	Grade III-IV	Deng et al., 2016	33088,46154	8834,384615	24254,07692
miR-139-5p_mature	Notch1	Upregulation	inhibit proliferation	grade III-IV	Li et al., 2018	5433,230769	1781,076923	3652,153846
miR-153-3p_mature	BCL2	Upregulation	increase of radiosensitivity	grade III-IV	Sun et al., 2018	12779,07692	5860,692308	6918,384615
miR-153-5p_mature	SNAI1 mRNA	Upregulation	inhibit invasion	grade III-IV	Zhao et al., 2019	12779,07692	5860,692308	6918,384615
miR-154-5p_mature	PIWIL1	Upregulation	inhibit proliferation	grade III-IV	Wang et al. 2017	1565,461538	816,0769231	749,3846154
miR-184_mature	STC2	Upregulation	retard the propagation, invasiveness and migratory ability	grade III-IV	Feng et al., 2018	161,2307692	83,46153846	77,76923077
miR-1843_mature	0	0	0	0	0	103,6153846	35,30769231	68,30769231
miR-190a-5p_mature	0	0	0	0	0	11057,23077	7055,692308	4001,538462
miR-203a-5p_mature	IFN response	upregulation	inhibited proliferation and migration	grade III-IV	Yang et al. 2017	2058,307692	785,4615385	1272,846154
miR-21-5p_mature	SPRY1 via the PTEN/PI3K/AKT	upregulation	promote proliferation and inhibit senescence and apoptosis	grade III-IV	Chai et al., 2018	247737,4615	475642,5385	-227905,0769
miR-210-5p_mature	BDNF	upregulation	inhibited the migration and invasion	grade III-IV	Liu et al., 2019	1271,923077	2521,076923	-1249,153846
miR-212-5p_mature	BRCA1	upregulation	increase of radioresistance	grade III-IV	He et al., 2018	118,8461538	39,38461538	79,46153846
miR-218-5p_mature	LHFPL3	upregulation	preventing the invasiveness	grade III-IV	Li et al., 2019	42028,5641	9504,435897	32524,12821
miR-23a-5p_mature	ATP5A1 or ATP5B	downregulation	preventing the microvascular proliferation	grade III-IV	Xu et al., 2016	9894,307692	17874,76923	-7980,461538
miR-25-5p_mature	0	0	0	0	0	13189,23077	20738,53846	-7549,307692
miR-29b-1-5p_mature	PTEN	upregulation	promotes proliferation and invasion	grade III-IV	Zhao et al., 2019	191879,5385	92615,69231	99263,84615
miR-29b-2-5p_mature	PTEN	upregulation	promotes proliferation and invasion	grade III-IV	Zhao et al., 2019	193389,3846	93498,15385	99891,23077
miR-29c-5p_mature	PTEN	upregulation	promotes proliferation and invasion	grade III-IV	Zhao et al., 2019	294511,3077	117029,9231	177481,3846
miR-323a-5p_mature	BRI3 and CDK6	upregulation	promotes proliferation and invasion	grade III-IV	Zhang et al., 2017	6662,384615	2487,923077	4174,461538
miR-326_mature	ARRB1	upregulation	inhibit proliferation	grade III-IV	Nawaz et al., 2016	289,1538462	119,9230769	169,2307692
miR-328-5p_mature	abrogated EZH2 effects	upregulation	inhibit proliferation and invasion	grade III-IV	Wang et al., 2016	753,6923077	379,0769231	374,6153846
miR-330-5p_mature	ITGA5 mRNA	upregulation	inhibit proliferation and invasion and migration	grade III-IV	Feng et al., 2017	902,6923077	298,3846154	604,3076923
miR-338-5p_mature	FOXD1	upregulation	inhibit proliferation and invasion and migration	grade III-IV	Ma et al., 2018	93175,61538	27895,30769	65280,30769

miRNA	Targets	Status	Functional Assay	Tumor Grade	Reference	Total number miRNA surrounding sample	Total number miRNA glioma sample	mean difference
miR-339-5p_mature	FOXD1-AS1 silencing	upregulation	promotes proliferation and invasion	grade III-IV	Gao et al., 2019	1813,307692	2555,538462	-742,2307692
miR-33a-5p_mature	suppression SIRT6	upregulation	promotes proliferation	grade III-IV	Chang et al., 2017	2042,307692	878,3076923	1164
miR-362-5p_mature	PAX3	upregulation	inhibit proliferation and invasion	grade III-IV	Xu et al., 2019	124	170,2307692	-46,23076923
miR-369-5p_mature	ignote	upregulation	inhibited proliferation and migration	grade III-IV	Shahar et al., 2016	2708,923077	1287,230769	1421,692308
miR-379-5p_mature	FOXP2	upregulation	preventing the microvascular proliferation	grade III-IV	He et al., 2018	15548,84615	6949,384615	8599,461538
miR-381-5p_mature	NEFL	upregulation	increase Temolozomide-resistance	grade III-IV	Wang et al., 2015	4586	1412,384615	3173,615385
miR-382-5p_mature	YBX1	downregulation	inhibited proliferation, migration, invasion	grade III-IV	Wang et al., 2019	8712,307692	4890,769231	3821,538462
miR-411-5p_mature	ECONEXIN	upregulation	promotes proliferation	grade III-IV	Deguchi et al., 2017	11505,38462	4529,230769	6976,153846
miR-495-5p_mature	MYB	upregulation	inhibit proliferation and invasion	grade III-IV	Zhang et al., 2016	376,8461538	165	211,8461538
miR-496_mature	HCG11	upregulation	promotes proliferation	grade III-IV	Chen et al., 2019	90,76923077	20,23076923	70,53846154
miR-615-5p_mature	EGFR	upregulation	inhibit proliferation and invasion and migration	grade III-IV	Ji et al., 2018	9,461538462	37	-27,53846154
miR-629-5p_mature	0	0	0	0	0	428,8461538	661,1538462	-232,3076923
miR-668-5p_mature	0	0	0	0	0	51,84615385	17,07692308	34,76923077
miR-7-5p_mature	RAF1	upregulation	inhibit proliferation	grade III-IV	Liu et al., 2014	192467,2692	41678,03846	150789,2308
miR-92b-5p_mature	Sonic Hedgehog	upregulation	promotes proliferation	grade III-IV	Uziel et al.,2009	1666,769231	3286,461538	-1619,692308
miR-96-5p_mature	PDCD4	upregulation	increase of radioresistance	grade III-IV	Guo et al., 2018	841,7692308	1195,153846	-353,3846154
miR-769-5p_mature	ignote	upregulation	inhibit proliferation	Grade I-II	Liu et al., 2013	6697	2932,692308	3764,307692
miR-874-5p_mature	0	0	0	0	0	1284,692308	394,8461538	889,8461538
miR-132-5p_mature	Gli1	upregulation	inhibited proliferation and migration	grade III-IV	Wang et al., 2018	5201,769231	1324,769231	3877
miR-491-5p_mature	TRIM28	upregulation	inhibit proliferation and invasion	grade III-IV	Qi et al., 2016	799	293,7692308	505,2307692
miR-6516-5p_mature	0	0	0	0	0	35,07692308	13,15384615	21,92307692
miR-1322_mature	0	0	0	0	0	9964,076923	4487,615385	5476,461538
miR-138-5p_mature						15080,26923	8066,153846	7014,115385
miR-582-5p_mature	Caspase 3, Caspase 9, and Bim	upregulation	inhibit proliferation and invasion	Grade III-IV	Floyd et al., 2014	539,6923077	319,3076923	220,3846154
miR-628-5p_mature	DDX59	upregulation	inhibit proliferation and invasion	Grade III-IV	Xie et al., 2019	1818,692308	786,3076923	1032,384615
miR-1287-5p_mature	EGFR	downregulation	promotes proliferation	Grade III-IV	Wolter et al., 2016	131,7692308	84,53846154	47,23076923
miR-1296-5p_mature	0	0	0	0	0	613,6923077	220,5384615	393,1538462
miR-203b-5p_mature	ATM	upregulation	inhibit proliferation	Grade III-IV	Yang et al. 2017	68,07692308	14,61538462	53,46153846
miR-487a-5p_mature	0	0	0	0	0	148,9230769	52	96,92307692
miR-504-5p_mature	FZD7	upregulation	inhibit invasion	grade III-IV	Liu et al., 2019	520,6153846	186,3076923	334,3076923
miR-584-5p_mature	ROCK1	upregulation	inhibit proliferation	grade III-IV	Xu et al., 2017	1251,538462	344,1538462	907,3846154
miR-642a-5p_mature	0	0	0	0	0	10,38461538	4,307692308	6,076923077

miRNA	Targets	Status	Functional Assay	Tumor Grade	Reference	Total number miRNA surrounding sample	Total number miRNA glioma sample	mean difference
miR-664b-5p_mature	0	0	0	0	0	44,07692308	16,61538462	27,46153846
miR-942-5p_mature	0	0	0	0	0	41,46153846	60	-18,53846154
miR-2110_mature	0	0	0	0	0	52,23076923	30,15384615	22,07692308
miR-33b-5p_mature	MYC	upregulation	promotes proliferation	grade III-IV	Wang et al. 2017	282,7692308	69,23076923	213,5384615
miR-488-5p_mature	PVT1	upregulation	inhibit proliferation	grade III-IV	Xue et al., 2018	6253,769231	3965,230769	2288,538462
miR-548av-5p_mature	0	0	0	0	0	16,92307692	27,93589744	-11,01282051
miR-552-5p_mature	0	0	0	0	0	20,38461538	10,92307692	9,461538462
miR-664a-5p_mature	0	0	0	0	0	315,4615385	205,7692308	109,6923077
miR-760_mature	FOXA1	upregulation	inhibit proliferation	grade III-IV	Li et al., 2019	72,38461538	32,07692308	40,30769231
miR-891a-5p_mature	0	0	0	0	0	98,69230769	358,4615385	-259,7692308
miR-124-3p_mature	Fra-2	upregulation	inhibit proliferation	grade III-IV	Luo et al., 2018	22283,15385	6541	15742,15385
miR-329-5p_mature	E2F1	upregulation	inhibit proliferation	grade III-IV	Xiao et al., 2013	905,0769231	393,5384615	511,5384615
miR-432-5p_mature	ZFAS1	upregulation	enhanced cisplatin sensitivity	grade III-IV	Yang et al. 2019	3072,461538	1542,153846	1530,307692
miR-889-5p_mature	0					2175,923077	632,3076923	1543,615385
miR-410-5p_mature	MET	upregulation	inhibit proliferation	grade III-IV	Chen et al., 2012	60	17,84615385	42,15384615
miR-1185-5p_mature	0					1036,307692	389,1538462	647,1538462
miR-490-5p_mature	AT-hook 2	upregulation	inhibit proliferation	grade III-IV	Zhang et al., 2019	230,2307692	83,30769231	146,9230769
miR-873-5p_mature	Bcl2	upregulation	enhanced cisplatin sensitivity	grade III-IV	Chen et al., 2015	2526,076923	792,3076923	1733,769231
miR-105-5p_mature	0	0	0	0	0	101,9230769	52,30769231	49,61538462
miR-1197_mature	0	0	0	0	0	366	90,30769231	275,6923077
miR-1243_mature	0	0	0	0	0	8,769230769	3,846153846	4,923076923
miR-1250-5p_mature	0	0	0	0	0	87,53846154	34,46153846	53,07692308
miR-1252-5p_mature	0	0	0	0	0	55,84615385	17	38,84615385
miR-1283_mature	ATF4	upregulation	inhibit proliferation	grade III-IV	Chen et al., 2019	52,53846154	15,84615385	36,69230769
miR-1286_mature	0	0	0	0	0	13,53846154	3,384615385	10,15384615
miR-208b-5p_mature	0	0	0	0	0	68,15384615	119,2307692	-51,07692308
miR-211-5p_mature	ignote	downregulation	inhibit proliferation and invasion	grade III-IV	Zhang et al., 2017	149,8461538	36,53846154	113,3076923
miR-3180-5p_mature	0	0	0	0	0	9,256410256	4,223076923	5,033333333
miR-3200-5p_mature	0	0	0	0	0	1119,692308	495,9230769	623,7692308
miR-383-5p_mature	VEGF	upregulation	inhibit proliferation and invasion	grade III-IV	Zhao et al., 2017	584,6153846	181,6923077	402,9230769
miR-433-5p_mature	CREB	upregulation	inhibit proliferation and chemosensitivity	grade III-IV	Sun et al., 2017	127,6923077	38	89,69230769
miR-4446-5p_mature	0	0	0	0	0	3,230769231	0,461538462	2,769230769

miRNA	Targets	Status	Functional Assay	Tumor Grade	Reference	Total number miRNA surrounding sample	Total number miRNA glioma sample	mean difference
miR-4677-5p_mature	0	0	0	0	0	54,15384615	72,07692308	-17,92307692
miR-4787-3p_mature	0	0	0	0	0	21,38461538	11,15384615	10,23076923
miR-4787-5p_mature	0	0	0	0	0	23,53846154	10,61538462	12,92307692
miR-516a-5p_mature	0	0	0	0	0	336	121,6923077	214,3076923
miR-520b-5p_mature	0	0	0	0	0	6,192307692	2,461538462	3,730769231
miR-539-5p_mature	DIXDC1	upregulation	inhibit proliferation and invasion	grade III-IV	Quan et al., 2017	2419,461538	762,8461538	1656,615385
miR-544a_mature	Park7	upregulation	inhibit proliferation and invasion	grade III-IV	Jin et al., 2016	238	35,53846154	202,4615385
miR-548aw_mature	0	0	0	0	0	33,76923077	9,230769231	24,53846154
miR-5584-5p_mature	0	0	0	0	0	21,53846154	5,769230769	15,76923077
miR-5586-5p_mature	0	0	0	0	0	48,61538462	17,38461538	31,23076923
miR-5699-5p_mature	0	0	0	0	0	44,69230769	27,15384615	17,53846154
miR-6511b-5p_mature	0	0	0	0	0	53,69230769	25,97435897	27,71794872
miR-655-5p_mature	0	0	0	0	0	251,7692308	106,3846154	145,3846154
miR-656-5p_mature	BMPR1A	upregulation	inhibit proliferation	grade III-IV	Guo et al., 2014	218,6923077	83	135,6923077
miR-876-5p_mature	KIF20A	upregulation	inhibit proliferation	grade III-IV	Tang et al., 2019	350,3076923	108,6153846	241,6923077
miR-888-5p_mature	0	0	0	0	0	52,46153846	181,4615385	-129
miR-892a_mature	0	0	0	0	0	20,76923077	77,61538462	-56,84615385
miR-6503-5p_mature	0	0	0	0	0	1	6,538461538	-5,538461538
miR-890_mature	0	0	0	0	0	3,461538462	13,69230769	-10,23076923
miR-891b_mature	0	0	0	0	0	26,15384615	89	-62,84615385
miR-892b_mature	0	0	0	0	0	9,230769231	39	-29,76923077
miR-548v_mature	0	0	0	0	0	52,38461538	8,230769231	44,15384615
let-7d-5p_star	MYC	downregulation	inhibit proliferation	grade III-IV	Wang et al., 2016	468,5384615	287,8461538	180,6923077
let-7e-5p_star	NRAS	downregulation	inhibit proliferation and invasion	grade III-IV	Gong et al., 2016	65,19230769	41,23076923	23,96153846
let-7g-5p_star	VSIG4	downregulation	inhibit proliferation	grade III-IV	Zhang et al., 2016	259,4615385	195,2307692	64,23076923
miR-101-5p_star	TRIM44	upregulation	inhibit proliferation	grade III-IV	Li et al., 2019	248,5384615	95,53846154	153
miR-103a-2-5p_star	MOV10, circ-DICER1, ZIC4, and Hsp90β	downregulation	inhibit proliferation and invasion	grade III-IV	He et al., 2019	12,46153846	7,538461538	4,923076923
miR-106b-5p_star	ignote	downregulation	promotes proliferation	Grade I-II	Wang et al., 2012	298,8461538	504,7692308	-205,9230769
miR-1307-5p_star	0					434,0769231	303,5384615	130,5384615
miR-136-5p_star	Bcl-2	upregulation	inhibit proliferation	grade III-IV	Liu et al., 2017	3306,923077	1776,384615	1530,538462
miR-137-5p_star	FOXK1	upregulation	inhibit proliferation	grade III-IV	Ji et al., 2018	13,23076923	4,384615385	8,846153846

miRNA	Targets	Status	Functional Assay	Tumor Grade	Reference	Total number miRNA surrounding sample	Total number miRNA glioma sample	mean difference
miR-139-5p_star	GFAP	upregulation	enhanced chemosensitivity	grade III-IV	Wang et al. 2018	737,4615385	267,1538462	470,3076923
miR-148a-5p_star	DNMT1-RUNX3	upregulation	inhibit proliferation and invasion	grade III-IV	Li et al., 2019	6,153846154	15,15384615	-9
miR-152-5p_star	lncRNA H19	downregulation	promotes proliferation	grade III-IV	Chen et al., 2018	5,230769231	11,07692308	-5,846153846
miR-153-3p_star	SNAI1 mRNA	Upregulation	inhibit invasion	grade III-IV	Zhao et al., 2019	27,76923077	11,69230769	16,07692308
miR-154-5p_star	0	0	0	0	0	80,15384615	29,84615385	50,30769231
miR-1843_star	0	0	0	0	0	106,9230769	28,76923077	78,15384615
miR-185-5p_star	ANXA2	downregulation	promotes proliferation	grade III-IV	Wu et al., 2019	36,84615385	20,38461538	16,46153846
miR-21-5p_star	SPRY1 via the PTEN/PI3K/AKT	upregulation	promote proliferation and inhibit senescence and apoptosis	grade III-IV	Chai et al., 2018	785,2307692	1906,307692	-1121,076923
miR-299-5p_star	GOLPH3/MAPK/ERK	downregulation	enhanced chemosensitivity	grade III-IV	Li et al., 2013	785,9230769	290,3076923	495,6153846
miR-29a-5p_star	PTEN	upregulation	promotes proliferation and invasion	grade III-IV	Zhao Y et al., 2019	462,9230769	319	143,9230769
miR-29b-2-5p_star	PTEN	upregulation	promotes proliferation and invasion	grade III-IV	Zhao Y et al., 2019	548,6153846	262,3076923	286,3076923
miR-29c-5p_star	PTEN	upregulation	promotes proliferation and invasion	grade III-IV	Zhao Y et al., 2019	860,1538462	396,3076923	463,8461538
miR-31-5p_star	FOXD2-AS1	upregulation	promotes proliferation	grade III-IV	Wang et al., 2019	97,53846154	40,23076923	57,30769231
miR-323a-5p_star	IGF- 1R	upregulation	inhibit proliferation	grade III-IV	Lian et al., 2014	10,46153846	2,230769231	8,230769231
miR-324-5p_star	EZH2	upregulation	inhibit proliferation and invasion	grade III-IV	Zhi et al., 2017	284,2307692	181,1538462	103,0769231
miR-330-5p_star	ITGA5	upregulation	inhibit proliferation and invasion	grade III-IV	Feng et al., 2017	555,9230769	163,2307692	392,6923077
miR-338-5p_star	FOXD1	upregulation	inhibit proliferation and invasion and migration	grade III-IV	Ma et al., 2018	126,0769231	31,30769231	94,76923077
miR-342-5p_star	E2F1	upregulation	inhibit proliferation and invasion	grade III-IV	Huang et al., 2019	410,3846154	262	148,3846154
miR-361-5p_star	SND1	upregulation	inhibit proliferation	grade III-IV	Liu et al., 2018	3402,153846	1963,615385	1438,538462
miR-376a-5p_star	ignote	downregulation	promotes proliferation	grade III-IV	Huang et al., 2017	804,3846154	327,9230769	476,4615385
miR-377-5p_star	E2F1	upregulation	inhibit proliferation and invasion	grade III-IV	Huang et al., 2019	35,30769231	15,61538462	19,69230769
miR-379-5p_star	MOV10, circ-DICER1, ZIC4, and Hsp90β	downregulation	inhibit proliferation and invasion	grade III-IV	He et al., 2019	138,3076923	75,23076923	63,07692308
miR-381-5p_star	NEFL	upregulation	increase Temolozomide-resistance	grade III-IV	Wang et al., 2015	29,15384615	11,30769231	17,84615385
miR-411-5p_star	0	0	0	0	0	61,07692308	29	32,07692308
miR-485-5p_star	PAX3	downregulation	inhibit proliferation	grade III-IV	Wang et al., 2018	233,5384615	98,84615385	134,6923077
miR-501-5p_star	NUCKS1	upregulation	promotes proliferation	Grade I-II	Giunti et al., 2019	10,46153846	16,84615385	-6,384615385
miR-505-5p_star	Wnt/β-catenin	upregulation	inhibit proliferation	grade III-IV	Zhang et al., 2018	14,46153846	24,61538462	-10,15384615
miR-542-5p_star	AKT	upregulation	inhibit invasion	grade III-IV	Cai at al., 2015	165,3846154	377,8461538	-212,4615385
miR-551b-5p_star	0	0	0	0	0	8,153846154	27,46153846	-19,30769231
miR-629-5p_star	0	0	0	0	0	5,307692308	11,84615385	-6,538461538
miR-744-5p_star	MAP2K4	upregulation	inhibit proliferation and invasion	grade III-IV	Hübner et al., 2018	43,46153846	21,88461538	21,57692308

miRNA	Targets	Status	Functional Assay	Tumor Grade	Reference	Total number miRNA surrounding sample	Total number miRNA glioma sample	mean difference
miR-92b-5p_star	PTEN;	upregulation	promotes proliferation	grade III-IV	Xu et al., 2017	81,23076923	203,6153846	-122,3846154
miR-93-5p_star	RBL2	upregulation	promotes proliferation and invasion	grade III-IV	Liu et al., 2018	52,5	81,73076923	-29,23076923
miR-95-5p_star	0	0	0	0	0	322,9230769	125,3846154	197,5384615
miR-219a-5p_star	Sal-like protein	upregulation	inhibit proliferation	grade III-IV	Jiang et al., 2017	15873,76923	6781,153846	9092,615385
miR-874-5p_star	0	0	0	0	0	191,6923077	61,92307692	129,7692308
miR-132-5p_star	Gli1	upregulation	inhibited proliferation and migration	grade III-IV	Wang et al., 2018	734	240,7692308	493,2307692
miR-376b-5p_star	ignote	downregulation	promotes proliferation	grade III-IV	Huang et al., 2017	736,0769231	411,2307692	324,8461538
miR-376c-5p_star	ignote	downregulation	promotes proliferation	grade III-IV	Huang et al., 2017	746,3076923	419,5384615	326,7692308
miR-491-5p_star	TRIM28	upregulation	inhibit proliferation and invasion	grade III-IV	Qi et al., 2016	76,84615385	24,30769231	52,53846154
miR-6516-5p_star	0	0	0	0	0	19,30769231	8,384615385	10,92307692
miR-1322_star	0	0	0	0	0	4,692307692	1,153846154	3,538461538
miR-582-5p_star	Caspase 3, Caspase 9, and Bim.	upregulation	inhibit proliferation and invasion	Grade III-IV	Floyd et al., 2014	407,0769231	154,8461538	252,2307692
miR-487b-5p_star	0	0	0	0	0	42,92307692	17,30769231	25,61538462
miR-376a-2-5p_star	ignote	downregulation	promotes proliferation	grade III-IV	Huang et al., 2017	127,4615385	84,38461538	43,07692308
miR-628-5p_star	DDX59	upregulation	inhibit proliferation and invasion	Grade III-IV	Xie et al., 2019	854,5384615	399,2307692	455,3076923
miR-1296-5p_star	0	0	0	0	0	16,46153846	4,307692308	12,15384615
miR-454-5p_star	NFATc2	upregulation	inhibit proliferation	grade III-IV	Zuo et al., 2019	29,69230769	45,46153846	-15,76923077
miR-487a-5p_star	0	0	0	0	0	87,07692308	32,53846154	54,53846154
miR-642a-5p_star	0	0	0	0	0	8,923076923	2,615384615	6,307692308
miR-664b-5p_star	AT-hook 2	upregulation	inhibit proliferation	grade III-IV	Zhang et al., 2019	9,230769231	3,384615385	5,846153846
miR-329-5p_star	0	0	0	0	0	61,69230769	25	36,69230769
miR-885-5p_star	HOXB-AS1	upregulation	promotes proliferation	grade III-IV	Chen et al., 2019	45,38461538	20,23076923	25,15384615
miR-543_star	GATA3	upregulation	promotes proliferation	grade III-IV	Guo et al., 2019	35,07692308	16,07692308	19
miR-490-5p_star	AT-hook 2	upregulation	inhibit proliferation	grade III-IV	Zhang et al., 2019	55,92307692	17,61538462	38,30769231
miR-873-5p_star	Bcl2	upregulation	enhanced cisplatin sensitivity	grade III-IV	Chen et al., 2015	100,8461538	33,15384615	67,69230769
miR-2682-5p_star	0	0	0	0	0	25,61538462	9,846153846	15,76923077
miR-3200-5p_star	0	0	0	0	0	13,69230769	7,076923077	6,615384615
miR-383-5p_star	VEGF	upregulation	inhibit proliferation and invasion	grade III-IV	Zhao et al., 2017	27,23076923	7,769230769	19,46153846
miR-433-5p_star	CREB	upregulation	inhibit proliferation and chemosensitivity	grade III-IV	Sun et al., 2017	14	1,846153846	12,15384615
miR-539-5p_star	DIXDC1	upregulation	inhibit proliferation and invasion	grade III-IV	Quan et al., 2017	45,76923077	12	33,76923077
miR-544a_star	Park7	upregulation	inhibit proliferation and invasion	grade III-IV	Jin et al., 2016	40,65384615	5,230769231	35,42307692
miR-5586-5p_star	0	0	0	0	0	12,53846154	4,769230769	7,769230769

miRNA	Targets	Status	Functional Assay	Tumor Grade	Reference	Total number miRNA surrounding sample	Total number miRNA glioma sample	mean difference
miR-5699-5p_star	0	0	0	0	0	27,07692308	14,23076923	12,84615385
miR-758-5p_star	ZBTB20	upregulation	inhibit proliferation	grade III-IV	Liu et al., 2018	102,3076923	42,84615385	59,46153846

Table 3

All the miRNAs were subsequently compared individually to verify the distribution between the glioma sample and the surrounding tissue sample through the Kolmogorov-Smirnova test, a non-parametric test that verifies the shape of the sample distributions, which allowed to select the miRNAs present in the two samples presenting a normal distribution (illustrated in table 4)

Surrounding miRNAs Kolmogorov-Smirnova				Gliomas miRNAs Kolmogorov-Smirnova			
	Statistic	df	Sig.		Statistic	df	Sig.
miR-210-5p_mature	0,142	13	0.200*	miR-210-5p_mature	0,125	13	0.200*
miR-25-5p_mature	0,147	13	0.200*	miR-25-5p_mature	0,173	13	0.200*
miR-339-5p_mature	0,167	13	0.200*	miR-339-5p_mature	0,177	13	0.200*
miR-362-5p_mature	0,177	13	0.200*	miR-362-5p_mature	0,178	13	0.200*
miR-369-5p_mature	0,177	13	0.200*	miR-369-5p_mature	0,186	13	0.200*
miR-92b-5p_mature	0,133	13	0.200*	miR-92b-5p_mature	0,167	13	0.200*
miR-132-5p_mature	0,192	13	0.200*	miR-132-5p_mature	0,16	13	0.200*
miR-2110_mature	0,158	13	0.200*	miR-2110_mature	0,181	13	0.200*
miR-664a-5p_mature	0,151	13	0.200*	miR-664a-5p_mature	0,172	13	0.200*
miR-105-5p_mature	0,153	13	0.200*	miR-105-5p_mature	0,179	13	0.200*
miR-3180-5p_mature	0,133	13	0.200*	miR-3180-5p_mature	0,174	13	0.200*
miR-4677-5p_mature	0,191	13	0.200*	miR-4677-5p_mature	0,143	13	0.200*
miR-4787-3p_mature	0,191	13	0.200*	miR-4787-3p_mature	0,145	13	0.200*
miR-4787-5p_mature	0,177	13	0.200*	miR-4787-5p_mature	0,185	13	0.200*
miR-5699-5p_mature	0,173	13	0.200*	miR-5699-5p_mature	0,173	13	0.200*
miR-655-5p_mature	0,096	13	0.200*	miR-655-5p_mature	0,188	13	0.200*
let-7e-5p_star	0,129	13	0.200*	let-7e-5p_star	0,152	13	0.200*
miR-106b-5p_star	0,16	13	0.200*	miR-106b-5p_star	0,19	13	0.200*
miR-324-5p_star	0,137	13	0.200*	miR-324-5p_star	0,189	13	0.200*
miR-361-5p_star	0,192	13	0.200*	miR-361-5p_star	0,141	13	0.200*
miR-379-5p_star	0,109	13	0.200*	miR-379-5p_star	0,145	13	0.200*
miR-411-5p_star	0,167	13	0.200*	miR-411-5p_star	0,135	13	0.200*
miR-501-5p_star	0,139	13	0.200*	miR-501-5p_star	0,124	13	0.200*
miR-505-5p_star	0,156	13	0.200*	miR-505-5p_star	0,1	13	0.200*
miR-542-5p_star	0,189	13	0.200*	miR-542-5p_star	0,136	13	0.200*
miR-92b-5p_star	0,153	13	0.200*	miR-92b-5p_star	0,174	13	0.200*
miR-5699-5p_star	0,158	13	0.200*	miR-5699-5p_star	0,159	13	0.200*

Table 4

We performed then a paired Student's T test in order to verify if the expression of miRNA were statistically different between glioma and surrounding tissue samples; results were considered statistically significant for p-value < 0.05. All the miRNA considered resulted statistically different between the two groups; in particular 10 miRNA (miR-25-5p_mature; miR-339-5p_mature; miR-362-5p_mature; miR-92b-5p_mature; miR-4677-5p_mature; miR-106b-5p_star; miR-501-5p_star; miR-505-5p_star; miR-542-5p_star; miR-92b-5p_star) resulted more expressed in glioma samples, and the other 15 (miR-25-5p_mature; miR-339-5p_mature; miR-362-5p_mature; miR-92b-5p_mature; miR-4677-5p_mature; miR-106b-5p_star; miR-501-5p_star; miR-505-5p_star; miR-542-5p_star; miR-92b-5p_star) in surrounding tissue samples (Table 5)•.

miRNA	Mean miRNA copies value		p-value
	Mean value surrounding sample	Mean value glioma sample	
miR-25-5p_mature	13189,23077	20738,53846	0,005910603
miR-339-5p_mature	1813,307692	2555,538462	0,019301026
miR-362-5p_mature	124	170,2307692	0,048399867
miR-369-5p_mature	2708,923077	1287,230769	0,048373497
miR-92b-5p_mature	1666,769231	3286,461538	0,006662824
miR-132-5p_mature	5201,769231	1324,769231	0,014935277
miR-2110_mature	52,23076923	30,15384615	0,036332154
miR-664a-5p_mature	315,4615385	205,7692308	0,026356233
miR-105-5p_mature	101,9230769	52,30769231	0,0415525
miR-3180-5p_mature	9,256410256	4,223076923	0,022890307
miR-4677-5p_mature	54,15384615	72,07692308	0,043961808
miR-4787-3p_mature	21,38461538	11,15384615	0,019578883
miR-4787-5p_mature	23,53846154	10,61538462	0,004721968
miR-5699-5p_mature	44,69230769	27,15384615	0,004826651
miR-655-5p_mature	251,7692308	106,3846154	0,006070423
let-7e-5p_star	65,19230769	41,23076923	0,047372498
miR-106b-5p_star	298,8461538	504,7692308	0,012677956
miR-324-5p_star	284,2307692	181,1538462	0,022673039
miR-361-5p_star	3402,153846	1963,615385	0,005785739
miR-379-5p_star	138,3076923	75,23076923	0,041725195
miR-411-5p_star	61,07692308	29	0,016353379
miR-501-5p_star	10,46153846	16,84615385	0,034523997
miR-505-5p_star	14,46153846	24,61538462	0,029782656
miR-542-5p_star	165,3846154	377,8461538	0,007966039
miR-92b-5p_star	81,23076923	203,6153846	0,001048841

Table 5

6.3 Texture analysis and Radiogenomics data

In this study or purpose was to identify the potential association between advanced imaging features extracted from brain MR and the mRNA expression. All the features were tested with correlation analysis tests and we considered only those that showed statistically significant correlation (positive or negative with p values < 0.001) in the tissue specimens obtained from the neoplasms and from the normal brain tissues.

One of the main advantages of the MRI is the potentiality to acquire the same tissue with different weightings in terms of physical properties of the radiofrequency (RF) signal by creating multiple different images of the same tissue, each one characterized by different phenotype determined by the variable tissue properties according to the RF and echo-waiting timing.

In this study we had assessed the multiple features (HISTO Kurtosis; HISTO Energy (or Uniformity); HISTO_Kurtosis; HISTO_Entropy _log2; FLAIR HISTO_Kurtosis; HISTO_Kurtosis and HISTO_Entropy_ log2) in different imaging weightings (C.E. T1; T2; FLAIR; DWI).

[C.E. T1] We found that some features (HISTO_Kurtosis) showed significantly strong negative correlation with the following miRNA (miR-369-5p_mature; miR-4787-3p_mature; miR-4787-5p_mature;) with the following rho values respectively, -0,6217, -0,75686, -0,67589.

[C.E. T1] HISTO_Energy (Uniformity) shows significantly strong negative correlation whit miR5699_5p_mature with the following rho values 0,644258.

[T2] Also HISTO_Kurtosis shows significantly strong negative correlation whit Mirna 411-5p_ star with the following rho values -0,65822.

[Flair] in this MR sequence the HISTO Kurtosis values detected show strong positive correlations with the two forms of miR-92 (miR-92b-5p_mature and miR-92b-5p_star) with the following rho values respectively 0,672699 and 0,67669.

[DWI] We found that some features (Entropy) showed significantly strong correlation with the following miRNA (miR-369-5p_mature, miR-132-5p_mature, miR-655-5p_mature miR-361-5p_star, miR-379-5p_star) with the following rho values respectively, 0,738630559, 0,668265048, 0,705840954, 0,623838883, 0,736459576.

[DWI] At the same time, we found that Kurtosis is significant correlated (with a negative association) with miR-369-5p_mature and miR-4787-3p_mature with the following rho values -0,622411899 and -0,649857583 respectively.

miRNA	C.E. T1 HISTO Kurtosis		C.E. T1 HISTO_Energy (=Uniformity)		T2 HISTO_Kurtosis		T2 HISTO_Entropy_log2		FLAIR HISTO_Kurtosis		DWI HISTO_Kurtosis		DWI HISTO_Entropy_log2	
	ρ_{xy}	R^2	ρ_{xy}	R^2	ρ_{xy}	R^2	ρ_{xy}	R^2	ρ_{xy}	R^2	ρ_{xy}	R^2	ρ_{xy}	R^2
miR-339-5p_mature	/	/	/	/	/	/	-0,79635	0,0927	/	/	/	/	/	/
miR-369-5p_mature	-0,6217	0,11	/	/	/	/	/	/	/	/	-0,62241	0,2069	0,738631	0,0987
miR-92b-5p_mature	/	/	/	/	/	/	/	/	0,672699	0,4579	/	/	/	/
miR-4787-3p_mature	-0,75686	0,11	/	/	/	/	/	/	/	/	-0,64986	0,0987	/	/
miR-4787-5p_mature	-0,67589	0,4568	/	/	/	/	/	/	/	/	/	/	/	/
miR-5699-5p_mature	/	/	0,644258	0,0047	/	/	/	/	/	/	/	/	/	/
miR-655-5p_mature	/	/	/	/	/	/	/	/	/	/	/	/	0,705841	0,2069
miR-361-5p_star	/	/	/	/	/	/	/	/	/	/	/	/	0,623839	0,2069
miR-379-5p_star	/	/	/	/	/	/	/	/	/	/	/	/	0,73646	0,2069
miR-411-5p_star	/	/	/	/	-0,65822	0,3428	/	/	/	/	/	/	/	/
miR-92b-5p_star	/	/	/	/	/	/	/	/	0,67669	0,4579	/	/	/	/

Table 6 (ρ_{xy} = Pearson's correlation coefficient; R^2=coefficient of determination)

(ρ_{xy} = Pearson's correlation coefficient; R^2=coefficient of determination)

- Mirna 339-5p_mature (ρ_{xy} = -0,79635; R^2 = 0,0927). strong negative correlation T2 HISTO_Entropy_log2
- Mirna 369-5p_mature (ρ_{xy} = -0,6217; R^2 = 0,11). strong negative correlation C.E. T1 HISTO Kurtosis
- Mirna 369-5p_mature (ρ_{xy} = -0,62241; R^2 = 0,2069). strong negative correlation DWI HISTO_Kurtosis
- Mirna 369-5p_mature (ρ_{xy} = 0,738631; R^2 = 0,0987). strong positive correlation DWI HISTO_Entropy_ log2
- Mirna 92-5p_mature (ρ_{xy} = 0,672699; R^2 = 0,4579). strong positive correlation FLAIR HISTO_Kurtosis
- Mirna 4787-3p_mature (ρ_{xy} = -0,75686; R^2 = 0,11). strong negative correlation C.E. T1 HISTO Kurtosis
- Mirna 4787-3p_mature (ρ_{xy} = -0,64986; R^2 = 0,0987). strong negative correlation DWI HISTO_Kurtosis
- Mirna 4787-5p_mature (ρ_{xy} = -0,67589; R^2 = 0,4568). strong negative correlation C.E. T1 HISTO Kurtosis
- Mirna 5699-5p_mature (ρ_{xy} = 0,644258; R^2 = 0,0047). strong positive correlation C.E. T1 HISTO_Energy (=Uniformity)
- Mirna 655-5p_mature (ρ_{xy} = 0,705841; R^2 = 0,2069). strong positive correlation DWI HISTO_Entropy_ log2
- Mirna 361-5p_star (ρ_{xy} = 0,623839; R^2 = 0,2069). strong positive correlation DWI HISTO_Entropy_ log2
- Mirna 379-5p_ star (ρ_{xy} = 0,73646; R^2 = 0,2069). strong positive correlation DWI HISTO_Entropy_ log2
- Mirna 411-5p_ star (ρ_{xy} = -0,65822; R^2 = 0,3428). strong negative correlation T2 HISTO_Kurtosis
- Mirna 92b-5p_star (ρ_{xy} = 0,67669; R^2 = 0,4579). strong positive correlation FLAIR HISTO_Kurtosis

The graphs for each individual miRNA in relation to the respective MR features are below.

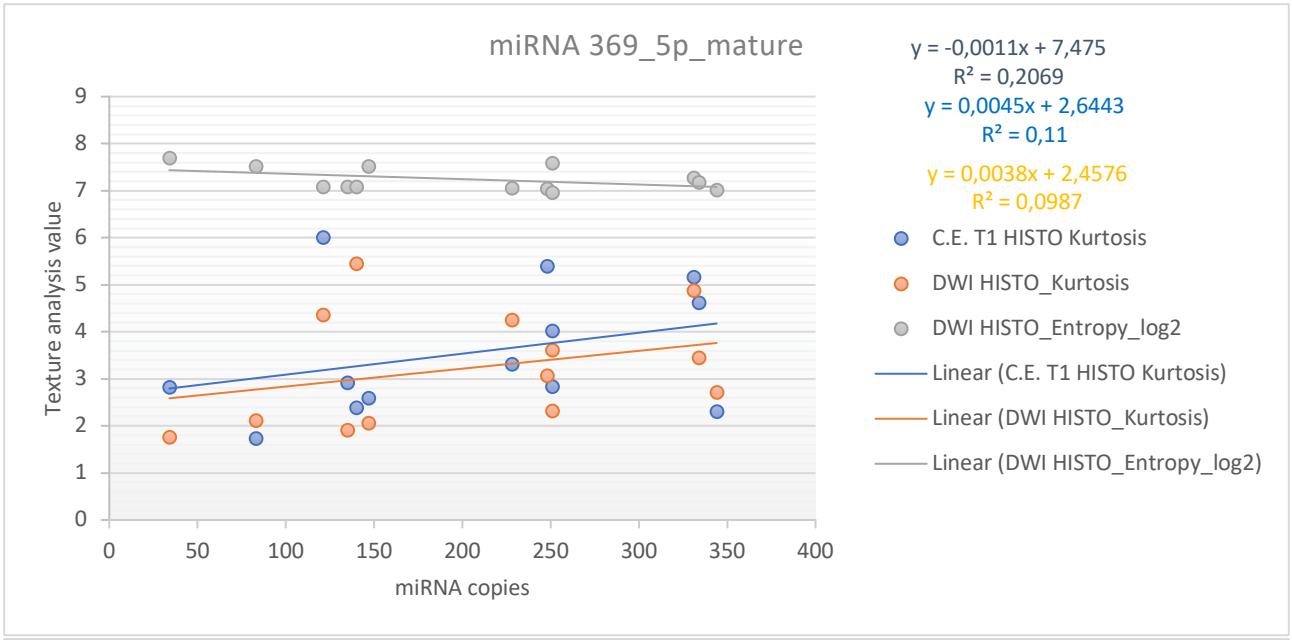

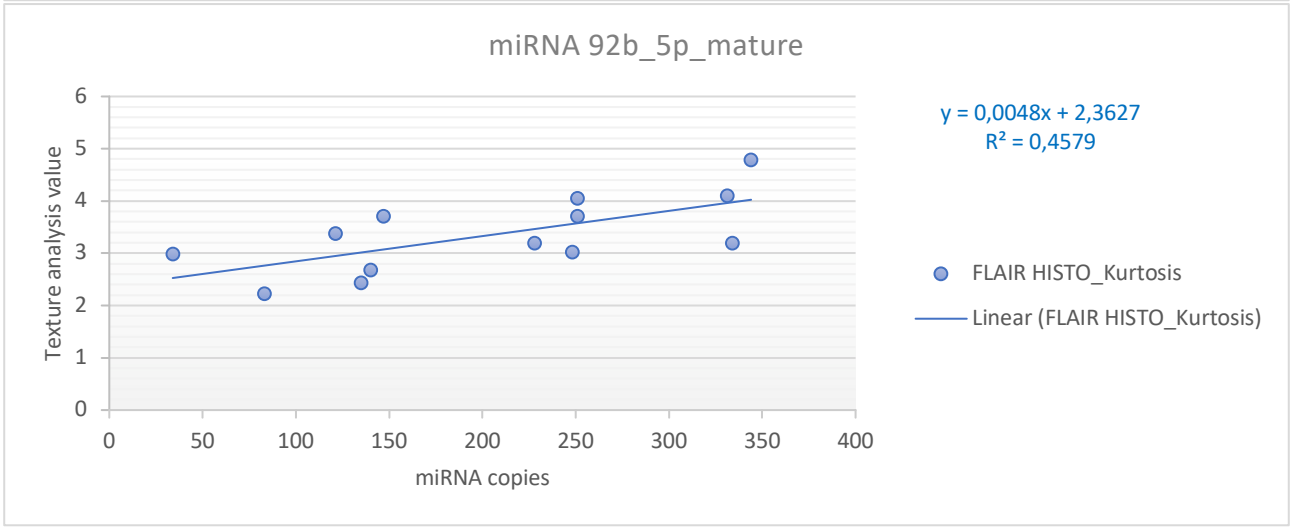

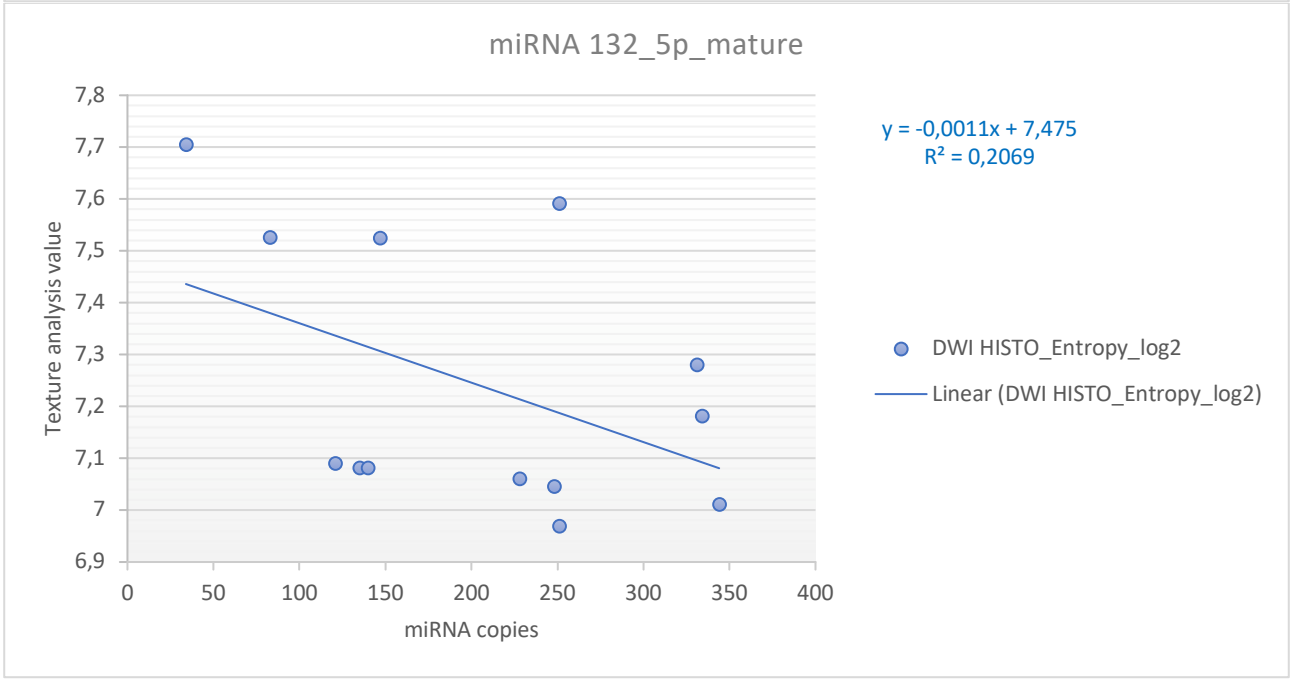

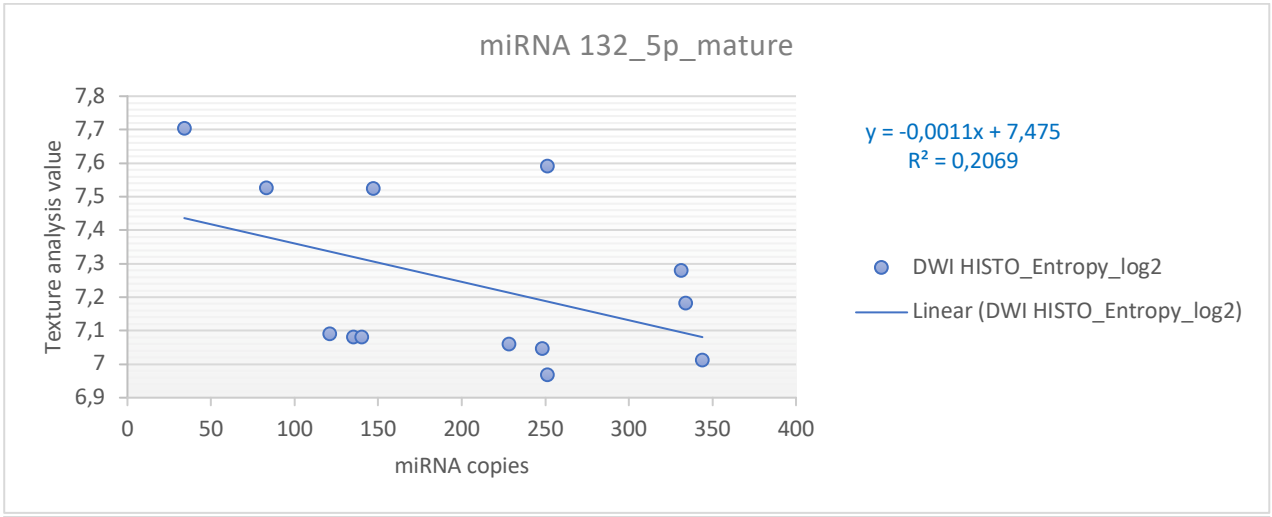
miRNA 132_5p_mature
Texture analysis value
7,8
7,7
7,6
7,5
7,4
7,3
7,2
7,1
7
6,9
0
50
100
150
200
250
300
350
400
miRNA copies
y = -0,0011x + 7,475
R² = 0,2069
DWI HISTO_Entropy_log2
Linear (DWI HISTO_Entropy_log2)

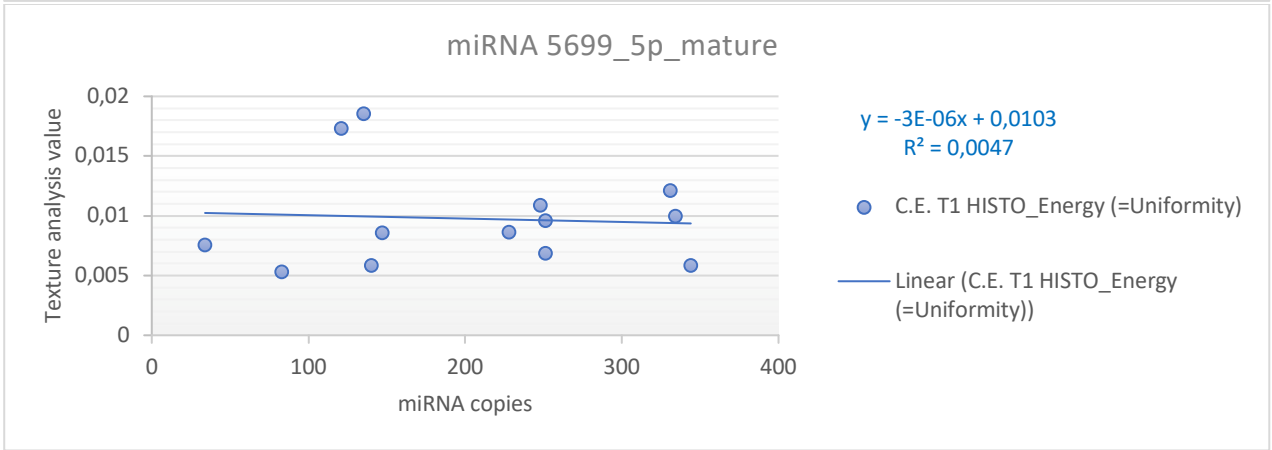
miRNA 5699_5p_mature
Texture analysis value
0,02
0,015
0,01
0,005
0
0
100
200
300
400
miRNA copies
y = -3E-06x + 0,0103
R² = 0,0047
C.E. T1 HISTO_Energy (=Uniformity)
Linear (C.E. T1 HISTO_Energy (=Uniformity))

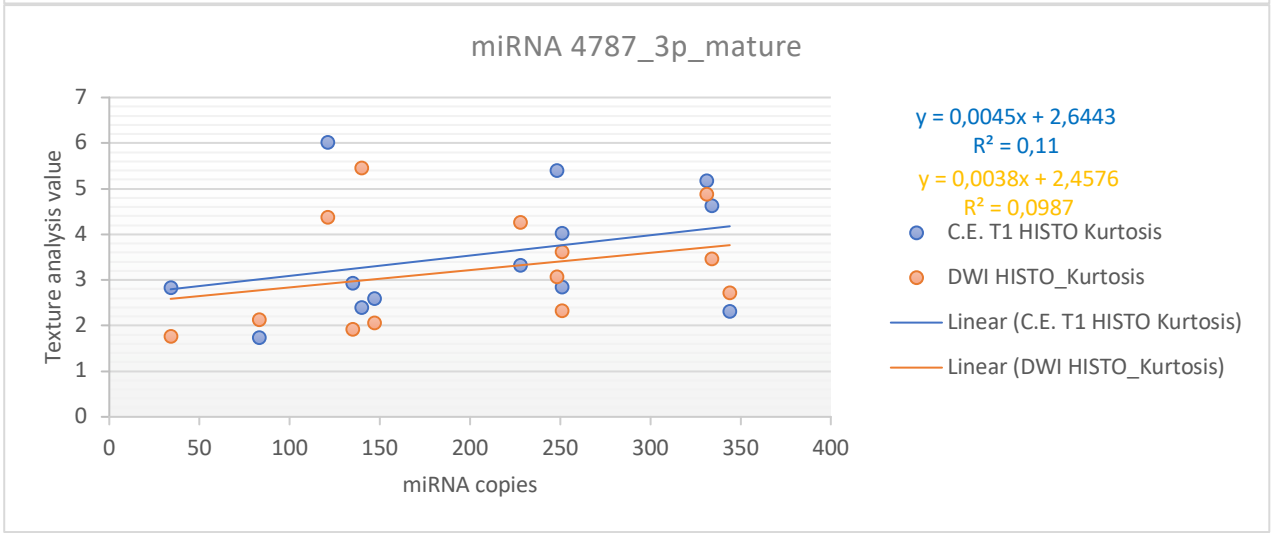
miRNA 4787_3p_mature
Texture analysis value
7
6
5
4
3
2
1
0
0
50
100
150
200
250
300
350
400
miRNA copies
y = 0,0045x + 2,6443
R² = 0,11
y = 0,0038x + 2,4576
R² = 0,0987
C.E. T1 HISTO Kurtosis
DWI HISTO_Kurtosis
Linear (C.E. T1 HISTO Kurtosis)
Linear (DWI HISTO_Kurtosis)

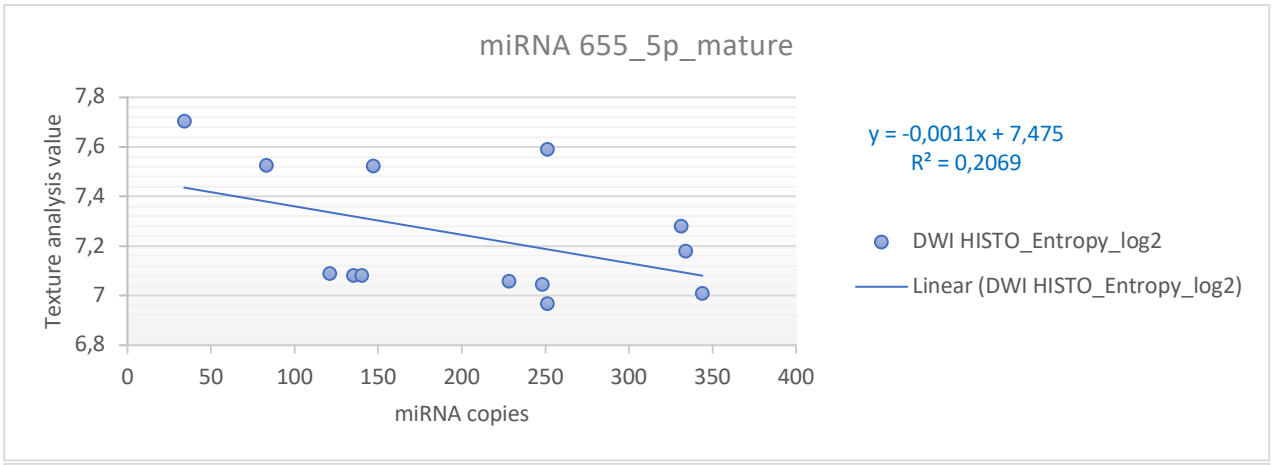
miRNA 655_5p_mature
Texture analysis value
7,8
7,6
7,4
7,2
7
6,8
0
50
100
150
200
250
300
350
400
miRNA copies
y = -0,0011x + 7,475
R² = 0,2069
DWI HISTO_Entropy_log2
Linear (DWI HISTO_Entropy_log2)

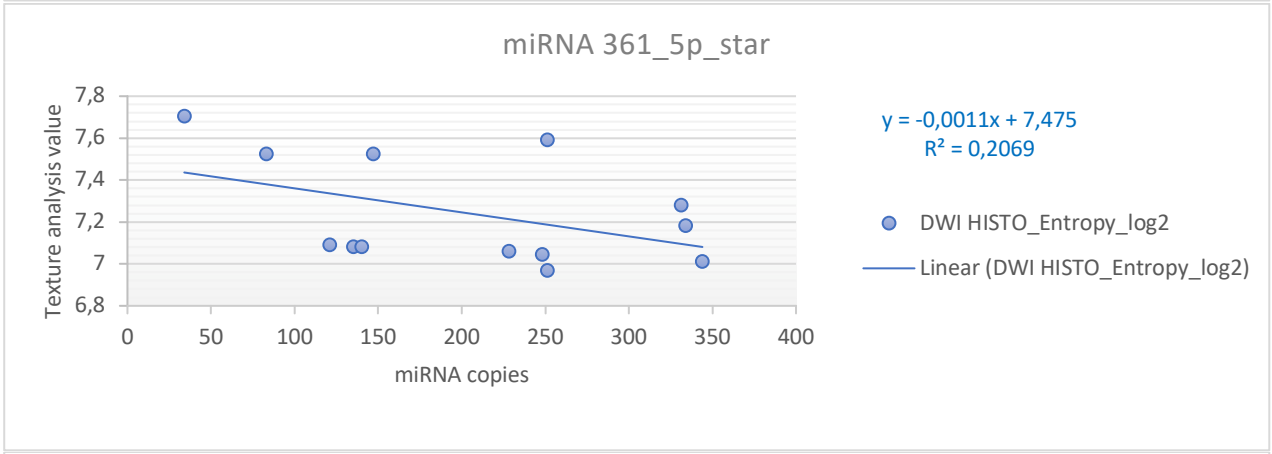
miRNA 361_5p_star
Texture analysis value
7,8
7,6
7,4
7,2
7
6,8
0
50
100
150
200
250
300
350
400
miRNA copies
y = -0,0011x + 7,475
R² = 0,2069
DWI HISTO_Entropy_log2
Linear (DWI HISTO_Entropy_log2)

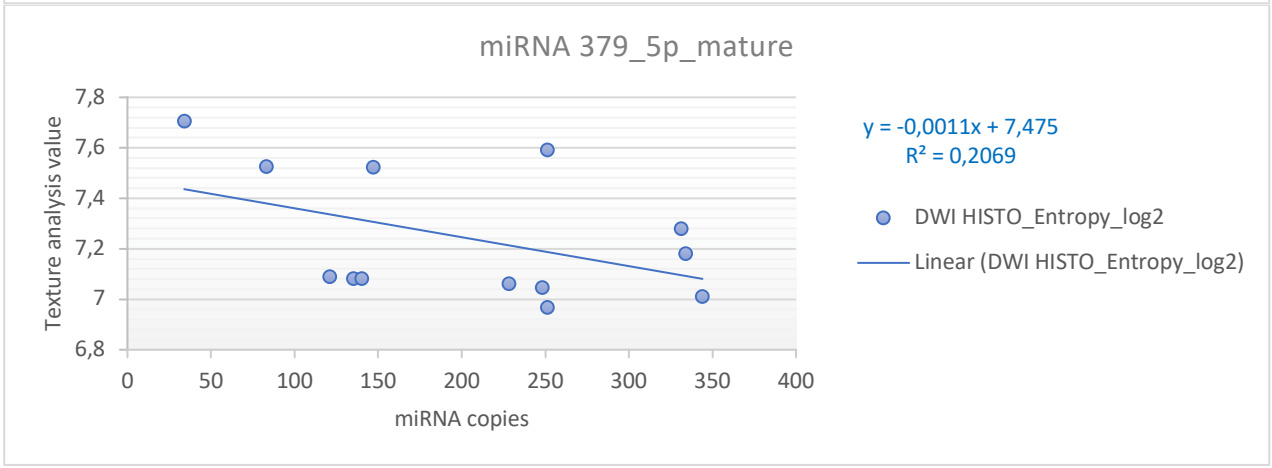
miRNA 379_5p_mature
Texture analysis value
7,8
7,6
7,4
7,2
7
6,8
0
50
100
150
200
250
300
350
400
miRNA copies
y = -0,0011x + 7,475
R² = 0,2069
DWI HISTO_Entropy_log2
Linear (DWI HISTO_Entropy_log2)

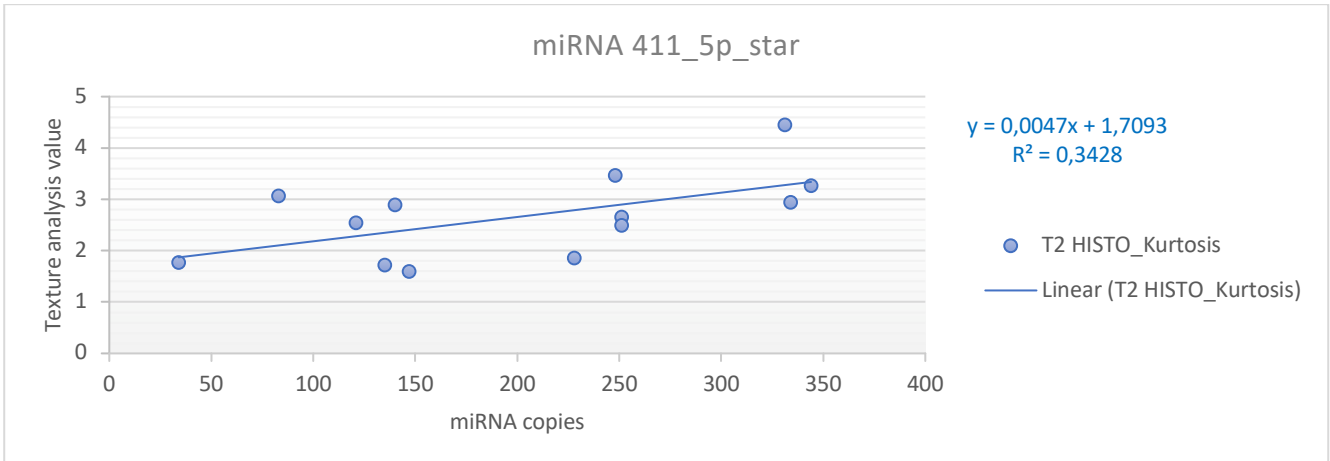
miRNA 411_5p_star
Texture analysis value
5
4
3
2
1
0
0
50
100
150
200
250
300
350
400
miRNA copies
y = 0,0047x + 1,7093
R² = 0,3428
T2 HISTO_Kurtosis
Linear (T2 HISTO_Kurtosis)

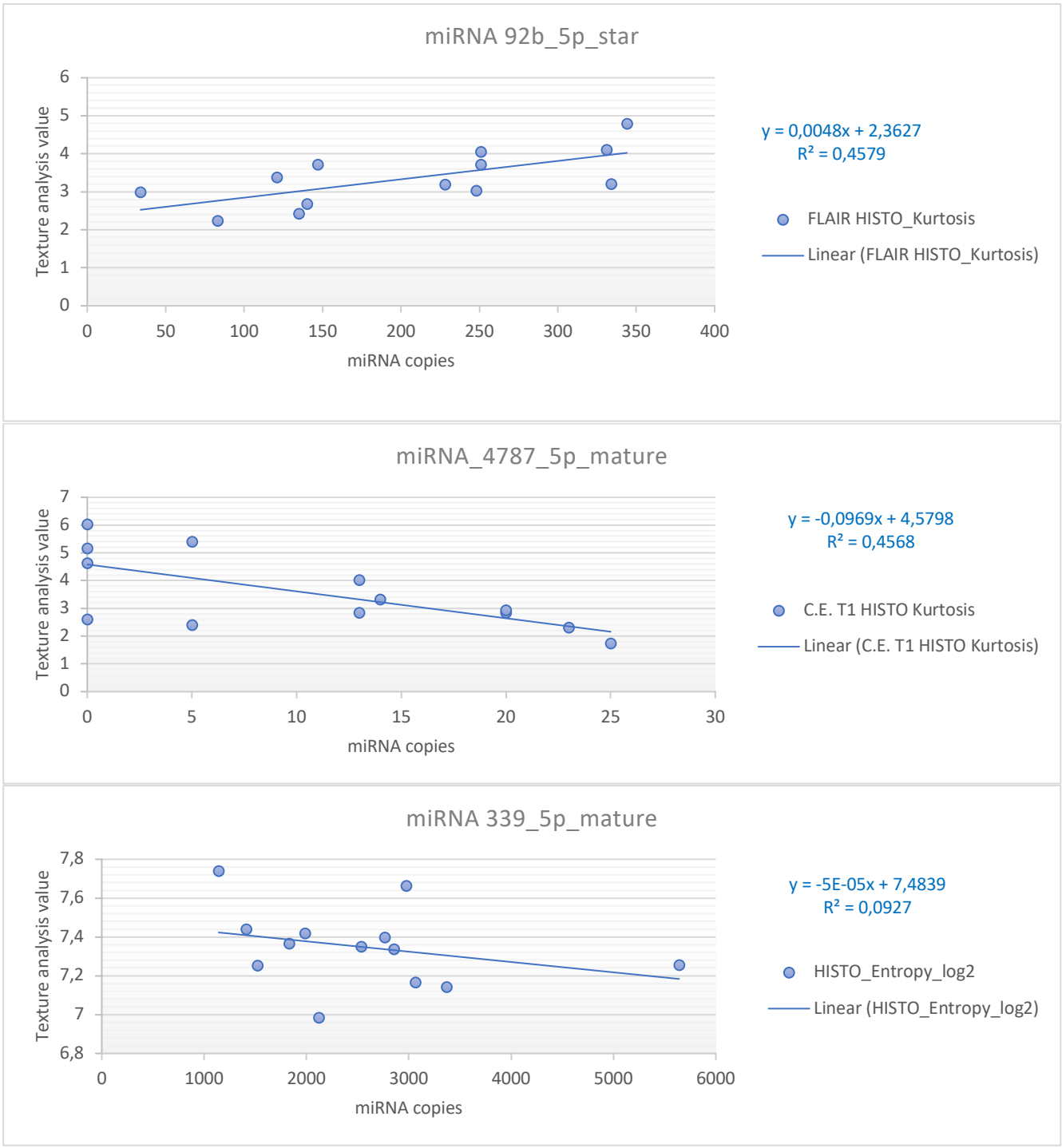

6.3 Limits of the study

The current data available for study for now are limited to a small number of patients, so further confirmation results or less will be obtained when they are included.

Only diffuse gliomas that are histologically considered to be grade III and IV according to WHO were included in the study, a post-irradiation glioma recurrence was also included.

The first selection was based on the possibility of having a glioma sample and a surrounding tissue sample. The reason is often due to surgical approach strategies that did not allow the surrounding tissue to be taken (stereotactic biopsy or needle biopsy with neuronavigator)

A further selection and relative decrease in patients depended on the low quality of RIN values (RNA Integrity number). There are multiple possible reasons why we observed low RIN index:

- once the tissue is extracted from the brain, degrading phenomena start adding up before soaking the samples in the RNA later;
- possible cell death events, likely affecting tumor tissue and its surroundings, therefore altering nucleic acids;
- the site of extraction relies on the surgical approach, thus determining different quality samples (grey matter vs white matter; tumoral cellularity vs necrotic cellularity).

6.4 Future expectation

The research project will continue with the study of each single miRNA examined, furthermore the collection of biological samples and MR images is still ongoing, with the aim of validating a study protocol of MR imaging to improve the pre diagnostic process. -operative and obtain a set to determine the presence of miRNAs with an exam already used in the standard protocols of all neurosurgical departments. Studies have already shown that through texture analysis a differential diagnosis can be made between gliomas and mestastases, differentiating them with a sensitivity of 80% and a specificity of 90% (Skogen et al. 2019).

7 Discussion

Gliomas are considered rare neoplasms, every year around 5/100000 represents however the most important share of tumors of the central nervous system followed by metastases. The glioma, in its various forms, can develop at any age. Despite the important and numerous discoveries in all areas of preclinical and clinical research, the management of primary brain tumors represents one of the most complex challenges in the neurosurgical, radiological and oncological fields. Today the therapeutic strategy of gliomas starts from the outcome of the histological and molecular examination, feeling a longer time frame than the speed with which high definition radiological images are obtained.

Surgical resection makes it possible to remove the tumor mass, immediately resolving the symptoms related to cerebral hypertension, but even in surgery we immediately identify limits: to perform a surgical operation it is necessary to make sure that it is possible to arrive at the target lesion, and that the surgical path does not affect the functional integrity of the patient, and under these conditions perform a supra-maximal surgery. These conditions rarely occur simultaneously, so the human cost of surgical treatment is very high.

With the research and the above data, we have explored the possibility of making a diagnosis not only of glioma, but of being able to identify a diagnostic marker already at the time of finding the pathology. Already some studies have already shown that through texture analysis a differential diagnosis can be made between gliomas and cases, differentiating them with a sensitivity of 80% and a specificity of 90% (Skogen et al. 2019).

The data collected in this study show a perfect dualism: analyzing the miRNA data abstracted from the glioma, comparing it with the texture analysis of the tumor mass in the main MR sequences used daily, performing the same work on surrounding tissue miRNA data with texture analysis of normal tissue of the same physical location and the same volume of the same patient have obtained a very clear result: although diffirently expressed in positive or negative the miRNAs between the surrounding sample and the glioma sample, and taking the surrounding sample as a healthy reference, we noted that in all the features in the different MR sequences there is no significantly significant correlation between the amounts of surrounding miRNAs; on the contrary, the MR features extracted from the gliomas show strong correlations with miRNAs closely related to the statistically significant increase or decrease.

For example we can note how miRNA 92, in its -star (upregulate in surrounding samples)and -mature (upregulate in glioma samples) forms, known to play in his mature form an oncogenic role in tumourigenesis, is significantly increased in glioma samples and presents a strong positive correlation in FLAIR HISTO_Kurtosis.

miRNA 92 in the literature is recognized as implicated in all phases of the pathogenesis of glioma, plays an important role on proliferation, migration, invasion and apoptosis of glioma cells (Wang et al., 2018).

If confirmed its early identification in MR, it could make it a potential molecular target for sartorial therapies.

Yet, miRNA 92 is not the only isolated miRNA. We found several miRNA's, each of them shares its own relative positive or negative correlation.

Mirna 369-5p_ has a mature and strong positive correlation with DWi HISTO_Entropy log2; Mirna5699-5p_ has a mature and strong positive correltion with contrast-enhanced HISTO_Energy (=Uniformity); Mirna 655-5p_ has a mature and strong positive correlation with DWi HISTO_Entropy_ log2; Mirna 361-5p_star has a strong positive correlation with DWi HISTO_Entropy_ log2; Mirna 379-5p_ star has a strong positive correlation DWi HISTO_Entropy_ log2. Whereas, the following miRNA's exhibit a strong negative correlation with these texture analysis features: Mirna 339-5p_mature strong negative correlation T2 HISTO_Entropy_log2; Mirna 369-5p_mature strong negative correlation C.E. T1 HISTO Kurtosis; Mirna 369-5p_mature strong negative correlation DWI HISTO_Kurtosis; Mirna 4787-3p_mature strong negative correlation C.E. T1 HISTO Kurtosis; Mirna 4787-3p_mature strong negative correlation DWI HISTO_Kurtosis; Mirna 4787-5p_mature strong negative correlation C.E. T1 HISTO Kurtosis; Mirna 411-5p_ star (ρ_{xy} = -0,65822; R^2 = 0,3428). strong negative correlation T2 HISTO_Kurtosis.

Therefore, cross-analysis of these data creates a radiologically detectable molecular trace, that might potentially become in the near future the least invasive and cheapest way to diagnose with certainty such disease and that might identify useful treatment targets.

8 Conclusion

These results confirm that the advanced extraction of data from imaging features produce biomarkers that are statistically associated with some sub-types miRNA features.

The innovation from this research is that we found not only the potential association between imaging-derived features and some class of miRNA but also that we could derive from the imaging information related to the miRNA distribution and expression, by confirm that the so-called radiomics is a promising area of intersection between morphological features and biology

This would imply that we could start considered these characteristics as advanced biomarkers for the identification from imaging of biological features (miRNA imaging-derived surrogates) that

would help the stratification of biological behavior of the tumor that is partially associated to the miRNA expression, as widely demonstrated in previously published literature

9 Ethics approval and consent to participate

In October 2017, we asked the Independent Ethics Committee of the A.O.U. Cagliari to assess the compliance with the Italian and European legistation. We received the approval on May 30th 2018. On June 26th 2018, the project was approved by the General Management of the A.O. Brotzu thus becoming operative.

10 Funding

Funds made available by the “Fondazione di Sardegna” were used to carry out this research project.

11 References

- *1*International Human Genome Sequencing Consortium. Finishing the euchromaticsequence of the human genome. Nature. 2004 Oct 21;431(7011):931-45. PubMed PMID: 15496913.
- Aerts HJ, Velazquez ER, Leijenaar RT, Parmar C, Grossmann P, Carvalho S,Bussink J, Monshouwer R, Haibe-Kains B, Rietveld D, Hoebers F, Rietbergen MM,Leemans CR, Dekker A, Quackenbush J, Gillies RJ, Lambin P. Decoding tumourphenotype by noninvasive imaging using a quantitative radiomics approach. Nat Commun. 2014 Jun 3;5:4006. doi: 10.1038/ncomms5006. Erratum in: Nat Commun.2014;5:4644. Cavalho, Sara [corrected to Carvalho, Sara]. PubMed PMID: 24892406; PubMed Central PMCID: PMC4059926.
- Aerts HJ. The Potential of Radiomic-Based Phenotyping in Precision Medicine: A Review. JAMA Oncol. 2016 Dec 1;2(12):1636-1642. doi: 10.1001/jamaoncol.2016.2631.Review. PubMed PMID: 27541161.
- Agrawal R, Pandey P, Jha P, Dwivedi V, Sarkar C, Kulshreshtha R. Hypoxic signature of microRNAs in glioblastoma: insights from small RNA deep sequencing. BMC Genomics. 2014 Aug 17;15:686. doi: 10.1186/1471-2164-15-686. PubMed PMID: 25129238; PubMed Central PMCID: PMC4148931.
- Alexander AL, Lee JE, Lazar M, Field AS. Diffusion tensor imaging of the brain.Neurotherapeutics. 2007;4(3):316–329. doi:10.1016/j.nurt.2007.05.011
- Anderson MD, Colen RR, Tremont-Lukats IW. Imaging mimics of primary malignant tumors of the central nervous system (CNS). Curr Oncol Rep. 2014;16(8):399. doi: 10.1007/s11912-014-0399-8. Review. PubMed PMID: 24927848.
- Baraniskin A, Kuhnhenn J, Schlegel U, Maghnouj A, Zöllner H, Schmiegel W, Hahn S, Schroers R. Identification of microRNAs in the cerebrospinal fluid as biomarker for the diagnosis of glioma. Neuro Oncol. 2012 Jan;14(1):29-33. doi:10.1093/neuonc/nor169. Epub 2011 Sep 21. PubMed PMID: 21937590; PubMed Central PMCID: PMC3245991.
- Bartel DP. MicroRNAs: genomics, biogenesis, mechanism, and function. Cell.2004 23;116(2):281-97. Review. PubMed PMID: 14744438.
- Bartel DP. MicroRNAs: target recognition and regulatory functions. Cell. 2009 Jan 23;136(2):215-33. doi: 10.1016/j.cell.2009.01.002. Review. PubMed PMID: 19167326; PubMed Central PMCID: PMC3794896.
- Berezikov E. Evolution of microRNA diversity and regulation in animals. Nat Rev Genet. 2011 Nov 18;12(12):846-60. doi: 10.1038/nrg3079. Review. PubMed PMID: 22094948.
- Bernstein E, Caudy AA, Hammond SM, Hannon GJ. Role for a bidentate ribonuclease in the initiation step of RNA interference. Nature. 2001 Jan 18;409(6818):363-6. PubMed PMID: 11201747.
- Bernstein E, Kim SY, Carmell MA, Murchison EP, Alcorn H, Li MZ, Mills AA, Elledge SJ, Anderson KV, Hannon GJ. Dicer is essential for mouse development. Nat Genet. 2003 Nov;35(3):215-7. Epub 2003 Oct 5. Erratum in: Nat Genet. 2003 Nov;35(3):287. PubMed PMID: 14528307.
- Bettegowda C, Agrawal N, Jiao Y, Sausen M, Wood LD, Hruban RH, Rodriguez FJ,Cahill DP, McLendon R, Riggins G, Velculescu VE, Oba-Shinjo SM, Marie SK,Vogelstein B, Bigner D, Yan H, Papadopoulos N, Kinzler KW. Mutations in CIC andFUBP1 contribute to human oligodendroglioma. Science. 2011 Sep 9;333(6048):1453-5. doi: 10.1126/science.1210557. Epub 2011 Aug 4. PubMed PMID:21817013; PubMed Central PMCID: PMC3170506.
- Bier A, Giladi N, Kronfeld N, Lee HK, Cazacu S, Finniss S, Xiang C, Poisson L, deCarvalho AC, Slavin S, Jacoby E, Yalon M, Toren A, Mikkelsen T, Brodie C. MicroRNA-137 is downregulated in glioblastoma and

inhibits the stemness of glioma stem cells by targeting RTVP-1. Oncotarget. 2013 May;4(5):665-76. PubMed PMID:23714687; PubMed Central PMCID: PMC3742828.

- Blenkiron C, Miska EA. miRNAs in cancer: approaches, aetiology, diagnostics and therapy. Hum Mol Genet. 2007 Apr 15;16 Spec No 1:R106-13. Review. PubMed PMID: 17613543.
- Cai J, Zhao J, Zhang N, Xu X, Li R, Yi Y, Fang L, Zhang L, Li M, Wu J, Zhang H. MicroRNA-542-3p Suppresses Tumor Cell Invasion via Targeting AKT Pathway in Human Astrocytoma. J Biol Chem. 2015 Oct 9;290(41):24678-88. doi: 10.1074/jbc.M115.649004. Epub 2015 Aug 18. PubMed PMID: 26286747; PubMed Central PMCID: PMC4598981.
- Castellano G, Bonilha L, Li LM, Cendes F. Texture analysis of medical images. Clin Radiol.2004 Dec;59(12):1061-9. Review. PubMed PMID: 15556588.
- Chai C, Song LJ, Han SY, Li XQ, Li M. MicroRNA-21 promotes glioma cell proliferation and inhibits senescence and apoptosis by targeting SPRY1 via the PTEN/PI3K/AKT signaling pathway. CNS Neurosci Ther. 2018 May;24(5):369-380. doi: 10.1111/cns.12785. Epub 2018 Jan 5. PubMed PMID: 29316313; PubMed Central PMCID: PMC6489721.
- Chan JA, Krichevsky AM, Kosik KS. MicroRNA-21 is an antiapoptotic factor in human glioblastoma cells. Cancer Res. 2005 Jul 15;65(14):6029-33. PubMed PMID: 16024602.
- Chang M, Qiao L, Li B, Wang J, Zhang G, Shi W, Liu Z, Gu N, Di Z, Wang X, TianY. Suppression of SIRT6 by miR-33a facilitates tumor growth of glioma throughapoptosis and oxidative stress resistance. Oncol Rep. 2017 Aug;38(2):1251-1258.doi: 10.3892/or.2017.5780. Epub 2017 Jul 3. PubMed PMID: 28677777.
- Chen CZ, Li L, Lodish HF, Bartel DP. MicroRNAs modulate hematopoietic lineage differentiation. Science. 2004 Jan 2;303(5654):83-6. Epub 2003 Dec 4. PubMed PMID: 14657504.
- Chen H, Zhang Y, Su H, Shi H, Xiong Q, Su Z. Overexpression of miR-1283 Inhibits Cell Proliferation and Invasion of Glioma Cells by Targeting ATF4. Oncol Res. 2019 Feb 21;27(3):325-334. doi: 10.3727/096504018X15251282086836. Epub 2018 May 1. PubMed PMID: 29716673.
- Chen L, Wang Y, He J, Zhang C, Chen J, Shi D. Long non-coding RNA H19 promotes proliferation and invasion in human glioma cells by downregulating miR-152. Oncol Res. 2018 Feb 8. doi: 10.3727/096504018X15178768577951. [Epub ahead of print]PubMed PMID: 29422115.
- Chen L, Zhang J, Feng Y, Li R, Sun X, Du W, Piao X, Wang H, Yang D, Sun Y, Li X, Jiang T, Kang C, Li Y, Jiang C. MiR-410 regulates MET to influence the proliferation and invasion of glioma. Int J Biochem Cell Biol. 2012 Nov;44(11):1711-7. doi: 10.1016/j.biocel.2012.06.027. Epub 2012 Jun 27. PubMed PMID: 22750473.
- Chen L, Zhang J, Han L, Zhang A, Zhang C, Zheng Y, Jiang T, Pu P, Jiang C, Kang C. Downregulation of miR-221/222 sensitizes glioma cells to temozolomide by regulating apoptosis independently of p53 status. Oncol Rep. 2012 Mar;27(3):854-60. doi: 10.3892/or.2011.1535. Epub 2011 Nov 8. PubMed PMID:22075712.
- Chen Q, Lu G, Cai Y, Li Y, Xu R, Ke Y, Zhang S. MiR-124-5p inhibits the growth of high-grade gliomas through posttranscriptional regulation of LAMB1. Neuro Oncol. 2014 May;16(5):637-51. doi: 10.1093/neuonc/not300. Epub 2014 Feb 3. PubMed PMID: 24497408; PubMed Central PMCID: PMC3984553.
- Chen W, Yang Y, Chen B, Lu P, Zhan L, Yu Q, Cao K, Li Q. MiR-136 targets E2F1 to reverse cisplatin chemosensitivity in glioma cells. J Neurooncol. 2014 Oct;120(1):43-53. doi: 10.1007/s11060-014-1535-x. Epub 2014 Aug 20. PubMed PMID: 25139024.

- Chen X, Li LQ, Qiu X, Wu H. Long non-coding RNA HOXB-AS1 promotes proliferation, migration and invasion of glioblastoma cells viaHOXB-AS1/miR-885-3p/HOXB2 axis. Neoplasma. 2019 May 23;66(3):386-396. doi:10.4149/neo_2018_180606N377. PubMed PMID: 30784279.
- Chen X, Yang F, Zhang T, Wang W, Xi W, Li Y, Zhang D, Huo Y, Zhang J, Yang A,Wang T. MiR-9 promotes tumorigenesis and angiogenesis and is activated by MYC and OCT4 in human glioma. J Exp Clin Cancer Res. 2019 Feb 22;38(1):99. doi:10.1186/s13046-019-1078-2. PubMed PMID: 30795814; PubMed Central PMCID:PMC6385476.
- Chen X, Zhang Y, Shi Y, Lian H, Tu H, Han S, Peng B, Liu W, He X. MiR-873 acts as a novel sensitizer of glioma cells to cisplatin by targeting Bcl-2. Int J Oncol. 2015 Oct;47(4):1603-11. doi: 10.3892/ijo.2015.3143. Epub 2015 Aug 31. PubMed PMID: 26323558.
- Chen Y, Bao C, Zhang X, Lin X, Huang H, Wang Z. Long non-coding RNA HCG11 modulates glioma progression through cooperating with miR-496/CPEB3 axis. Cell Prolif. 2019 Jul 16:e12615. doi: 10.1111/cpr.12615. [Epub ahead of print] PubMed PMID: 31310044.
- Ciafrè SA, Galardi S, Mangiola A, Ferracin M, Liu CG, Sabatino G, Negrini M,Maira G, Croce CM, Farace MG. Extensive modulation of a set of microRNAs in primary glioblastoma. Biochem Biophys Res Commun. 2005 Sep 9;334(4):1351-8.PubMed PMID: 16039986.
- Conti A, Aguennouz M, La Torre D, Tomasello C, Cardali S, Angileri FF, Maio F,Cama A, Germanò A, Vita G, Tomasello F. miR-21 and 221 upregulation and miR-181b downregulation in human grade II-IV astrocytic tumors. J Neurooncol. 2009 Jul;93(3):325-32. doi: 10.1007/s11060-009-9797-4. Epub 2009 Jan 22. PubMed PMID:19159078.
- Crocetti E, Trama A, Stiller C, Caldarella A, Soffietti R, Jaal J, Weber DC,Ricardi U, Slowinski J, Brandes A; RARECARE working group. Epidemiology of glial and non-glial brain tumours in Europe. Eur J Cancer. 2012 Jul;48(10):1532-42.doi: 10.1016/j.ejca.2011.12.013. Epub 2012 Jan 7. PubMed PMID: 22227039.
- Cunha PP, Costa PM, Morais CM, Lopes IR, Cardoso AM, Cardoso AL, Mano M, Jurado AS, Pedroso de Lima MC. High-throughput screening uncovers miRNAs enhancing glioblastoma cell susceptibility to tyrosine kinase inhibitors. Hum Mol Genet. 2017 Nov 15;26(22):4375-4387. doi: 10.1093/hmg/ddx323. PubMed PMID: 28973155.
- D'Urso PI, D'Urso OF, Storelli C, Mallardo M, Gianfreda CD, Montinaro A, Cimmino A, Pietro C, Marsigliante S. miR-155 is up-regulated in primary and secondary glioblastoma and promotes tumour growth by inhibiting GABA receptors.Int J Oncol. 2012 Jul;41(1):228-34. doi: 10.3892/ijo.2012.1420. Epub 2012 Mar 28.PubMed PMID: 22470130.
- Debruyne DN, Turchi L, Burel-Vandenbos F, Fareh M, Almairac F, Virolle V, Figarella-Branger D, Baeza-Kallee N, Lagadec P, Kubiniek V, Paquis P, Fontaine D,Junier MP, Chneiweiss H, Virolle T. DOCK4 promotes loss of proliferation in glioblastoma progenitor cells through nuclear beta-catenin accumulation and subsequent miR-302-367 cluster expression. Oncogene. 2018 Jan 11;37(2):241-254.doi: 10.1038/onc.2017.323. Epub 2017 Sep 18. PubMed PMID: 28925399.
- Deguchi S, Katsushima K, Hatanaka A, Shinjo K, Ohka F, Wakabayashi T, Zong H, Natsume A, Kondo Y. Oncogenic effects of evolutionarily conserved noncoding RNA ECONEXIN on gliomagenesis. Oncogene. 2017 Aug 10;36(32):4629-4640. doi:10.1038/onc.2017.88. Epub 2017 Apr 3. PubMed PMID: 28368417.

• Deng D, Xue L, Shao N, Qu H, Wang Q, Wang S, Xia X, Yang Y, Zhi F. miR-137 acts as a tumor suppressor in astrocytoma by targeting RASGRF1. Tumour Biol. 2016 Mar;37(3):3331-40. doi: 10.1007/s13277-015-4110-y. Epub 2015 Oct 6. PubMed PMID: 26440052.
• Deng D, Xue L, Shao N, Qu H, Wang Q, Wang S, Xia X, Yang Y, Zhi F. miR-137 acts as a tumor suppressor in astrocytoma by targeting RASGRF1. Tumour Biol. 2016 Mar;37(3):3331-40. doi: 10.1007/s13277-015-4110-y. Epub 2015 Oct 6. PubMed PMID:26440052.
• Denli AM, Tops BB, Plasterk RH, Ketting RF, Hannon GJ. Processing of primary microRNAs by the Microprocessor complex. Nature. 2004 Nov 11;432(7014):231-5.Epub 2004 Nov 7. PubMed PMID: 15531879.
• Dews M, Fox JL, Hultine S, Sundaram P, Wang W, Liu YY, Furth E, Enders GH, El-Deiry W, Schelter JM, Cleary MA, Thomas-Tikhonenko A. The myc-miR-17~92 axis blunts TGF{beta} signaling and production of multiple TGF{beta}-dependent antiangiogenic factors. Cancer Res. 2010 Oct 15;70(20):8233-46. doi:10.1158/0008-5472.CAN-10-2412. Epub 2010 Oct 12. PubMed PMID: 20940405; PubMed Central PMCID: PMC3007123.
• Di Bari M, Bevilacqua V, De Jaco A, Laneve P, Piovesana R, Trobiani L, Talora C, Caffarelli E, Tata AM. Mir-34a-5p Mediates Cross-Talk between M2 Muscarinic Receptors and Notch-1/EGFR Pathways in U87MG Glioblastoma Cells: Implication in Cell Proliferation. Int J Mol Sci. 2018 May 31;19(6). pii: E1631. doi:10.3390/ijms19061631. PubMed PMID: 29857516; PubMed Central PMCID: PMC6032387.
• Dimou L, Götz M. Glial cells as progenitors and stem cells: new roles in the healthy and diseased brain. Physiol Rev. 2014 Jul;94(3):709-37. doi:10.1152/physrev.00036.2013. Review. PubMed PMID: 24987003.
• Dong H, Hao X, Cui B, Guo M. MiR-429 suppresses glioblastoma multiforme by targeting SOX2. Cell Biochem Funct. 2017 Jul;35(5):260-268. doi:10.1002/cbf.3271. PubMed PMID: 28749077.
• Dontula R, Dinasarapu A, Chetty C, Pannuru P, Herbert E, Ozer H, Lakka SS. MicroRNA 203 Modulates Glioma Cell Migration via Robo1/ERK/MMP-9 Signaling. GenesCancer. 2013 Jul;4(7-8):285-96. Doi 10.1177/1947601913500141. PubMed PMID:24167656; PubMed Central PMCID: PMC3807644.
• Ellingson BM, Bendszus M, Boxerman J, et al. Consensus recommendations for a standardized Brain Tumor Imaging Protocol in clinical trials. Neuro Oncol. 2015;17(9):1188–1198. doi:10.1093/neuonc/nov095
• Ellingson BM, Wen PY, van den Bent MJ, Cloughesy TF. Pros and cons of current brain tumor imaging. Neuro Oncol. 2014 Oct;16 Suppl 7:vii2-11. doi:10.1093/neuonc/nou224. Review. PubMed PMID: 25313235; PubMed Central PMCID: PMC4195528.
• Ernst A, Campos B, Meier J, Devens F, Liesenberg F, Wolter M, Reifenberger G, Herold-Mende C, Lichter P, Radlwimmer B. De-repression of CTGF via the miR-17-92 cluster upon differentiation of human glioblastoma spheroid cultures. Oncogene.2010 Jun 10;29(23):3411-22. doi: 10.1038/onc.2010.83. Epub 2010 Mar 22. PubMed PMID: 20305691.
• Essig M, Shiroishi MS, Nguyen TB, et al. Perfusion MRI: the five most frequently asked technical questions. AJR Am J Roentgenol. 2013;200(1):24–34. doi:10.2214/AJR.12.9543
• Fan H, Yuan R, Cheng S, Xiong K, Zhu X, Zhang Y. Overexpressed miR-183 promoted glioblastoma radioresistance via down-regulating LRIG1. Biomed Pharmacother. 2018 Jan;97:1554-1563. doi: 10.1016/j.biopha.2017.11.050. Epub 2017 Nov 22. PubMed PMID: 29793318
• Fan YH, Ye MH, Wu L, Lv SG, Wu MJ, Xiao B, Liao CC, Ji QK, Chai Y, Zhu XG. Overexpression of miR-98 inhibits cell invasion in glioma cell lines via downregulation of IKKε. Eur Rev Med Pharmacol Sci. 2015 Oct;19(19):3593-604.PubMed PMID: 26502849.

• Feltbower RG, Picton S, Bridges LR, Crooks DA, Glaser AW, McKinney PA.Epidemiology of central nervous system tumors in children and young adults (0-29 years), Yorkshire, United Kingdom. Pediatr Hematol Oncol. 2004 Oct-Nov;21(7):647-60. PubMed PMID: 15626021.

• Feng L, Ma J, Ji H, Liu Y, Hu W. MiR-184 Retarded the Proliferation, Invasiveness and Migration of Glioblastoma Cells by Repressing Stanniocalcin-2. Pathol Oncol Res. 2018 Oct;24(4):853-860. doi: 10.1007/s12253-017-0298-z. Epub 2017 Sep 8. PubMed PMID: 28887636.

• Feng L, Ma J, Ji H, Liu Y, Hu W. miR-330-5p suppresses glioblastoma cell proliferation and invasiveness through targeting ITGA5. Biosci Rep. 2017 Jun 21;37(3). pii: BSR20170019. doi: 10.1042/BSR20170019. Print 2017 Jun 30. PubMed PMID: 28336765; PubMed Central PMCID: PMC5479020.

• Floyd DH, Zhang Y, Dey BK, Kefas B, Breit H, Marks K, Dutta A, Herold-Mende C,Synowitz M, Glass R, Abounader R, Purow BW. Novel anti-apoptotic microRNAs 582-5p and 363 promote human glioblastoma stem cell survival via direct inhibition of caspase 3, caspase 9, and Bim. PLoS One. 2014 May 7;9(5):e96239. doi: 10.1371/journal.pone.0096239. eCollection 2014. PubMed PMID: 24805821; PubMed Central PMCID: PMC4013090.

• Fox JL, Dews M, Minn AJ, Thomas-Tikhonenko A. Targeting of TGFβ signature and its essential component CTGF by miR-18 correlates with improved survival in glioblastoma. RNA. 2013 Feb;19(2):177-90. doi: 10.1261/rna.036467.112. Epub 2012 Dec 18. PubMed PMID: 23249750; PubMed Central PMCID: PMC3543081.

• Franceschi E, Tosoni A, Minichillo S, Depenni R, Paccapelo A, Bartolini S,Michiara M, Pavesi G, Urbini B, Crisi G, Cavallo MA, Tosatto L, Dazzi C, Biasini C, Pasini G, Balestrini D, Zanelli F, Ramponi V, Fioravanti A, Giombelli E, De Biase D, Baruzzi A, Brandes AA; PERNO Study Group. The Prognostic Roles of Gender and O6-Methylguanine-DNA Methyltransferase Methylation Status in Glioblastoma Patients: The Female Power. World Neurosurg. 2018 Apr;112:e342-e347. doi: 10.1016/j.wneu.2018.01.045. Epub 2018 Jan 11. PubMed PMID: 29337169.

• Gabriely G, Teplyuk NM, Krichevsky AM. Context effect: microRNA-10b in cancer cell proliferation, spread and death. Autophagy. 2011 Nov;7(11):1384-6. doi:10.4161/auto.7.11.17371. Epub 2011 Nov 1. PubMed PMID: 21795860.

• Gállego Pérez-Larraya J, Lahutte M, Petrirena G, Reyes-Botero G, González Aguilar A, Houillier C, Guillevin R, Sanson M, Hoang-Xuan K, Delattre JY. Response assessment in recurrent glioblastoma treated with irinotecan-bevacizumab: comparative analysis of the Macdonald, RECIST, RANO, and RECIST + F criteria. Neuro Oncol. 2012 May;14(5):667-73. doi:10.1093/neuonc/nos070. Epub 2012 Apr 4. PubMed PMID: 22492961; PubMed Central PMCID: PMC3337315.

• Gao J, Bai S, Wang Y, Zhao S, He Z, Wang R. MiR-374b targets GATA3 to promote progression and development of glioblastoma via regulating SEMA3B. Neoplasma. 2019 Jul 23;66(4):543-554. doi: 10.4149/neo_2018_180830N659. Epub 2019 Mar 7. PubMed PMID: 30868892.

• Gao YF, Liu JY, Mao XY, He ZW, Zhu T, Wang ZB, Li X, Yin JY, Zhang W, Zhou HH, Liu ZQ. LncRNA FOXD1-AS1 acts as a potential oncogenic biomarker in glioma. CNS Neurosci Ther. 2019 May 17. doi: 10.1111/cns.13152. [Epub ahead of print] PubMed PMID: 31102349.

• Gaur AB, Holbeck SL, Colburn NH, Israel MA. Downregulation of Pdcd4 by mir-21 facilitates glioblastoma proliferation in vivo. Neuro Oncol. 2011 Jun;13(6):580-90. doi: 10.1093/neuonc/nor033. PubMed PMID: 21636706; PubMed Central PMCID: PMC3107097.

- GBD 2016 Brain and Other CNS Cancer Collaborators. Global, regional, and national burden of brain and other CNS cancer, 1990-2016: a systematic analysis for the Global Burden of Disease Study 2016. Lancet Neurol. 2019 Apr;18(4):376-393. doi: 10.1016/S1474-4422(18)30468-X. Epub 2019 Feb 21. PubMed PMID: 30797715; PubMed Central PMCID: PMC6416167.
- Genovese G, Ergun A, Shukla SA, Campos B, Hanna J, Ghosh P, Quayle SN, Rai K, Colla S, Ying H, Wu CJ, Sarkar S, Xiao Y, Zhang J, Zhang H, Kwong L, Dunn K, Wiedemeyer WR, Brennan C, Zheng H, Rimm DL, Collins JJ, Chin L. microRNA regulatory network inference identifies miR-34a as a novel regulator of TGF-β signaling in glioblastoma. Cancer Discov. 2012 Aug;2(8):736-49. Epub 2012 Jun 29.PubMed PMID: 22750848; PubMed Central PMCID: PMC3911772.
- Ghosh M, Shubham S, Mandal K, Trivedi V, Chauhan R, Naseera S. Survival and prognostic factors for glioblastoma multiforme: Retrospectivesingle-institutional study. Indian J Cancer. 2017 Jan-Mar;54(1):362-367. doi:10.4103/ijc.IJC_157_17. PubMed PMID: 29199724.
- Giaume C. Astroglial Wiring is Adding Complexity to Neuroglial Networking. Front Neuroenergetics. 2010;2:129. Published 2010 Sep 20. doi:10.3389/fnene.2010.00129
- Giunti L, Da Ros M, De Gregorio V, Magi A, Landini S, Mazzinghi B, Buccoliero AM, Genitori L, Giglio S, Sardi I. A microRNA profile of pediatric glioblastoma: The role of NUCKS1 upregulation. Mol Clin Oncol. 2019 Mar;10(3):331-338. doi: 10.3892/mco.2019.1795. Epub 2019 Jan 2. PubMed PMID: 30847170; PubMed Central PMCID: PMC6388501
- Gong W, Zheng J, Liu X, Ma J, Liu Y, Xue Y. Knockdown of NEAT1 restrained the malignant progression of glioma stem cells by activating microRNA let-7e.Oncotarget. 2016 Sep 20;7(38):62208-62223. doi: 10.18632/oncotarget.11403. PubMed PMID: 27556696; PubMed Central PMCID: PMC5308721.
- Gore JC, Li M, Gao Y, Wu TL, Schilling KG, Huang Y, Mishra A, Newton AT,Rogers BP, Chen LM, Anderson AW, Ding Z. Functional MRI and resting state connectivity in white matter - a mini-review. Magn Reson Imaging. 2019 Jul 31;63:1-11. doi:10.1016/j.mri.2019.07.017. (Epub ahead of print) PubMed PMID:31376477.
- Graves P, Zeng Y. Biogenesis of mammalian microRNAs: a global view. Genomics Proteomics Bioinformatics. 2012 Oct;10(5):239-45. doi:10.1016/j.gpb.2012.06.004.Epub 2012 Sep 29. Review. PubMed PMID: 23200133; PubMed Central PMCID:PMC5054211.
- Gu JJ, Gao GZ, Zhang SM. MiR-218 inhibits the tumorgenesis and proliferation of glioma cells by targeting Robo1. Cancer Biomark. 2016;16(3):309-17. doi:10.3233/CBM-160568. PubMed PMID: 26889813.
- Gu X, Gong H, Shen L, Gu Q. MicroRNA-129-5p inhibits human glioma cell proliferation and induces cell cycle arrest by directly targeting DNMT3A. Am JTransl Res. 2018 Sep 15;10(9):2834-2847. eCollection 2018. PubMed PMID: 30323870;PubMed Central PMCID: PMC6176228.
- Gundersen V, Storm-Mathisen J, Bergersen LH. Neuroglial Transmission. Physiol Rev. 2015 Jul;95(3):695-726. doi: 10.1152/physrev.00024.2014. Review. PubMedPMID: 26084688
- Guo AC, Cummings TJ, Dash RC, Provenzale JM. Lymphomas and high-grade astrocytomas: comparison of water diffusibility and histologic characteristics. Radiology. 2002 Jul;224(1):177-83. PubMed PMID: 12091680.
- Guo M, Jiang Z, Zhang X, Lu D, Ha AD, Sun J, Du W, Wu Z, Hu L, Khadarian K, Shen J, Lin Z. miR-656 inhibits glioma tumorigenesis through repression of BMPR1A. Carcinogenesis. 2014 Aug;35(8):1698-706. doi: 10.1093/carcin/bgu030. Epub 2014 Jan 30. PubMed PMID: 24480809.

• Guo P, Yu Y, Tian Z, Lin Y, Qiu Y, Yao W, Zhang L. Upregulation of miR-96 promotes radioresistance in glioblastoma cells via targeting PDCD4. Int J Oncol. 2018 Oct;53(4):1591-1600. doi: 10.3892/ijo.2018.4498. Epub 2018 Jul 23. PubMed PMID: 30066909.
• Ha M, Kim VN. Regulation of microRNA biogenesis. Nat Rev Mol Cell Biol. 2014 Aug;15(8):509-24. doi: 10.1038/nrm3838. Epub 2014 Jul 16. Review. PubMed PMID: 25027649.
• Hao Y, Zhang S, Sun S, Zhu J, Xiao Y. MiR-595 targeting regulation of SOX7 expression promoted cell proliferation of human glioblastoma. Biomed Pharmacother. 2016 May;80:121-126. doi: 10.1016/j.biopha.2016.03.008. Epub 2016 Mar 19. PubMed PMID: 27133048.
• He L, Hannon GJ. MicroRNAs: small RNAs with a big role in gene regulation. Nat Rev Genet. 2004 Jul;5(7):522-31. Review. Erratum in: Nat Rev Genet. 2004 Aug;5(8):631. PubMed PMID: 15211354.
• He Q, Zhao L, Liu X, Zheng J, Liu Y, Liu L, Ma J, Cai H, Li Z, Xue Y. MOV10 binding circ-DICER1 regulates the angiogenesis of glioma via miR-103a-3p/miR-382-5p mediated ZIC4 expression change. J Exp Clin Cancer Res.2019 Jan 8;38(1):9. doi: 10.1186/s13046-018-0990-1. PubMed PMID: 30621721; PubMed Central PMCID: PMC6323715.
• He Q, Zhao L, Liu Y, Liu X, Zheng J, Yu H, Cai H, Ma J, Liu L, Wang P, Li Z,Xue Y. circ-SHKBP1 Regulates the Angiogenesis of U87 Glioma-Exposed Endothelial Cells through miR-544a/FOXP1 and miR-379/FOXP2 Pathways. Mol Ther Nucleic Acids. 2018 Mar 2;10:331-348. doi: 10.1016/j.omtn.2017.12.014. Epub 2017 Dec 30. PubMed PMID: 29499945; PubMed Central PMCID: PMC5862134.
• He X, Fan S. hsa-miR-212 modulates the radiosensitivity of glioma cells by targeting BRCA1. Oncol Rep. 2018 Mar;39(3):977-984. doi: 10.3892/or.2017.6156. Epub 2017 Dec 15. PubMed PMID: 29286157; PubMed Central PMCID: PMC5802039
• Hegi ME, Diserens AC, Gorlia T, Hamou MF, de Tribolet N, Weller M, Kros JM,Hainfellner JA, Mason W, Mariani L, Bromberg JE, Hau P, Mirimanoff RO, Cairncross JG, Janzer RC, Stupp R. MGMT gene silencing and benefit from temozolomide in glioblastoma. N Engl J Med. 2005 Mar 10;352(10):997-1003. PubMed PMID: 15758010.
• Horská A, Barker PB. Imaging of brain tumors: MR spectroscopy and metabolic imaging. Neuroimaging Clin N Am. 2010;20(3):293–310. doi:10.1016/j.nic.2010.04.003
• Houillier C, Wang X, Kaloshi G, Mokhtari K, Guillevin R, Laffaire J, Paris S, Boisselier B, Idbaih A, Laigle-Donadey F, Hoang-Xuan K, Sanson M, Delattre JY.IDH1 or IDH2 mutations predict longer survival and response to temozolomide in low-grade gliomas. Neurology. 2010 Oct 26;75(17):1560-6. doi: 10.1212/WNL.0b013e3181f96282. PubMed PMID: 20975057.
• Hsieh TH, Chien CL, Lee YH, Lin CI, Hsieh JY, Chao ME, Liu DJ, Chu SS, Chen W,Lin SC, Ho DM, Liu RS, Lin CH, Wong TT, Wang HW. Downregulation of SUN2, a novel tumor suppressor, mediates miR-221/222-induced malignancy in central nervous system embryonal tumors. Carcinogenesis. 2014 Oct;35(10):2164-74. doi:10.1093/carcin/bgu105. Epub 2014 May 15. PubMed PMID: 24832085.
• Huang Q, Wang C, Hou Z, Wang G, Lv J, Wang H, Yang J, Zhang Z, Zhang H. Serum microRNA-376 family as diagnostic and prognostic markers in human gliomas. Cancer Biomark. 2017;19(2):137-144. doi: 10.3233/CBM-160146. PubMed PMID: 28211798.
• Huang SW, Ali ND, Zhong L, Shi J. MicroRNAs as biomarkers for human glioblastoma: progress and potential. Acta Pharmacol Sin. 2018 Feb 8. doi: 10.1038/aps.2017.173. [Epub ahead of print] Review. PubMed PMID: 29417946.

- Huang Y, Chi C. Glioma cell proliferation is inhibited by miR-342-3p, miR-377 / E2F1 signaling pathway. Neoplasma. 2019 Jul 23;66(4):524-531. doi: 10.4149/neo_2018_180805N574. PubMed PMID: 30868897.
- Hübner M, Hinske CL, Effinger D, Wu T, Thon N, Kreth FW, Kreth S. Intronic miR-744 Inhibits Glioblastoma Migration by Functionally Antagonizing Its Host Gene MAP2K4. Cancers (Basel). 2018 Oct 25;10(11). pii: E400. doi: 10.3390/cancers10110400. PubMed PMID: 30366472; PubMed Central PMCID: PMC6266622
- Jahng GH, Li KL, Ostergaard L, Calamante F. Perfusion magnetic resonance imaging: a comprehensive update on principles and techniques. Korean J Radiol. 2014;15(5):554–577. doi:10.3348/kjr.2014.15.5.554
- Jansen M, Yip S, Louis DN. Molecular pathology in adult gliomas: diagnostic, prognostic, and predictive markers. Lancet Neurol. 2010;9(7):717–726. doi:10.1016/S1474-4422(10)70105-8
- Jenkins RB, Blair H, Ballman KV, Giannini C, Arusell RM, Law M, Flynn H, Passe S, Felten S, Brown PD, Shaw EG, Buckner JC. A t(1;19)(q10;p10) mediates the combined deletions of 1p and 19q and predicts a better prognosis of patients with oligodendroglioma. Cancer Res. 2006 Oct 15;66(20):9852-61. PubMed PMID: 17047046.
- Jeuken J, Sijben A, Alenda C, Rijntjes J, Dekkers M, Boots-Sprenger S, McLendon R, Wesseling P. Robust detection of EGFR copy number changes and EGFR variant III: technical aspects and relevance for glioma diagnostics. Brain Pathol. 2009 Oct;19(4):661-71. doi: 10.1111/j.1750-3639.2009.00320.x. PubMed PMID: 19744038; PubMed Central PMCID: PMC4332625.
- Ji Y, Sun Q, Zhang J, Hu H. MiR-615 inhibits cell proliferation, migration and invasion by targeting EGFR in human glioblastoma. Biochem Biophys Res Commun. 2018 May 15;499(3):719-726. doi: 10.1016/j.bbrc.2018.03.217. Epub 2018 Apr 3.PubMed PMID: 29605294.
- Ji ZG, Jiang HT, Zhang PS. FOXK1 promotes cell growth through activating wnt/β-catenin pathway and emerges as a novel target of miR-137 in glioma. Am J Transl Res. 2018 Jun 15;10(6):1784-1792. eCollection 2018. PubMed PMID: 30018719;PubMed Central PMCID: PMC6038085.
- Jiang B, Li M, Ji F, Nie Y. MicroRNA-219 exerts a tumor suppressive role in glioma via targeting Sal-like protein 4. Exp Ther Med. 2017 Dec;14(6):6213-6221. doi: 10.3892/etm.2017.5292. Epub 2017 Oct 12. PubMed PMID: 29285179; PubMed Central PMCID: PMC5740761.
- Jin S, Dai Y, Li C, Fang X, Han H, Wang D. MicroRNA-544 inhibits glioma proliferation, invasion and migration but induces cell apoptosis by targeting PARK7. Am J Transl Res. 2016 Apr 15;8(4):1826-37. eCollection 2016. PubMed PMID: 27186306; PubMed Central PMCID: PMC4859911.
- Karsy M, Arslan E, Moy F. Current Progress on Understanding MicroRNAs in Glioblastoma Multiforme. Genes Cancer. 2012 Jan;3(1):3-15. doi:10.1177/1947601912448068. PubMed PMID: 22893786; PubMed Central PMCID:PMC3415667.
- Kim J, Zhang Y, Skalski M, Hayes J, Kefas B, Schiff D, Purow B, Parsons S, Lawler S, Abounader R. microRNA-148a is a prognostic oncomiR that targets MIG6 and BIM to regulate EGFR and apoptosis in glioblastoma. Cancer Res. 2014 Mar 1;74(5):1541-53. doi: 10.1158/0008-5472.CAN-13-1449. Epub 2014 Jan 14. PubMed PMID: 24425048; PubMed Central PMCID: PMC3947487.
- Kim TM, Huang W, Park R, Park PJ, Johnson MD. A developmental taxonomy of glioblastoma defined and maintained by MicroRNAs. Cancer Res. 2011 May 1;71(9):3387-99. doi: 10.1158/0008-5472.CAN-10-4117. Epub 2011 Mar 8. PubMedPMID: 21385897; PubMed Central PMCID: PMC3085663.

• Kouri FM, Hurley LA, Daniel WL, Day ES, Hua Y, Hao L, Peng CY, Merkel TJ, Queisser MA, Ritner C, Zhang H, James CD, Sznajder JI, Chin L, Giljohann DA,Kessler JA, Peter ME, Mirkin CA, Stegh AH. miR-182 integrates apoptosis, growth, and differentiation programs in glioblastoma. Genes Dev. 2015 Apr 1;29(7):732-45.doi: 10.1101/gad.257394.114. PubMed PMID: 25838542; PubMed Central PMCID:PMC4387715.

• Kumar A, Nayak S, Pathak P, Purkait S, Malgulawar PB, Sharma MC, Suri V,Mukhopadhyay A, Suri A, Sarkar C. Identification of miR-379/miR-656 (C14MC)cluster downregulation and associated epigenetic and transcription regulatory mechanism in oligodendrogliomas. J Neurooncol. 2018 Aug;139(1):23-31. doi: 10.1007/s11060-018-2840-6. Epub 2018 Jun 21. PubMed PMID: 29931616; PubMedCentral PMCID: PMC6061222.

• Lagos-Quintana M, Rauhut R, Lendeckel W, Tuschl T. Identification of novel genes coding for small expressed RNAs. Science. 2001 Oct 26;294(5543):853-8.PubMed PMID: 11679670.

• Laws ER, Parney IF, Huang W, Anderson F, Morris AM, Asher A, Lillehei KO,Bernstein M, Brem H, Sloan A, Berger MS, Chang S; Glioma Outcomes Investigators. Survival following surgery and prognostic factors for recently diagnosed malignant glioma: data from the Glioma Outcomes Project. J Neurosurg. 2003 Sep;99(3):467-73. PubMed PMID: 12959431.

• Lee D, Sun S, Zhang XQ, Zhang PD, Ho AS, Kiang KM, Fung CF, Lui WM, Leung GK. MicroRNA-210 and Endoplasmic Reticulum Chaperones in the Regulation of Chemoresistance in Glioblastoma. J Cancer. 2015 Jan 16;6(3):227-32. doi:10.7150/jca.10765. eCollection 2015. PubMed PMID: 25663939; PubMed Central PMCID:PMC4317757.

• Lee H, Hwang SJ, Kim HR, Shin CH, Choi KH, Joung JG, Kim HH. Neurofibromatosis 2 (NF2) controls the invasiveness of glioblastoma through YAP-dependent expression of CYR61/CCN1 and miR-296-3p. Biochim Biophys Acta. 2016 Apr;1859(4):599-611. doi: 10.1016/j.bbagrm.2016.02.010. Epub 2016 Feb 24. PubMed PMID: 26923924.

• Lee H, Shin CH, Kim HR, Choi KH, Kim HH. MicroRNA-296-5p Promotes Invasiveness through Downregulation of Nerve Growth Factor Receptor and Caspase-8. Mol Cells. 2017 Apr;40(4):254-261. doi:10.14348/molcells.2017.2270. Epub 2016 Dec 8. PubMedPMID: 27927008; PubMed Central PMCID: PMC5424271.

• Lee RC, Ambros V. An extensive class of small RNAs in Caenorhabditis elegans. Science. 2001 Oct 26;294(5543):862-4. PubMed PMID: 11679672.

• Lee RC, Feinbaum RL, Ambros V. The C. elegans heterochronic gene lin-4 encodes small RNAs with antisense complementarity to lin-14. Cell. 1993 Dec 3;75(5):843-54. PubMed PMID: 8252621.

• Lee Y, Ahn C, Han J, Choi H, Kim J, Yim J, Lee J, Provost P, Rådmark O, Kim S,Kim VN. The nuclear RNase III Drosha initiates microRNA processing. Nature. 2003 Sep 25;425(6956):415-9. PubMed PMID: 14508493.

• Lee Y, Jeon K, Lee JT, Kim S, Kim VN. MicroRNA maturation: stepwise processing and subcellular localization. EMBO J. 2002 Sep 2;21(17):4663-70. PubMed PMID:12198168; PubMed Central PMCID: PMC126204.

• Leece R, Xu J, Ostrom QT, Chen Y, Kruchko C, Barnholtz-Sloan JS. Globalincidence of malignant brain and other central nervous system tumors by histology, 2003-2007. Neuro Oncol. 2017 Oct 19;19(11):1553-1564.

- Li J, Li Q, Lin L, Wang R, Chen L, Du W, Jiang C, Li R. Targeting the Notch1 oncogene by miR-139-5p inhibits glioma metastasis and epithelial-mesenchymal transition (EMT). BMC Neurol. 2018 Aug 31;18(1):133. doi: 10.1186/s12883-018-1139-8. PubMed PMID: 30170559; PubMed Central PMCID:PMC6117922.
- Li L, Shao MY, Zou SC, Xiao ZF, Chen ZC. MiR-101-3p inhibits EMT to attenuate proliferation and metastasis in glioblastoma by targeting TRIM44. J Neurooncol. 2019 Jan;141(1):19-30. doi: 10.1007/s11060-018-2973-7. Epub 2018 Dec 11. PubMed PMID: 30539341.
- Li L, Shao MY, Zou SC, Xiao ZF, Chen ZC. MiR-101-3p inhibits EMT to attenuate proliferation and metastasis in glioblastoma by targeting TRIM44. J Neurooncol. 2019 Jan;141(1):19-30. doi: 10.1007/s11060-018-2973-7. Epub 2018 Dec 11. PubMed PMID: 30539341.
- Li Q, Lu J, Xia J, Wen M, Wang C. Long non-coding RNA LOC730100 enhances proliferation and invasion of glioma cells through competitively sponging miR-760 from FOXA1 mRNA. Biochem Biophys Res Commun. 2019 May 7;512(3):558-563. doi:10.1016/j.bbrc.2019.03.124. Epub 2019 Mar 23. PubMed PMID: 30914197.
- Li WB, Chen HY, Zhang W, Yan W, Shi R, Li SW, Jiang T. Relationship betweenmagnetic resonance imaging features and miRNA gene expression in patients with glioblastoma multiforme. Chin Med J (Engl). 2013;126(15):2881-5. PubMed PMID:23924460.
- Li X, Liu Y, Granberg KJ, Wang Q, Moore LM, Ji P, Gumin J, Sulman EP, CalinGA, Haapasalo H, Nykter M, Shmulevich I, Fuller GN, Lang FF, Zhang W. Two mature products of MIR-491 coordinate to suppress key cancer hallmarks in glioblastoma. Oncogene. 2015 Mar 26;34(13):1619-1628. doi: 10.1038/onc.2014.98. Epub 2014 Apr 21. PubMed PMID: 24747968; PubMed Central PMCID: PMC4205227.
- Li Y, Chen F, Chu J, Wu C, Li Y, Li H, Ma H. miR-148-3p Inhibits Growth of Glioblastoma Targeting DNA Methyltransferase-1 (DNMT1). Oncol Res. 2019 Aug 8;27(8):911-921. doi: 10.3727/096504019X15516966905337. Epub 2019 Apr 8. PubMed PMID: 30982493.
- Li Z, Qian R, Zhang J, Shi X. MiR-218-5p targets LHFPL3 to regulate proliferation, migration, and epithelial-mesenchymal transitions of human glioma cells. Biosci Rep. 2019 Mar 1;39(3). pii: BSR20180879. doi: 10.1042/BSR20180879. Print 2019 Mar 29. PubMed PMID: 30314994; PubMed Central PMCID: PMC6395304.
- Li Z, Wang Y, Yu J, Guo Y, Cao W. Deep Learning based Radiomics (DLR) and its usage in noninvasive IDH1 prediction for low grade glioma. Sci Rep. 2017 Jul 14;7(1):5467. doi: 10.1038/s41598-017-05848-2. PubMed PMID: 28710497; PubMed Central PMCID: PMC5511238.
- Lian HW, Zhou Y, Jian ZH, Liu RZ. MiR-323-5p acts as a tumor suppressor by targeting the insulin-like growth factor 1 receptor in human glioma cells. Asian Pac J Cancer Prev. 2014;15(23):10181-5. PubMed PMID: 25556445.
- Lin Y, Wu Z. MicroRNA-128 inhibits proliferation and invasion of glioma cells by targeting COX-2. Gene. 2018 Jun 5;658:63-69. doi: 10.1016/j.gene.2018.03.020. Epub 2018 Mar 7. PubMed PMID: 29524580.
- Liu DK, Wei YJ, Guo Y, Wang J, Wang GH. MiRNA-93 functions as an oncogene in glioma by directly targeting RBL2. Eur Rev Med Pharmacol Sci. 2018 Apr;22(8):2343-2350. doi: 10.26355/eurrev_201804_14825. PubMed PMID: 29762838.
- Liu DK, Wei YJ, Guo Y, Wang J, Wang GH. MiRNA-93 functions as an oncogene in glioma by directly targeting RBL2. Eur Rev Med Pharmacol Sci. 2018 Apr;22(8):2343-2350. doi: 10.26355/eurrev_201804_14825. PubMed PMID:29762838.

• Liu F, Xiong Y, Zhao Y, Tao L, Zhang Z, Zhang H, Liu Y, Feng G, Li B, He L, MaJ, Qin S, Yang Y. Identification of aberrant microRNA expression pattern in pediatric gliomas by microarray. Diagn Pathol. 2013 Sep 20;8:158. doi: 10.1186/1746-1596-8-158. PubMed PMID: 24053158; PubMed Central PMCID:PMC3853583.
• Liu H, Xie X, Yang X, Li Y, Wang Y, Xu D. Enhanced inflammatory damage by microRNA-136 targeting Klotho expression in HK-2 cells by modulating JAK/STAT pathway. Pharmazie. 2017 May 1;72(5):265-271. doi: 10.1691/ph.2017.6990. PubMed PMID: 29441871.

• Liu J, Jiang J, Hui X, Wang W, Fang D, Ding L. Mir-758-5p Suppresses Glioblastoma Proliferation, Migration and Invasion by Targeting ZBTB20. Cell Physiol Biochem. 2018;48(5):2074-2083. doi: 10.1159/000492545. Epub 2018 Aug 10. PubMed PMID: 30099442.
• Liu J, Yang J, Yu L, Rao C, Wang Q, Sun C, Shi C, Hua D, Zhou X, Luo W, Wang R, Li W, Yu S. miR-361-5p inhibits glioma migration and invasion by targetingSND1. Onco Targets Ther. 2018 Aug 28;11:5239-5252. doi: 10.2147/OTT.S171539.eCollection 2018. PubMed PMID: 30214229; PubMed Central PMCID: PMC6118279.
• Liu N, Wang Z, Liu D, Xie P. HOXC13-AS-miR-122-5p-SATB1-C-Myc feedback loop promotes migration, invasion and EMT process in glioma. Onco Targets Ther. 2019 Sep 2;12:7165-7173. doi: 10.2147/OTT.S220027. eCollection 2019. PubMed PMID:31564901; PubMed Central PMCID: PMC6731462
• Liu PJ, Ye YX, Wang YX, Du JX, Pan YH, Fang XB. MiRNA-92a promotes cell proliferation and invasion through binding to KLF4 in glioma. Eur Rev Med Pharmacol Sci. 2019 Aug;23(15):6612-6620. doi: 10.26355/eurrev_201908_18550. PubMed PMID: 31378903.
• Liu Q, Guan Y, Li Z, Wang Y, Liu Y, Cui R, Wang Y. miR-504 suppresses mesenchymal phenotype of glioblastoma by directly targeting the FZD7-mediated Wnt-β-catenin pathway. J Exp Clin Cancer Res. 2019 Aug 16;38(1):358. doi: 10.1186/s13046-019-1370-1. PubMed PMID: 31419987; PubMed Central PMCID: PMC6697940.
• Liu Q, Zou R, Zhou R, Gong C, Wang Z, Cai T, Tan C, Fang J. miR-155 Regulates Glioma Cells Invasion and Chemosensitivity by p38 Isforms In Vitro. J Cell Biochem. 2015 Jul;116(7):1213-21. doi: 10.1002/jcb.25073. PubMed PMID: 25535908.
• Liu S, Jiang T, Zhong Y, Yu Y. miR-210 inhibits cell migration and invasion by targeting the brain-derived neurotrophic factor in glioblastoma. J Cell Biochem. 2019 Feb 11. doi: 10.1002/jcb.28414. [Epub ahead of print] PubMed PMID:30746749.
• Liu Y, Han L, Bai Y, Du W, Yang B. Down-regulation of MicroRNA-133 predictspoor overall survival and regulates the growth and invasive abilities in glioma. Artif Cells Nanomed Biotechnol. 2018 Feb;46(1):206-210. doi:10.1080/21691401.2017.1304551. Epub 2017 Apr 4. PubMed PMID: 28376685.
• Liu Z, Liu Y, Li L, Xu Z, Bi B, Wang Y, Li JY. MiR-7-5p is frequently downregulated in glioblastoma microvasculature and inhibits vascular endothelial cell proliferation by targeting RAF1. Tumour Biol. 2014 Oct;35(10):10177-84. doi:10.1007/s13277-014-2318-x. Epub 2014 Jul 16. PubMed PMID: 25027403.
• Lopez-Bertoni H, Lal B, Michelson N, Guerrero-Cázares H, Quiñones-Hinojosa A, Li Y, Laterra J. Epigenetic modulation of a miR-296-5p:HMGA1 axis regulates Sox2 expression and glioblastoma stem cells. Oncogene. 2016 Sep 15;35(37):4903-13.doi: 10.1038/onc.2016.22. Epub 2016 Feb 22. PubMed PMID: 26898758; PubMed Central PMCID: PMC6151872.
• Louis DN, Ohgaki H, Wiestler OD, Cavenee WK, Burger PC, Jouvet A, Scheithauer BW, Kleihues P. The 2007 WHO classification of tumours of the central nervous system. Acta Neuropathol. 2007 Aug;114(2):97-109.

Epub 2007 Jul 6. Review. Erratum in: Acta Neuropathol. 2007 Nov;114(5):547. PubMed PMID: 17618441; PubMed Central PMCID: PMC1929165.

- Louis DN, Perry A, Reifenberger G, von Deimling A, Figarella-Branger D, Cavenee WK, Ohgaki H, Wiestler OD, Kleihues P, Ellison DW. The 2016 World Health Organization Classification of Tumors of the Central Nervous System: a summary.
- Luo L, Chi H, Ling J. MiR-124-3p suppresses glioma aggressiveness via targeting of Fra-2. Pathol Res Pract. 2018 Nov;214(11):1825-1834. doi: 10.1016/j.prp.2018.09.017. Epub 2018 Sep 15. PubMed PMID: 30243808.
- Lv QL, Zhu HT, Li HM, Cheng XH, Zhou HH, Chen SH. Down-regulation of miRNA-320c promotes tumor growth and metastasis and predicts poor prognosis in human glioma. Brain Res Bull. 2018 May;139:125-132. doi:10.1016/j.brainresbull.2018.02.009. Epub 2018 Feb 10. PubMed PMID: 29438779.
- Lv S, Sun B, Dai C, Shi R, Zhou X, Lv W, Zhong X, Wang R, Ma W. The Downregulation of MicroRNA-146a Modulates TGF-β Signaling Pathways Activity in Glioblastoma. Mol Neurobiol. 2015 Dec;52(3):1257-1262. doi:10.1007/s12035-014-8938-8. Epub 2014 Oct 19. Retraction in: Mol Neurobiol. 2017 Apr;54(3):2379. PubMed PMID: 25326894.
- Ma L, Weinberg RA. Micromanagers of malignancy: role of microRNAs in regulating metastasis. Trends Genet. 2008 Sep;24(9):448-56. doi:10.1016/j.tig.2008.06.004. Epub 2008 Jul 31. Review. PubMed PMID:18674843.
- Ma XL, Shang F, Ni W, Zhu J, Luo B, Zhang YQ. MicroRNA-338-5p plays a tumor suppressor role in glioma through inhibition of the MAPK-signaling pathway by binding to FOXD1. J Cancer Res Clin Oncol. 2018 Dec;144(12):2351-2366. doi:10.1007/s00432-018-2745-y. Epub 2018 Sep 17. PubMed PMID: 30225541.
- Macdonald DR, Cascino TL, Schold SC Jr, Cairncross JG. Response criteria for phase II studies of supratentorial malignant glioma. J Clin Oncol. 1990 Jul;8(7):1277-80. PubMed PMID: 2358840.
- Mei J, Bachoo R, Zhang CL. MicroRNA-146a inhibits glioma development by targeting Notch1. Mol Cell Biol. 2011 Sep;31(17):3584-92. doi:10.1128/MCB.05821-11. Epub 2011 Jul 5. PubMed PMID: 21730286; PubMed Central PMCID: PMC3165557.
- Meng W, Jiang L, Lu L, Hu H, Yu H, Ding D, Xiao K, Zheng W, Guo H, Ma W. Anti-miR-155 oligonucleotide enhances chemosensitivity of U251 cell to taxol by inducing apoptosis. Cell Biol Int. 2012 Jul;36(7):653-9. doi:10.1042/CBI20100918. PubMed PMID: 22276743.
- Metzker ML. Sequencing technologies - the next generation. Nat Rev Genet. 2010 Jan;11(1):31-46. doi: 10.1038/nrg2626. Epub 2009 Dec 8. Review. PubMed PMID:19997069.
- Miele E, Buttarelli FR, Arcella A, Begalli F, Garg N, Silvano M, Po A, Baldi C, Carissimo G, Antonelli M, Spinelli GP, Capalbo C, Donofrio V, Morra I, Nozza P, Gulino A, Giangaspero F, Ferretti E. High-throughput microRNA profiling of pediatric high-grade gliomas. Neuro Oncol. 2014 Jan;16(2):228-40. doi: 10.1093/neuonc/not215. Epub 2013 Dec 4. PubMed PMID: 24305714; PubMed Central PMCID: PMC3895388.
- Miles KA, Ganeshan B, Hayball MP. CT texture analysis using the filtration histogram method: what do the measurements mean?. Cancer Imaging. 2013;13(3):400–406. Published 2013 Sep 23. doi:10.1102/1470-7330.2013.9045
- Mo X, Cao Q, Liang H, Liu J, Li H, Liu F. MicroRNA-610 suppresses the proliferation of human glioblastoma cells by repressing CCND2 and AKT3. Mol Med Rep. 2016 Mar;13(3):1961-6. doi: 10.3892/mmr.2016.4760. Epub 2016 Jan 12. PubMed PMID: 26782072; PubMed Central PMCID: PMC4768983.

• Nan Y, Guo H, Guo L, Wang L, Ren B, Yu K, Huang Q, Zhong Y. MiRNA-451 Inhibits Glioma Cell Proliferation and Invasion Through the mTOR/HIF-1α/VEGF Signaling Pathway by Targeting CAB39. Hum Gene Ther Clin Dev. 2018 Sep;29(3):156-166. doi: 10.1089/humc.2018.133. PubMed PMID: 30180756.
• Natukka T, Raitanen J, Haapasalo H, Auvinen A. Incidence trends of adult malignant brain tumors in Finland, 1990-2016. Acta Oncol. 2019
• Nawaz Z, Patil V, Paul Y, Hegde AS, Arivazhagan A, Santosh V, Somasundaram K. PI3 kinase pathway regulated miRNome in glioblastoma: identification of miR-326 as a tumour suppressor miRNA. Mol Cancer. 2016 Nov 21;15(1):74. PubMed PMID:27871300; PubMed Central PMCID: PMC5117574.
• Ning X, Shi Z, Liu X, Zhang A, Han L, Jiang K, Kang C, Zhang Q. DNMT1 and EZH2 mediated methylation silences the microRNA-200b/a/429 gene and promotes tumor progression. Cancer Lett. 2015 Apr 10;359(2):198-205. doi:10.1016/j.canlet.2015.01.005. Epub 2015 Jan 13. PubMed PMID: 25595591.
• Niu H, Wang K, Zhang A, Yang S, Song Z, Wang W, Qian C, Li X, Zhu Y, Wang Y.miR-92a is a critical regulator of the apoptosis pathway in glioblastoma with inverse expression of BCL2L11. Oncol Rep. 2012 Nov;28(5):1771-7. doi:10.3892/or.2012.1970. Epub 2012 Aug 10. Erratum in: Oncol Rep. 2014 Sep;32(3):1319. PubMed PMID: 22895567.
• Ohgaki H, Dessen P, Jourde B, Horstmann S, Nishikawa T, Di Patre PL, Burkhard C, Schüler D, Probst-Hensch NM, Maiorka PC, Baeza N, Pisani P, Yonekawa Y, Yasargil MG, Lütolf UM, Kleihues P. Genetic pathways to glioblastoma: a population-based study. Cancer Res. 2004 Oct 1;64(19):6892-9. PubMed PMID:15466178.
• Ohgaki H, Kleihues P. The definition of primary and secondary glioblastoma. Clin Cancer Res. 2013 Feb 15;19(4):764-72. doi: 10.1158/1078-0432.CCR-12-3002.Epub 2012 Dec 3. Review. PubMed PMID: 23209033.
• Ostrom QT, Bauchet L, Davis FG, Deltour I, Fisher JL, Langer CE, Pekmezci M, Schwartzbaum JA, Turner MC, Walsh KM, Wrensch MR, Barnholtz-Sloan JS. The epidemiology of glioma in adults: a "state of the science" review. Neuro Oncol. 2014 Jul;16(7):896-913. Review. PubMed PMID: 24842956; PubMed Central PMCID: PMC4057143.
• Ozsolak F, Poling LL, Wang Z, Liu H, Liu XS, Roeder RG, Zhang X, Song JS, Fisher DE. Chromatin structure analyses identify miRNA promoters. Genes Dev. 2008 Nov 15;22(22):3172-83. doi: 10.1101/gad.1706508. PubMed PMID: 19056895; PubMedCentral PMCID: PMC2593607.
• Papagiannakopoulos T, Shapiro A, Kosik KS. MicroRNA-21 targets a network of key tumor-suppressive pathways in glioblastoma cells. Cancer Res. 2008 Oct 1;68(19):8164-72. doi: 10.1158/0008-5472.CAN-08-1305. PubMed PMID: 18829576.
• Park H, Huang X, Lu C, Cairo MS, Zhou X. MicroRNA-146a and microRNA-146b regulate human dendritic cell apoptosis and cytokine production by targeting TRAF6 and IRAK1 proteins. J Biol Chem. 2015 Jan 30;290(5):2831-41. doi: 10.1074/jbc.M114.591420. Epub 2014 Dec 11. PubMed PMID: 25505246; PubMed Central PMCID: PMC4317016.
• Park JE, Kim HS. Radiomics as a Quantitative Imaging Biomarker: Practical Considerations and the Current Standpoint in Neuro-oncologic Studies. Nucl Med Mol Imaging. 2018 Apr;52(2):99-108. doi: 10.1007/s13139-017-0512-7. Epub 2018 Feb 1. Review. PubMed PMID: 29662558; PubMed Central PMCID: PMC5897262.
• Parmar C, Grossmann P, Bussink J, Lambin P, Aerts HJWL. Machine Learning methods for Quantitative Radiomic Biomarkers. Sci Rep. 2015 Aug 17;5:13087. doi: 10.1038/srep13087. PubMed PMID: 26278466; PubMed Central PMCID: PMC4538374.

• Pasquinelli AE, Reinhart BJ, Slack F, Martindale MQ, Kuroda MI, Maller B,Hayward DC, Ball EE, Degnan B, Müller P, Spring J, Srinivasan A, Fishman M, Finnerty J, Corbo J, Levine M, Leahy P, Davidson E, Ruvkun G. Conservation of the sequence and temporal expression of let-7 heterochronic regulatory RNA. Nature. 2000 Nov 2;408(6808):86-9. PubMed PMID: 11081512

• Paul R, Hawkins SH, Schabath MB, Gillies RJ, Hall LO, Goldgof DB. Predicting malignant nodules by fusing deep features with classical radiomics features. Med Imaging (Bellingham). 2018 Jan;5(1):011021. doi: 10.1117/1.JMI.5.1.011021. Epub 2018 Mar 21. PubMed PMID: 29594181; PubMed Central PMCID: PMC5862127.

• Peeken JC, Bernhofer M, Wiestler B, Goldberg T, Cremers D, Rost B, Wilkens JJ,Combs SE, Nüsslin F. Radiomics in radiooncology - Challenging the medical physicist. Phys Med. 2018 Apr;48:27-36. doi: 10.1016/j.ejmp.2018.03.012. Epub 2018 Mar 27. Review. PubMed PMID: 29728226.

• Pellerino A, Franchino F, Soffietti R, Rudà R. Overview on current treatmentstandards in high-grade gliomas. Q J Nucl Med Mol Imaging. 2018Sep;62(3):225-238. doi: 10.23736/S1824-4785.18.03096-0. Epub 2018 Apr 26. Review. PubMed PMID: 29696949.

• Qi Z, Cai S, Cai J, Chen L, Yao Y, Chen L, Mao Y. miR-491 regulates glioma cells proliferation by targeting TRIM28 in vitro. BMC Neurol. 2016 Dec 1;16(1):248. PubMed PMID: 27905892; PubMed Central PMCID: PMC5131408.

• Qi Z, Cai S, Cai J, Chen L, Yao Y, Chen L, Mao Y. miR-491 regulates glioma cells proliferation by targeting TRIM28 in vitro. BMC Neurol. 2016 Dec 1;16(1):248. PubMed PMID: 27905892; PubMed Central PMCID: PMC5131408.

• Quan J, Qu J, Zhou L. MicroRNA-539 inhibits glioma cell proliferation and invasion by targeting DIXDC1. Biomed Pharmacother. 2017 Sep;93:746-753. doi:10.1016/j.biopha.2017.06.097. Epub 2017 Jul 10. PubMed PMID: 28704799.

• Quintavalle C, Donnarumma E, Iaboni M, Roscigno G, Garofalo M, Romano G, Fiore D, De Marinis P, Croce CM, Condorelli G. Effect of miR-21 and miR-30b/c on TRAIL-induced apoptosis in glioma cells. Oncogene. 2013 Aug 22;32(34):4001-8.doi: 10.1038/onc.2012.410. Epub 2012 Sep 10. PubMed PMID: 22964638.

• Rasmussen BK, Hansen S, Laursen RJ, Kosteljanetz M, Schultz H, Nørgård BM, Guldberg R, Gradel KO. Epidemiology of glioma: clinical characteristics, symptoms, and predictors of glioma patients grade I-IV in the the Danish Neuro-Oncology Registry. J Neurooncol. 2017 Dec;135(3):571-579. doi:10.1007/s11060-017-2607-5.

• Ręcławowicz D, Stempniewicz M, Biernat W, Limon J, Słoniewski P. Loss of genetic material within 1p and 19q chromosomal arms in low grade gliomas of central nervous system. Folia Neuropathol. 2013;51(1):26-32. PubMed PMID: 23553134.

• Reifenberger G, Wirsching HG, Knobbe-Thomsen CB, Weller M. Advances in the molecular genetics of gliomas - implications for classification and therapy. Nat Rev Clin Oncol. 2017 Jul;14(7):434-452. doi: 10.1038/nrclinonc.2016.204. Epub 2016 Dec 29. Review. PubMed PMID: 28031556.

• Riemenschneider MJ, Jeuken JW, Wesseling P, Reifenberger G. Molecular diagnostics of gliomas: state of the art. Acta Neuropathol. 2010Nov;120(5):567-84. doi: 10.1007/s00401-010-0736-4. Epub 2010 Aug 17. Review.PubMed PMID: 20714900; PubMed Central PMCID: PMC2955236.

• Rutman AM, Kuo MD. Radiogenomics: creating a link between molecular diagnostics and diagnostic imaging. Eur J Radiol. 2009 May;70(2):232-41. doi:10.1016/j.ejrad.2009.01.050. Epub 2009 Mar 19. Review. PubMed PMID:19303233.

- Saito Y, Liang G, Egger G, Friedman JM, Chuang JC, Coetzee GA, Jones PA. Specific activation of microRNA-127 with downregulation of the proto-oncogene BCL6 by chromatin-modifying drugs in human cancer cells. Cancer Cell. 2006 Jun;9(6):435-43. PubMed PMID: 16766263
- Sanger F, Nicklen S, Coulson AR. DNA sequencing with chain-terminating inhibitors. Proc Natl Acad Sci U S A. 1977 Dec;74(12):5463-7. PubMed PMID: 271968; PubMed Central PMCID: PMC431765.
- Sasayama T, Nishihara M, Kondoh T, Hosoda K, Kohmura E. MicroRNA-10b is overexpressed in malignant glioma and associated with tumor invasive factors,uPAR and RhoC. Int J Cancer. 2009 Sep 15;125(6):1407-13. doi: 10.1002/ijc.24522. PubMed PMID: 19536818.
- Sassen S, Miska EA, Caldas C. MicroRNA: implications for cancer. Virchows Arch. 2008 Jan;452(1):1-10. Epub 2007 Nov 27. Review. PubMed PMID: 18040713;PubMed Central PMCID: PMC2151131.
- Schirle NT, MacRae IJ. The crystal structure of human Argonaute2. Science. 2012 May 25;336(6084):1037-40. doi: 10.1126/science.1221551. Epub 2012 Apr 26.PubMed PMID: 22539551; PubMed Central PMCID: PMC3521581
- Scott GK, Mattie MD, Berger CE, Benz SC, Benz CC. Rapid alteration of microRNA levels by histone deacetylase inhibition. Cancer Res. 2006 Feb 1;66(3):1277-81.PubMed PMID: 16452179.
- Sehmer EA, Hall GJ, Greenberg DC, O'Hara C, Wallingford SC, Wright KA, Green AC. Incidence of glioma in a northwestern region of England, 2006-2010. Neuro Oncol. 2014 Jul;16(7):971-4. PubMed PMID: 24470555; PubMed Central PMCID:PMC4057131.
- Shahar T, Granit A, Zrihan D, Canello T, Charbit H, Einstein O, Rozovski U,Elgavish S, Ram Z, Siegal T, Lavon I. Expression level of miRNAs on chromosome 14q32.31 region correlates with tumor aggressiveness and survival of glioblastoma patients. J Neurooncol. 2016 Dec;130(3):413-422. Epub 2016 Aug 29. PubMed PMID:27573219.
- Shendure J, Ji H. Next-generation DNA sequencing. Nat Biotechnol. 2008 Oct;26(10):1135-45. doi: 10.1038/nbt1486. PubMed PMID: 18846087.
- Shi JA, Lu DL, Huang X, Tan W. miR-219 inhibits the proliferation, migration and invasion of medulloblastoma cells by targeting CD164. Int J Mol Med. 2014 Jul;34(1):237-43. doi: 10.3892/ijmm.2014.1749. Epub 2014 Apr 22. PubMed PMID:24756834.
- Shi L, Fei X, Wang Z, You Y. PI3K inhibitor combined with miR-125b inhibitor sensitize TMZ-induced anti-glioma stem cancer effects through inactivation of Wnt/β-catenin signaling pathway. In Vitro Cell Dev Biol Anim. 2015 Nov;51(10):1047-55. doi: 10.1007/s11626-015-9931-x. Epub 2015 Jul 14. PubMed PMID: 26170223.
- Shijun Wang, Ronald M. Summers Machine Learning and Radiology Med Image Anal. 2012 Jul; 16(5): 933–951. Published online 2012 Feb 23. doi: 10.1016/j.media.2012.02.005PMCID: PMC3372692
- Shu M, Zhou Y, Zhu W, Zhang H, Wu S, Chen J, Yan G. MicroRNA 335 is required for differentiation of malignant glioma cells induced by activation of cAMP/protein kinase A pathway. Mol Pharmacol. 2012 Mar;81(3):292-8. doi: 10.1124/mol.111.076166. Epub 2011 Dec 15. PubMed PMID: 22172575.
- Silber J, Jacobsen A, Ozawa T, Harinath G, Pedraza A, Sander C, Holland EC,Huse JT. miR-34a repression in proneural malignant gliomas upregulates expression of its target PDGFRA and promotes tumorigenesis. PLoS One. 2012;7(3):e33844. doi: 10.1371/journal.pone.0033844. Epub 2012 Mar 27. PubMed PMID: 22479456; PubMed Central PMCID: PMC3313940.

• Skogen K, Schulz A, Helseth E, Ganeshan B, Dormagen JB, Server A. Texture analysis on diffusion tensor imaging: discriminating glioblastoma from single brain metastasis. Acta Radiol. 2019 Mar;60(3):356-366. doi:10.1177/0284185118780889. Epub 2018 Jun 3. PubMed PMID: 29860889.

• Soffietti R, Baumert BG, Bello L, von Deimling A, Duffau H, Frénay M, Grisold W, Grant R, Graus F, Hoang-Xuan K, Klein M, Melin B, Rees J, Siegal T, Smits A,Stupp R, Wick W; European Federation of Neurological Societies. Guidelines on management of low-grade gliomas: report of an EFNS-EANO Task Force. Eur J Neurol.2010 Sep;17(9):1124-33. doi: 10.1111/j.1468-1331.2010.03151.x. PubMed PMID:20718851.

• Soni N, Priya S, Bathla G. Texture Analysis in Cerebral Gliomas: A Review of the Literature. AJNR Am J Neuroradiol. 2019 Jun;40(6):928-934. doi: 10.3174/ajnr.A6075. Epub 2019 May 23. Review. PubMed PMID: 31122918.

• Stommel JM, Kimmelman AC, Ying H, Nabioullin R, Ponugoti AH, Wiedemeyer R, Stegh AH, Bradner JE, Ligon KL, Brennan C, Chin L, DePinho RA. Coactivation of receptor tyrosine kinases affects the response of tumor cells to targeted therapies. Science. 2007 Oct 12;318(5848):287-90. Epub 2007 Sep 13. PubMed PMID: 17872411.

• Suhovskih AV, Kazanskaya GM, Volkov AM, Tsidulko AY, Aidagulova SV, GrigorievaEV. Suitability of RNALater solution as a tissue-preserving reagent for immunohistochemical analysis. Histochem Cell Biol. 2019 Sep;152(3):239-247. doi: 10.1007/s00418-019-01799-z. Epub 2019 Jun 14. PubMed PMID: 31197457.

• Sun D, Mu Y, Piao H. MicroRNA-153-3p enhances cell radiosensitivity by targeting BCL2 in human glioma. Biol Res. 2018 Dec 11;51(1):56. doi: 10.1186/s40659-018-0203-6. PubMed PMID: 30537994; PubMed Central PMCID: PMC6288870.

• Sun J, Jia Z, Li B, Zhang A, Wang G, Pu P, Chen Z, Wang Z, Yang W. MiR-19 regulates the proliferation and invasion of glioma by RUNX3 via β-catenin/Tcf-4 signaling. Oncotarget. 2017 Nov 28;8(67):110785-110796. doi:10.18632/oncotarget.22720. eCollection 2017 Dec 19. PubMed PMID: 29340016; PubMed Central PMCID: PMC5762284

• Sun S, Wang X, Xu X, Di H, Du J, Xu B, Wang Q, Wang J. MiR-433-3p suppresses cell growth and enhances chemosensitivity by targeting CREB in human glioma. Oncotarget. 2017 Jan 17;8(3):5057-5068. doi: 10.18632/oncotarget.13789. PubMed PMID: 27926502; PubMed Central PMCID: PMC5354892.

• Tamim S, Vo DT, Uren PJ, Qiao M, Bindewald E, Kasprzak WK, Shapiro BA, Nakaya HI, Burns SC, Araujo PR, Nakano I, Radek AJ, Kuersten S, Smith AD, Penalva LO.Genomic analyses reveal broad impact of miR-137 on genes associated with malignant transformation and neuronal differentiation in glioblastoma cells. PLoS One. 2014 Jan 22;9(1):e85591. doi: 10.1371/journal.pone.0085591. eCollection 2014. PubMed PMID: 24465609; PubMed Central PMCID: PMC3899048.

• Tang H, Wang Z, Liu Q, Liu X, Wu M, Li G. Disturbing miR-182 and -381 inhibits BRD7 transcription and glioma growth by directly targeting LRRC4. PLoS One. 2014 Jan 3;9(1):e84146. doi: 10.1371/journal.pone.0084146. eCollection 2014. PubMed PMID: 24404152; PubMed Central PMCID: PMC3880275.

• Tang J, Xu J, Zhi Z, Wang X, Wang Y, Zhou Y, Chen R. MiR-876-3p targets KIF20A to block JAK2/STAT3 pathway in glioma. Am J Transl Res. 2019 Aug 15;11(8):4957-4966. eCollection 2019. PubMed PMID: 31497212; PubMed Central PMCID: PMC6731397.

• Tang L. [Radiological evaluation of advanced gastric cancer: from image to big data radiomics]. Zhonghua Wei Chang Wai Ke Za Zhi. 2018 Oct 25;21(10):1106-1112. Review. Chinese. PubMed PMID: 30370508.

• Thust SC, Heiland S, Falini A, et al. Glioma imaging in Europe: A survey of 220 centres and recommendations for best clinical practice. Eur Radiol. 2018;28(8):3306–3317. doi:10.1007/s00330-018-5314-5
• Tian Y, Nan Y, Han L, Zhang A, Wang G, Jia Z, Hao J, Pu P, Zhong Y, Kang C.MicroRNA miR-451 downregulates the PI3K/AKT pathway through CAB39 in human glioma. Int J Oncol. 2012 Apr;40(4):1105-12. doi: 10.3892/ijo.2011.1306. Epub 2011 Dec 15. PubMed PMID: 22179124; PubMed Central PMCID: PMC3584578.
• Trakunram K, Champoochana N, Chaniad P, Thongsuksai P, Raungrut P. MicroRNA Isolation by Trizol-Based Method and Its Stability in Stored Serum and cDNA Derivatives. Asian Pac J Cancer Prev. 2019 Jun 1;20(6):1641-1647. doi: 10.31557/APJCP.2019.20.6.1641. PubMed PMID: 31244282.
• Upadhyay N, Waldman AD. Conventional MRI evaluation of gliomas. Br J Radiol. 2011 Dec;84 Spec No 2:S107-11. doi: 10.1259/bjr/65711810. Review. PubMed PMID: 22433821; PubMed Central PMCID: PMC3473894.
• Uziel T, Karginov FV, Xie S, Parker JS, Wang YD, Gajjar A, He L, Ellison D, Gilbertson RJ, Hannon G, Roussel MF. The miR-17~92 cluster collaborates with the Sonic Hedgehog pathway in medulloblastoma. Proc Natl Acad Sci U S A. 2009 Feb 24;106(8):2812-7. doi: 10.1073/pnas.0809579106. Epub 2009 Feb 5. PubMed PMID: 19196975; PubMed Central PMCID: PMC2636735.
• von Deimling A, Korshunov A, Hartmann C. The next generation of glioma biomarkers: MGMT methylation, BRAF fusions and IDH1 mutations. Brain Pathol. 2011 Jan;21(1):74-87. doi: 10.1111/j.1750-3639.2010.00454.x. Review. PubMed PMID: 21129061.
• Walker C, Baborie A, Crooks D, Wilkins S, Jenkinson MD. Biology, genetics and imaging of glial cell tumours. Br J Radiol. 2011 Dec;84 Spec No 2:S90-106. doi: 10.1259/bjr/23430927. Review. PubMed PMID: 22433833; PubMed Central PMCID:PMC3473897.
• Wang B, Sun F, Dong N, Sun Z, Diao Y, Zheng C, Sun J, Yang Y, Jiang D. MicroRNA-7 directly targets insulin-like growth factor 1 receptor to inhibit cellular growth and glucose metabolism in gliomas. Diagn Pathol. 2014 Nov 14;9:211. doi: 10.1186/s13000-014-0211-y. PubMed PMID: 25394492; PubMed Central PMCID: PMC4236426.
• Wang H, Cruz-Roa A, Basavanhally A, Gilmore H, Shih N, Feldman M, Tomaszewski J, Gonzalez F, Madabhushi A. Mitosis detection in breast cancer pathology images by combining handcrafted and convolutional neural network features. J Med Imaging (Bellingham). 2014 Oct;1(3):034003. doi: 10.1117/1.JMI.1.3.034003. Epub 2014 Oct 10. PubMed PMID: 26158062; PubMed Central PMCID: PMC4479031.
• Wang H, Yuan X, Zhou Z, Hu J, Zhang T, Hu S, Luo J, Li X. MicroRNAs might be promising biomarkers of human gliomas. Asian Pac J Cancer Prev. 2011;12(4):833-5.Review. PubMed PMID: 21790212.
• Wang J, Chen C, Yan X, Wang P. The role of miR-382-5p in glioma cell proliferation, migration and invasion. Onco Targets Ther. 2019 Jun 25;12:4993-5002. doi: 10.2147/OTT.S196322. eCollection 2019. PubMed PMID:31417288; PubMed Central PMCID: PMC6601051.
• Wang J, Li B, Wang C, Luo Y, Zhao M, Chen P. Long noncoding RNA FOXD2-AS1 promotes glioma cell cycle progression and proliferation through the FOXD2-AS1/miR-31/CDK1 pathway. J Cell Biochem. 2019 Dec;120(12):19784 19795. doi:10.1002/jcb.29284. Epub 2019 Jul 26. PubMed PMID: 31347720.
• Wang J, Wang ML, Wang CH, Sun SY, Zhang HB, Jiang YY, Xu QW, Wang Y, Gu SX. A novel functional polymorphism of GFAP decrease glioblastoma susceptibility through inhibiting the binding of miR-139. Aging

(Albany NY). 2018 May 10;10(5):988-999. doi: 10.18632/aging.101442. PubMed PMID: 29746255; PubMed Central PMCID: PMC5990380.

• Wang L, Guo S, Zhang H. MiR-98 Promotes Apoptosis of Glioma Cells via Suppressing IKBKE/NF-κB Pathway. Technol Cancer Res Treat. 2017 Dec;16(6):1226-1234. doi: 10.1177/1533034617745761. Epub 2017 Dec 11. PubMed PMID: 29333957; PubMed Central PMCID: PMC5762096.

• Wang Q, Lei D, Yuan Y, Zhao H. Accuracy of magnetic resonance imaging texture analysis in differentiating low-grade from high-grade gliomas: systematic review and meta-analysis. BMJ Open. 2019 Sep 5;9(9):e027144. doi:10.1136/bmjopen-2018-027144. PubMed PMID: 31492777; PubMed Central PMCID:PMC6731805.

• Wang R, Zuo X, Wang K, Han Q, Zuo J, Ni H, Liu W, Bao H, Tu Y, Xie P. MicroRNA-485-5p attenuates cell proliferation in glioma by directly targeting paired box 3. Am J Cancer Res. 2018 Dec 1;8(12):2507-2517. eCollection 2018.PubMed PMID: 30662807; PubMed Central PMCID: PMC6325470.

• Wang W, Zhang A, Hao Y, Wang G, Jia Z. The emerging role of miR-19 in glioma. J Cell Mol Med. 2018 Oct;22(10):4611-4616. Doi 10.1111/jcmm.13788. Epub 2018Aug 2. Review. PubMed PMID: 30073755; PubMed Central PMCID: PMC6156349.

• Wang X, Huang Z, Wu Q, Prager BC, Mack SC, Yang K, Kim LJY, Gimple RC, Shi Y, Lai S, Xie Q, Miller TE, Hubert CG, Song A, Dong Z, Zhou W, Fang X, Zhu Z, Mahadev V, Bao S, Rich JN. MYC-Regulated Mevalonate Metabolism Maintains Brain Tumor-Initiating Cells. Cancer Res. 2017 Sep 15;77(18):4947-4960. doi: 10.1158/0008-5472.CAN-17-0114. Epub 2017 Jul 20. PubMed PMID: 28729418; PubMed Central PMCID: PMC5600855.

• Wang X, Sun S, Tong X, Ma Q, Di H, Fu T, Sun Z, Cai Y, Fan W, Wu Q, Li Y, Wang Q, Wang J. MiRNA-154-5p inhibits cell proliferation and metastasis by targeting PIWIL1 in glioblastoma. Brain Res. 2017 Dec 1;1676:69-76. doi: 10.1016/j.brainres.2017.08.014. Epub 2017 Aug 24. PubMed PMID: 28842123.

• Wang X, Sun S, Tong X, Ma Q, Di H, Fu T, Sun Z, Cai Y, Fan W, Wu Q, Li Y, Wang Q, Wang J. MiRNA-154-5p inhibits cell proliferation and metastasis by targeting PIWIL1 in glioblastoma. Brain Res. 2017 Dec 1;1676:69-76. doi: 10.1016/j.brainres.2017.08.014. Epub 2017 Aug 24. PubMed PMID: 28842123.

• Wang X, Zhang H, Zhang A, Han L, Wang K, Liu R, Yang S, Pu P, Shen C, Kang C, Yu C. Upregulation of miR-20a and miR-106b is involved in the acquisition of malignancy of pediatric brainstem gliomas. Oncol Rep. 2012 Oct;28(4):1293-300.doi: 10.3892/or.2012.1927. Epub 2012 Jul 23. PubMed PMID: 22825541.

• Wang Y, Medvid R, Melton C, Jaenisch R, Blelloch R. DGCR8 is essential for microRNA biogenesis and silencing of embryonic stem cell self-renewal. Nat Genet. 2007 Mar;39(3):380-5. Epub 2007 Jan 28. PubMed PMID: 17259983; PubMed Central PMCID: PMC3008549.

• Wang Y, Wang L. miR-34a attenuates glioma cells progression and chemoresistance via targeting PD-L1. Biotechnol Lett. 2017 Oct;39(10):1485-1492. doi: 10.1007/s10529-017-2397-z. Epub 2017 Jul 18.PubMed PMID: 28721584.

• Wang Y, Wang M, Wei W, Han D, Chen X, Hu Q, Yu T, Liu N, You Y, Zhang J. Disruption of the EZH2/miRNA/β-catenin signaling suppresses aerobic glycolysis in glioma. Oncotarget. 2016 Aug 2;7(31):49450-49458. doi: 10.18632/oncotarget.10370. PubMed PMID: 27385092; PubMed Central PMCID: PMC5226520.

• Wang YZ, Han JJ, Fan SQ, Yang W, Zhang YB, Xu TJ, Xu GM. miR-132 weakensproliferation and invasion of glioma cells via the inhibition of Gli1. Eur Rev Med Pharmacol Sci. 2018 Apr;22(7):1971-1978. doi: 10.26355/eurrev_201804_14724. PubMed PMID: 29687851.

• Wang Z, Lin S, Zhang J, Xu Z, Xiang Y, Yao H, Ge L, Xie D, Kung HF, Lu G, Poon WS, Liu Q, Lin MC. Loss of MYC and E-box3 binding contributes to defective MYC-mediated transcriptional suppression of human MC-let-7a-1~let-7d in glioblastoma. Oncotarget. 2016 Aug 30;7(35):56266-56278. doi: 10.18632/oncotarget.10517. PubMed PMID: 27409345; PubMed Central PMCID: PMC5302913.
• Wang Z, Wang B, Shi Y, Xu C, Xiao HL, Ma LN, Xu SL, Yang L, Wang QL, Dang WQ, Cui W, Yu SC, Ping YF, Cui YH, Kung HF, Qian C, Zhang X, Bian XW. Oncogenic miR-20a and miR-106a enhance the invasiveness of human glioma stem cells by directly targeting TIMP-2. Oncogene. 2015 Mar 12;34(11):1407-19. doi:10.1038/onc.2014.75. Epub 2014 Apr 7. PubMed PMID: 24704830.
• Wang Z, Wang B, Shi Y, Xu C, Xiao HL, Ma LN, Xu SL, Yang L, Wang QL, Dang WQ, Cui W, Yu SC, Ping YF, Cui YH, Kung HF, Qian C, Zhang X, Bian XW. Oncogenic miR-20a and miR-106a enhance the invasiveness of human glioma stem cells by directly targeting TIMP-2. Oncogene. 2015 Mar 12;34(11):1407-19. doi: 10.1038/onc.2014.75. Epub 2014 Apr 7. PubMed PMID: 24704830.
• Wang Z, Yang J, Xu G, Wang W, Liu C, Yang H, Yu Z, Lei Q, Xiao L, Xiong J, Zeng L, Xiang J, Ma J, Li G, Wu M. Targeting miR-381-NEFL axis sensitizes glioblastoma cells to temozolomide by regulating stemness factors and multidrug resistance factors. Oncotarget. 2015 Feb 20;6(5):3147-64. PubMed PMID: 25605243; PubMed Central PMCID: PMC4413644.
• Wang ZL, Zhang CB, Wang Z, Meng XQ, Liu XJ, Han B, Duan CB, Cai JQ, Hao ZF, Chen MH, Jiang T, Li YL, Jiang CL, Wang HJ. MiR-134, epigenetically silenced in gliomas, could mitigate the malignant phenotype by targeting KRAS. Carcinogenesis. 2018 Mar 8;39(3):389-396. doi: 10.1093/carcin/bgy022. PubMed PMID: 29432532.
• Wang ZY, Xiong J, Zhang SS, Wang JJ, Gong ZJ, Dai MH. Up-Regulation of microRNA-183 Promotes Cell Proliferation and Invasion in Glioma By Directly Targeting NEFL. Cell Mol Neurobiol. 2016 Nov;36(8):1303-1310. Epub 2016 Feb 15.PubMed PMID: 26879754.
• Wei CW, Guo G, Mikulis DJ. Tumor effects on cerebral white matter as characterized by diffusion tensor tractography. Can J Neurol Sci. 2007 Feb;34(1):62-8. PubMed PMID: 17352349.
• Weisman ID, Bennett LH, Maxwell LR Sr, Woods MW, Burk D. Recognition of cancer in vivo by nuclear magnetic resonance. Science. 1972 Dec 22;178(4067):1288-90. PubMed PMID: 4640065.
• Weng HH, Noll KR, Johnson JM, Prabhu SS, Tsai YH, Chang SW, Huang YC, Lee JD, Yang JT, Yang CT, Tsai YH, Yang CY, Hazle JD, Schomer DF, Liu HL. Accuracy of Presurgical Functional MR Imaging for Language Mapping of Brain Tumors: A Systematic Review and Meta-Analysis. Radiology. 2018 Feb;286(2):512-523. doi: 10.1148/radiol.2017162971. Epub 2017 Oct 4. Review. PubMed PMID: 28980887.
• Wesseling P, van der Laak JA, Link M, Teepen HL, Ruiter DJ. Quantitative analysis of microvascular changes in diffuse astrocytic neoplasms with increasing grade of malignancy. Hum Pathol. 1998 Apr;29(4):352-8. PubMed PMID: 9563784.
• Wightman B, Ha I, Ruvkun G. Posttranscriptional regulation of the heterochronic gene lin-14 by lin-4 mediates temporal pattern formation in C.elegans. Cell. 1993 Dec 3;75(5):855-62. PubMed PMID: 8252622.
• Wolter M, Werner T, Malzkorn B, Reifenberger G. Role of microRNAs Located on Chromosome Arm 10q in Malignant Gliomas. Brain Pathol. 2016 May;26(3):344-58. doi: 10.1111/bpa.12294. Epub 2015 Sep 9. PubMed PMID: 26223576.

• Wu W, Yu T, Wu Y, Tian W, Zhang J, Wang Y. The miR155HG/miR-185/ANXA2 loop contributes to glioblastoma growth and progression. J Exp Clin Cancer Res. 2019Mar 21;38(1):133. doi: 10.1186/s13046-019-1132-0. PubMed PMID: 30898167; PubMed Central PMCID: PMC6427903.
• Xia L, Nie D, Wang G, Sun C, Chen G. FER1L4/miR-372/E2F1 works as a ceRNA system to regulate the proliferation and cell cycle of glioma cells. J Cell Mol Med. 2019 May;23(5):3224-3233. doi: 10.1111/jcmm.14198. Epub 2019 Mar 19. PubMed PMID: 30887657; PubMed Central PMCID: PMC6484322.
• Xiao B, Tan L, He B, Liu Z, Xu R. MiRNA-329 targeting E2F1 inhibits cell proliferation in glioma cells. J Transl Med. 2013 Jul 17;11:172. doi: 10.1186/1479-5876-11-172. PubMed PMID: 23866847; PubMed Central PMCID: PMC3750231.
• Xiao B, Tan L, He B, Liu Z, Xu R. MiRNA-329 targeting E2F1 inhibits cell proliferation in glioma cells. J Transl Med. 2013 Jul 17;11:172. doi: 10.1186/1479-5876-11-172. PubMed PMID: 23866847; PubMed Central PMCID: PMC3750231.
• Xie P, Wang Y, Liao Y, Han Q, Qiu Z, Chen Y, Zuo X. MicroRNA-628-5p inhibits cell proliferation in glioma by targeting DDX59. J Cell Biochem. 2019 Oct;120(10):17293-17302. doi: 10.1002/jcb.28991. Epub 2019 May 20. PubMed PMID: 31111544.
• Xie Q, Yan Y, Huang Z, Zhong X, Huang L. MicroRNA-221 targeting PI3-K/Akt signaling axis induces cell proliferation and BCNU resistance in human glioblastoma. Neuropathology. 2014 Oct;34(5):455-64. doi: 10.1111/neup.12129. Epub 2014 Apr 30. PubMed PMID: 24780067.
• Xu G, Fang P, Chen K, Xu Q, Song Z, Ouyang Z. MicroRNA-362-3p Targets PAX3 to Inhibit the Development of Glioma through Mediating Wnt/β-Catenin Pathway.Neuroimmunomodulation. 2019;26(3):119-128. doi: 10.1159/000499766. Epub 2019 Jun 5. PubMed PMID: 31167206.
• Xu G, Li JY. ATP5A1 and ATP5B are highly expressed in glioblastoma tumor cells and endothelial cells of microvascular proliferation. J Neurooncol. 2016 Feb;126(3):405-13. doi: 10.1007/s11060-015-1984-x. Epub 2015 Nov 2. PubMed PMID: 26526033.
• Xu S, Zhang J, Xue H, Guo X, Han X, Li T, Guo X, Gao X, Liu Q, Li G. MicroRNA-584-3p reduces the vasculogenic mimicry of human glioma cells by regulating hypoxia-induced ROCK1 dependent stress fiber formation. Neoplasma.b2017;64(1):13-21. doi: 10.4149/neo_2017_102. PubMed PMID: 27881000.
• Xu T, Wang H, Jiang M, Yan Y, Li W, Xu H, Huang Q, Lu Y, Chen J. The E3 ubiquitin ligase CHIP/miR-92b/PTEN regulatory network contributes to tumorigenesis of glioblastoma. Am J Cancer Res. 2017 Feb 1;7(2):289-300. eCollection 2017. PubMed PMID: 28337377; PubMed Central PMCID: PMC5336502.
• Xu T, Wang H, Jiang M, Yan Y, Li W, Xu H, Huang Q, Lu Y, Chen J. The E3 ubiquitin ligase CHIP/miR-92b/PTEN regulatory network contributes to tumorigenesis of glioblastoma. Am J Cancer Res. 2017 Feb 1;7(2):289-300. eCollection 2017. PubMed PMID: 28337377; PubMed Central PMCID: PMC5336502.
• Xu X, Bao Z, Liu Y, Jiang K, Zhi T, Wang D, Fan L, Liu N, Ji J. PBX3/MEK/ERK1/2/LIN28/let-7b positive feedback loop enhances mesenchymal phenotype to promote glioblastoma migration and invasion. J Exp Clin Cancer Res. 2018 Jul 17;37(1):158. doi: 10.1186/s13046-018-0841-0. PubMed PMID: 30016974;PubMed Central PMCID: PMC6050701.
• Xu Y, Xu W, Lu T, Dai Y, Liang W. miR-126 affects the invasion and migration of glioma cells through GATA4. Artif Cells Nanomed Biotechnol. 2017 Sep;45(6):1-7. doi: 10.1080/21691401.2016.1226179. Epub 2016 Sep 6. PubMed PMID: 27598297.

- Xue W, Chen J, Liu X, Gong W, Zheng J, Guo X, Liu Y, Liu L, Ma J, Wang P, Li Z, Xue Y. PVT1 regulates the malignant behaviors of human glioma cells by targeting miR-190a-5p and miR-488-3p. Biochim Biophys Acta Mol Basis Dis. 2018May;1864(5 Pt A):1783-1794. doi: 10.1016/j.bbadis.2018.02.022. Epub 2018 Mar 1.PubMed PMID: 29501773.
- Yan H, Parsons DW, Jin G, McLendon R, Rasheed BA, Yuan W, Kos I,Batinic-Haberle I, Jones S, Riggins GJ, Friedman H, Friedman A, Reardon D,Herndon J, Kinzler KW, Velculescu VE, Vogelstein B, Bigner DD. IDH1 and IDH2 mutations in gliomas. N Engl J Med. 2009 Feb 19;360(8):765-73. doi: 10.1056/NEJMoa0808710. PubMed PMID: 19228619; PubMed Central PMCID: PMC2820383.
- Yan W, Zhang W, Sun L, Liu Y, You G, Wang Y, Kang C, You Y, Jiang T. Identification of MMP-9 specific microRNA expression profile as potential targets of anti-invasion therapy in glioblastoma multiforme. Brain Res. 2011 Sep 9;1411:108-15. doi: 10.1016/j.brainres.2011.07.002. Epub 2011 Jul 13. PubMed PMID: 21831363.
- Yan Y, Peng Y, Ou Y, Jiang Y. MicroRNA-610 is downregulated in glioma cells,and inhibits proliferation and motility by directly targeting MDM2. Mol Med Rep. 2016 Sep;14(3):2657-64. doi: 10.3892/mmr.2016.5559. Epub 2016 Jul 27. PubMed PMID: 27485527.
- Yang CH, Wang Y, Sims M, Cai C, He P, Häcker H, Yue J, Cheng J, Boop FA,Pfeffer LM. MicroRNA203a suppresses glioma tumorigenesis through an ATM-dependent interferon response pathway. Oncotarget. 2017 Dec 6;8(68):112980-112991. doi: 10.18632/oncotarget.22945. eCollection 2017 Dec 22. PubMed PMID: 29348882; PubMed Central PMCID: PMC5762567.
- Yang CH, Wang Y, Sims M, Cai C, He P, Häcker H, Yue J, Cheng J, Boop FA, Pfeffer LM. MicroRNA203a suppresses glioma tumorigenesis through an ATM-dependentinterferon response pathway. Oncotarget. 2017 Dec 6;8(68):112980-112991. doi:10.18632/oncotarget.22945. eCollection 2017 Dec 22. PubMed PMID: 29348882; PubMed Central PMCID: PMC5762567.
- Yang G, Han B, Feng T. ZFAS1 knockdown inhibits viability and enhances cisplatin cytotoxicity by up-regulating miR-432-5p in glioma cells. Basic Clin Pharmacol Toxicol. 2019 Jun 27. doi: 10.1111/bcpt.13286. [Epub ahead of print] PubMed PMID: 31246330.
- Yeom KH, Lee Y, Han J, Suh MR, Kim VN. Characterization of DGCR8/Pasha, the essential cofactor for Drosha in primary miRNA processing. Nucleic Acids Res.2006;34(16):4622-9. Epub 2006 Sep 8. PubMed PMID: 16963499; PubMed Central PMCID:PMC1636349.
- Yip SSF, Liu Y, Parmar C, Li Q, Liu S, Qu F, Ye Z, Gillies RJ, Aerts HJWL.Associations between radiologist-defined semantic and automatically computed radiomic features in non-small cell lung cancer. Sci Rep. 2017 Jun 14;7(1):3519. doi: 10.1038/s41598-017-02425-5. PubMed PMID: 28615677; PubMed Central PMCID:PMC5471260.
- Zhang B, Yuan F, Liu J, Li Y, Zhou F, Liu X, Hao Z, Li Q, Zheng Y, Wang W. Hsa-miR-495 acts as a tumor suppressor gene in glioma via the negative regulation of MYB. Mol Med Rep. 2016 Jul;14(1):977-82. doi: 10.3892/mmr.2016.5327. Epub 2016 May 23. PubMed PMID: 27220777.
- Zhang C, Moore LM, Li X, Yung WK, Zhang W. IDH1/2 mutations target a key hallmark of cancer by deregulating cellular metabolism in glioma. Neuro Oncol. 2013 Sep;15(9):1114-26. doi: 10.1093/neuonc/not087. Epub 2013 Jul 21. Review. PubMed PMID: 23877318; PubMed Central PMCID: PMC3748922.
- Zhang C, Yang X, Fu C, Liu X. Combination with TMZ and miR-505 inhibits the development of glioblastoma by regulating the WNT7B/Wnt/β-catenin signaling pathway. Gene. 2018 Sep 25;672:172-179. doi: 10.1016/j.gene.2018.06.030. Epub 2018 Jun 12. PubMed PMID: 29906532.

- Zhang C, Zhang J, Hao J, Shi Z, Wang Y, Han L, Yu S, You Y, Jiang T, Wang J, Liu M, Pu P, Kang C. High level of miR-221/222 confers increased cell invasion and poor prognosis in glioma. J Transl Med. 2012 Jun 8;10:119. doi:10.1186/1479-5876-10-119. PubMed PMID: 22681957; PubMed Central PMCID:PMC3403924.
- Zhang F, Wu A, Wang Y, Liu J. miR-490-3p functions as a tumor suppressor in glioma by inhibiting high-mobility group AT-hook 2 expression. Exp Ther Med. 2019 Jul;18(1):664-670. doi: 10.3892/etm.2019.7606. Epub 2019 May 23. PubMed PMID: 31258704; PubMed Central PMCID: PMC6566118.
- Zhang H, Wang X, Chen X. Potential Role of Long Non-Coding RNA ANRIL in Pediatric Medulloblastoma Through Promotion on Proliferation and Migration by Targeting miR-323. J Cell Biochem. 2017 Dec;118(12):4735-4744. doi: 10.1002/jcb.26141. Epub 2017 Jun 12. PubMed PMID: 28513871.
- Zhang J, Lv J, Zhang F, Che H, Liao Q, Huang W, Li S, Li Y. MicroRNA-211 expression is down-regulated and associated with poor prognosis in human glioma. J Neurooncol. 2017 Jul;133(3):553-559. doi: 10.1007/s11060-017-2464-2. Epub 2017 May 27. PubMed PMID: 28551850.
- Zhang W, Dahlberg JE, Tam W. MicroRNAs in tumorigenesis: a primer. Am J Pathol. 2007 Sep;171(3):728-38. Review. PubMed PMID: 17724137; PubMed Central PMCID: PMC1959494.
- Zhang X, Yu J, Zhao C, Ren H, Yuan Z, Zhang B, Zhuang J, Wang J, Feng B. MiR-181b-5p modulates chemosensitivity of glioma cells to temozolomide by targeting Bcl-2. Biomed Pharmacother. 2019 Jan;109:2192-2202. doi: 10.1016/j.biopha.2018.11.074. Epub 2018 Nov 27. PubMed PMID: 30551476.
- Zhang XH, Qian Y, Li Z, Zhang NN, Xie YJ. Let-7g-5p inhibits epithelial-mesenchymal transition consistent with reduction of glioma stem cell phenotypes by targeting VSIG4 in glioblastoma. Oncol Rep. 2016 Nov;36(5):2967-2975. doi: 10.3892/or.2016.5098. Epub 2016 Sep 16. PubMed PMID: 27634309.
- Zhao LN, Wang P, Liu YH, Cai H, Ma J, Liu LB, Xi Z, Li ZQ, Liu XB, Xue YX. MiR-383 inhibits proliferation, migration and angiogenesis of glioma-exposed endothelial cells in vitro via VEGF-mediated FAK and Src signaling pathways. Cell Signal. 2017 Jan;30:142-153. doi: 10.1016/j.cellsig.2016.09.007. Epub 2016 Sep 28. PubMed PMID: 27693218.
- Zhao W, Yin CY, Jiang J, Kong W, Xu H, Zhang H. MicroRNA-153 suppresses cellinvasion by targeting SNAI1 and predicts patient prognosis in glioma. Oncol Lett. 2019 Jan;17(1):1189-1195. doi: 10.3892/ol.2018.9706. Epub 2018 Nov 15. PubMed PMID: 30655883; PubMed Central PMCID: PMC6313079.
- Zhao Y, Huang W, Kim TM, Jung Y, Menon LG, Xing H, Li H, Carroll RS, Park PJ, Yang HW, Johnson MD. MicroRNA-29a activates a multi-component growth and invasionprogram in glioblastoma. J Exp Clin Cancer Res. 2019 Jan 25;38(1):36. doi: 10.1186/s13046-019-1026-1. PubMed PMID: 30683134; PubMed Central PMCID:PMC6347789.
- Zhi T, Yu T, Pan M, Nie E, Wu W, Wang X, Liu N, You Y, Wang Y, Zhang J. EZH2 alteration driven by microRNA-524-5p and microRNA-324-5p promotes cell proliferation and temozolomide resistance in glioma. Oncotarget. 2017 Oct 24;8(56):96239-96248. doi: 10.18632/oncotarget.21996. eCollection 2017 Nov 10.PubMed PMID: 29221202; PubMed Central PMCID: PMC5707096.
- Zhou J, Wang W, Gao Z, Peng X, Chen X, Chen W, Xu W, Xu H, Lin MC, Jiang S. MicroRNA-155 promotes glioma cell proliferation via the regulation of MXI1. PLoS One. 2013 Dec 23;8(12):e83055. doi: 10.1371/journal.pone.0083055. eCollection 2013. PubMed PMID: 24376632; PubMed Central PMCID: PMC3871643.

• Zuo J, Yu H, Xie P, Liu W, Wang K, Ni H. miR-454-3p exerts tumor-suppressive functions by down-regulation of NFATc2 in glioblastoma. Gene. 2019 Aug 20;710:233-239. doi: 10.1016/j.gene.2019.06.008. Epub 2019 Jun 7. PubMed PMID: 31181312.